ANALYSIS OF THE TRIBOLOGICAL BEHAVIOUR OF STAINLESS AND BALL BEARING STEELS SLIDING IN THE PRESENCE OF SULPHUR EXTREME-PRESSURE ADDITIVES

Author: Sattar Jabar Dawud, B.Sc. M.Sc.

A thesis submitted for the degree of

M. Phil.

1985

ACKNOWLEDGEMENT

I would like to express my deep gratitude to my supervisor, Mr. J. Sullivan, for his advice and invaluable guidance throughout the work. Also, I would like to thank Dr. N.W. Grimes (Head of Department) and Professor T. Mulvey for their support and advice.

My sincere appreciation to all those who have helped and encouraged me.

A thesis submitted for the degree of M. Phil. by

SATTAR JABAR DAWUD

1985

ABSTRACT

Conventional wear tests using a Four-Ball Lubricant Tester with the British Standard SAE 52100 steel were supplemented by tests with a stainless steel (AISI 420). Four combinations of these two materials were studied, namely each material was used in turn for the upper (driven) ball and the lower (clamped) balls. The tribological behaviour of stainless and ball bearing steel were studied under extreme pressure and/or anti-wear lubrication conditions in the presence of sulphur and sulphur containing additives, in order to compare the wear behaviour of the AISI 420 stainless steel with the SAE 52100 steel, taking into account the influence of chromium in both materials. Electron Probe Microanalysis and Glancing Angle X-ray Diffraction combined with Scanning Electron Microscopy have been used to identify the thin films produced on the worn surfaces and to study the micro-structures of the subsurface layers. This investigation shows that the wear behaviour of a combination of materials is worsened by the greater use of the stainless steel in the rotating and stationary balls. The percentage of chromium does have a deleterious effect on the wear behaviour of the AISI 420 stainless steel, where the anti wear and extreme pressure actions were suppressed. These effects were investigated using surface analytical techniques by using the same and mixed specimens.

Key Words: Steels, Additives, Anti-wear, Extreme Pressure and Physical Analysis.

TABLE OF CONTENTS

Page No.

Page No.

Page No.

Page No.

Page No.

LIST OF FIGURES

Page No.

Page No.

Page No.

Page No.

Page No.

Page No.

Page No.

Page No.

Page No.

LIST OF TABLES

CHAPTER 1

INTRODUCTION

1.1 Tribology

Tribology is the science and technology of surfaces, surface topography, friction, lubrication and wear. It elucidates what happens when surfaces in relative motion interact. Also, it helps in the understanding of how lubrication can reduce or prevent wear.

Tribology is "a new interdisplinary approach to subjects previously treated separately (under various categories such as adhesion, lubrication, friction and wear, bearings, abrasion) by several disciplines, e.g. mechanical engineering, chemistry, metallurgy and physics".

1.2 Steels and High Carbon Chrome Steel (SAE 52100)

Steel is an alloy of iron containing carbon (0.05-1.5%) and usually quantities of other elements, such as silicon, manganese, sulphur, phosphorus and nitrogen. Two main types of steel are distinguished; (i) carbon steels, containing mainly iron and carbon, with only small amounts of other elements (silicon, manganese, sulphur, phosphorus and nitrogen); (ii) alloy steels containing, in addition to the carbon steel constituents, certain amounts of nickel, chromium and molybdenum.

Many different steels exist within these two categories depending on the amounts of carbon and other elements present and on the heat-treatment given to the steel.

Carbon steels are classified as (i) mild steel, (0.1-0.2% carbon); (ii) medium carbon steel (0.3-0.4% carbon), and (iii) high carbon steel (above 0.5% carbon).

If the carbon percentage is high, steels tend to be harder, whereas a low percentage gives the steels increased toughness and ductility.

The main function of other elements when added in relatively small amounts to a carbon steel is to change the mechanical properties of the steel. If chromium is added (1.0% or more) to steel, a considerable increase in hardness will be made with some loss in ductility. The increase in hardness is due mainly to the fact that chromium is a carbide stabiliser, and forms hard carbides, such as Cr_7C_3. Most ball bearings are produced from specially manufactured high carbon chrome steel. The use of this steel has improved the performance and life of steel ball bearings by substantially increasing their resistance to fatigue. In this investigation, a high carbon chrome steel (SAE 52100) was used, in which carbon constituted 0.90% to 1.10% and chromium 1.30% to 1.60%.

1.3 Stainless Steel and Martensitic Stainless Steel (AISI 420)

The surface of metals and metallic alloys is often subjected to rusting and corrosion, due to the effects of water, corrosive liquid, and moist air, also gases with which it comes into contact at elevated temperatures increase these effects.

Stainless steels are more resistant to rusting and staining than are plain carbon and lower alloy steels. The "stainlessness" is produced by addition of the element chromium to alloys of iron and carbon. Many of the stainless steels contain one or more alloying elements in addition

to chromium, such as nickel and molybdenum. These can effect the properties of the steel in different ways as regards both corrosion resistance and hardness of the steel.

Chromium may be added in amounts up to 21% and this has a pronounced effect in improving corrosion resistance, due to the formation of protective oxide layers[1]. This oxide layer is extremely thin, and such steels take a very high polish.

The protective layer is essentially chromium III oxide[2] and it is this layer that gives stainless steels good resistance to oxidising environments since the protective layer precludes the possibility of any further oxidation.

The "stainlessness" of stainless steels is primarily a function of their chromium content. The American Iron and Steel Institute (AISI) has chosen 4% chromium as the dividing line between alloy steel and stainless steel.

In 1912, Harry Brearley, Head of the Brown-Firth Research Laboratory in England, found out that a composition of 12.8% chromium and 0.24%, carbon was quite resistant to corrosion. This composition can be used for domestic purposes, such as cutlery.

A comprehensive range of precision balls is manufactured in corrosion resistant steel where a high level of resistance to corrosion or oxidation is required. The stainless steel used in this investigation is martensitic stainless steel, type AISI 420, which has a composition of less than 0.15% of carbon and 12 to 14.00% of chromium.

Most stainless steels and alloys are usually classified into three groups:-

(i) Martensitic steels contain 12 to 17% Cr with 0.1 to 1.0% C. When the carbon content is adequate and the heat treatment conditions are correct, then stainless steels can be very hard.

(ii) Ferritic steels contain 16 to 30% Cr with lower carbon contents than the martensitic steels. These stainless steels have a significantly better "stainlessness" but they cannot be hardened by heat treatment.

(iii) Austenitic steels contain nickel (or manganese) in addition to at least 16-18% Cr. These stainless steels cannot be hardened by heat treatment.

1.4 Characterisation of Wear

Wear can be defined as the progressive loss of substance from the operating surface of a body occurring as a result of relative motion at the surface. Wear arises from many mechanisms, such as adhesion, abrasion, corrosion, erosion and surface fatigue. Any of these mechanisms can operate and cause wear, either singly or in association with the other, in lubricated and unlubricated conditions.

Archard and Hirst[3] recognized two main types of wear, a mild type and a severe type. Mild wear is characterised by high contact resistance, small debris particle size, smooth oxidized wear surfaces and by oxidized wear debris. In mild wear, the surfaces wear away slowly. Severe wear is characterised by low contact resistance, large metallic

debris particles and gross plastic deformation. Severe wear also produces rough and deeply torn surfaces. Machines suffering from rapid severe wear cannot operate in this condition.

Quinn[4] maintains that most of the Burnwell and Strange[5] wear characterizations are special cases of those proposed by Archard and Hirst (mild and severe wear). Nevertheless, one can classify wear in detail as follows:-

1.4:1 Adhesive wear

Adhesive wear can take place where contact of the sliding surfaces increases the friction and interactions of the asperities. This may occur by means of a cold welding of asperity junctions, which then results in adhesive wear. Adhesive wear processes may lead to transfer of the fractured material from one surface to the other. The amount of adhesive transfer is determined by the mechanical properties of the interface, the nature of the surfaces and the ambient conditions. Any oxide or adsorbed film, such as oxygen, water vapour etc., would reduce the probability of an adhesive wear. Also, lubrication is a most effective method of reducing adhesive wear.

1.4:2 Abrasive wear

The form of wear which arises through the penetration and ploughing out of material from a surface by another body is called abrasive wear.

Abrasive wear can be produced when there is a great dissimilarity in hardness between the sliding surfaces. In this situation, the hard asperities of particles of a sliding surface would form grooves in the other softer surface. Industrial machinery suffers from abrasive wear, due to the loose particles between the two sliding surfaces, but it is worth noting that this could be controlled by using hard materials and by excluding all foreign matter from the sliding surfaces.

1.4:3 Corrosive wear

Corrosive wear is a form of chemical reaction of a solid, usually a metal, with some substance in the environment leading to the eventual destruction of the surface. The most commonly observed corrosion is the rusting of iron which is caused by moisture. Corrosion may occur between solid and liquid or gas, also even between solid and solid.

In general, corrosive wear may be classified as a "mild wear". The martensitic steels have good corrosion resistance, especially in the hardened condition. But, even the most highly alloyed stainless steels can suffer corrosion reactions under unfavourable conditions. Corrosion could be diminished by controlling the surrounding atmosphere and moisture.

1.4:4 Surface fatigue wear

Surface fatigue wear is a phenomenon which occurs with surfaces which are in contact and under sliding and rolling motion. This refers to failure of a component under the action of repeated cycles of stress. The high frequency of cyclic loading may lead to the nucleation of sub-

surface cracks which eventually propagate to the surface forming wide-scale fretting or flaking of the surfaces. Also, this would occur rather suddenly without any prior visible signs, after a relatively long life. This kind of wear is commonly found at sliding surfaces of journal roller bearings, cams, ball and roller bearings and gears. It is worth mentioning that the action of a corrosive medium may initiate a fatigue crack. Once a crack has been formed it will spread more rapidly as a result of the corrosive action combined with alternating stress. Surface fatigue could be the basic mechanism of many other types of wear.

1.4:5 Erosive wear

Erosion is a form of wear caused by high velocity impact of particles. Erosive wear may take place due to the impact of solid particles on solid components, for example, nozzles and blades of gas turbines may be subjected to the impact of solid particles in the products of combustion. Also erosive wear may occur due to the repeated impact of a fluid against solid surfaces.

Erosive wear could be minimised or prevented by some form of protective coating, like carbon fibre coating. This coating is quite useful for increasing the erosion resistance of turbine blades.

1.4:6 Fretting wear

Fretting wear is allied to corrosion fatigue and takes place between two tightly fitting surfaces which are subjected to vibrational stresses. In machinery, fretting wear is most commonly encountered with rubbing steel surfaces which become pitted and where copious amounts of debris are formed.

Waterhouse[6] and others have suggested that there are only three mechanisms which can cause fretting corrosion;

(i) The removal of metallic particles by grinding or by the formation of welds at the points of contact followed by tearing.

(ii) The removal of metal particles where the abrasive action is the most effective cause of wear.

(iii) The direct oxidation of the metal and the continuous removal of this oxide layer by the scraping of one surface over the other.

Holliday and Hirst[7] maintain that the important causes of fretting are the first two listed above, that abrasion due to oxide can in some circumstances lead to an extremely mild form of wear, and that the third process, if it occurs, is relatively unimportant.

1.5 Lubrication

Lubrication has been widely investigated by tribologists, from different aspects and is regarded as playing an important role wherever interacting surfaces move relative to each other.

When solid surfaces are in sliding contact both friction and wear occur. Friction is expressed as the resistance to motion encountered during sliding while wear is the resultant loss or destruction of surface material.

Lubrication reduces both friction and wear. The function of a lubricant is (i) to prevent interacting surfaces from coming into direct contact by interposing solid (such as graphite and molybenite), liquid

(such as oils) or gaseous (such as air and helium) substances between the sliding surfaces to facilitate their relative movement, (ii) to provide an easily sheared interfacial film, and (iii) to carry away any heat evolved in lubricated contacts.

Lubrication can be classified as (i) hydrodynamic, (ii) elasto-hydrodynamic and (iii) boundary.

1.5:1 Hydrodynamic lubrication

Hydrodynamic lubrication occurs where the moving surfaces are entirely separated by a thick film of lubricant. The thickness of the film depends upon viscosity, speed and load. This type of lubricant is observed in journal bearings. In hydrodynamic lubrication, friction is due to shearing within the fluid film and wear should be non-existent due to the fluid film which completely separates the two moving components. In fact, the thickness of this fluid film is generally much greater than the total surface roughness of both components (see Figure 1.1a). The minimum film thickness normally exceeds 2×10^{-7} m which is many times thicker than the surface roughness.

The three parameters (viscosity (6), speed (U) and load per unit area (P) are sometimes combined to form the dimensionless bearing-number, C, defined:-

$$C = \frac{\text{viscosity x speed}}{\text{unit load}}$$

By plotting the variation of coefficient of friction versus dimensionless bearing-number, a curve known as the Stribeck Curve is obtained, the various lubrication regimes can then be identified as shown in the diagram (Figure 1.2) and given by Dowson[8].

1.5:2 Elastohydrodynamic lubrication

Elastohydrodynamic lubrication is commonly characterized by a thin film, formed under high loads. In this situation the thin film is subjected to high pressure which leads to a marked increase in the viscosity of the fluid. Before breakdown (when limited metal to metal contact occurs) of this thin film of lubricant, the moving surfaces undergo elastic deformation in the contact zone. However very little wear takes place since the thickness of the film of lubrication is usually just a little greater than the roughness of both surfaces (see Figure 1.1b).

Elastohydrodynamic lubrication occurs in gears, ball and roller bearings, cams and some soft rubber seals. Both the physical properties of the lubricant and the sliding materials have to be known. The elastohydrodynamic analysis has predicted that lubrication films may be 10 or 100 times greater than those estimated by conventional hydrodynamic lubrication theory. For normal engineering contact, the film thickness is of the order 2.5×10^{-8} m to 2.5×10^{-6} m.

1.5:3 Boundary lubrication

Boundary lubrication is defined as a condition of lubrication in which a protective film exists between sliding pairs, but intermittent penetration of this film may take place by the surface asperities under some combination of high load, rough surfaces and small apparent area of contact (8-10) as shown in Figure (1.1c).

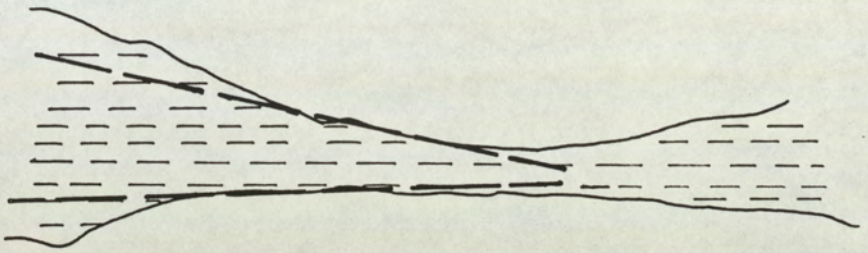

a) Hydrodynamic lubrication

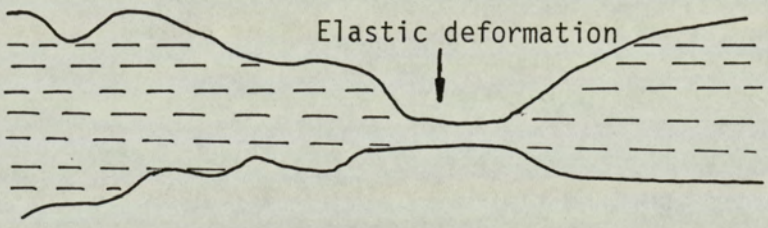

b) Elastohydrodynamic lubrication

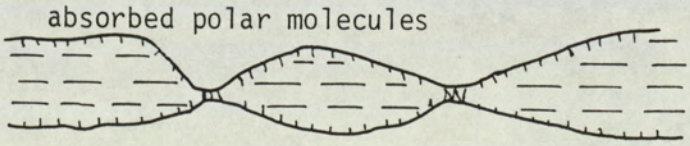

c) Boundary lubrication

Figure 1.1 Schematic diagrams of

(a) Hydrodynamic lubrication

(b) Elasto-hydrodynamic lubrication

and (c) Boundary lubrication.

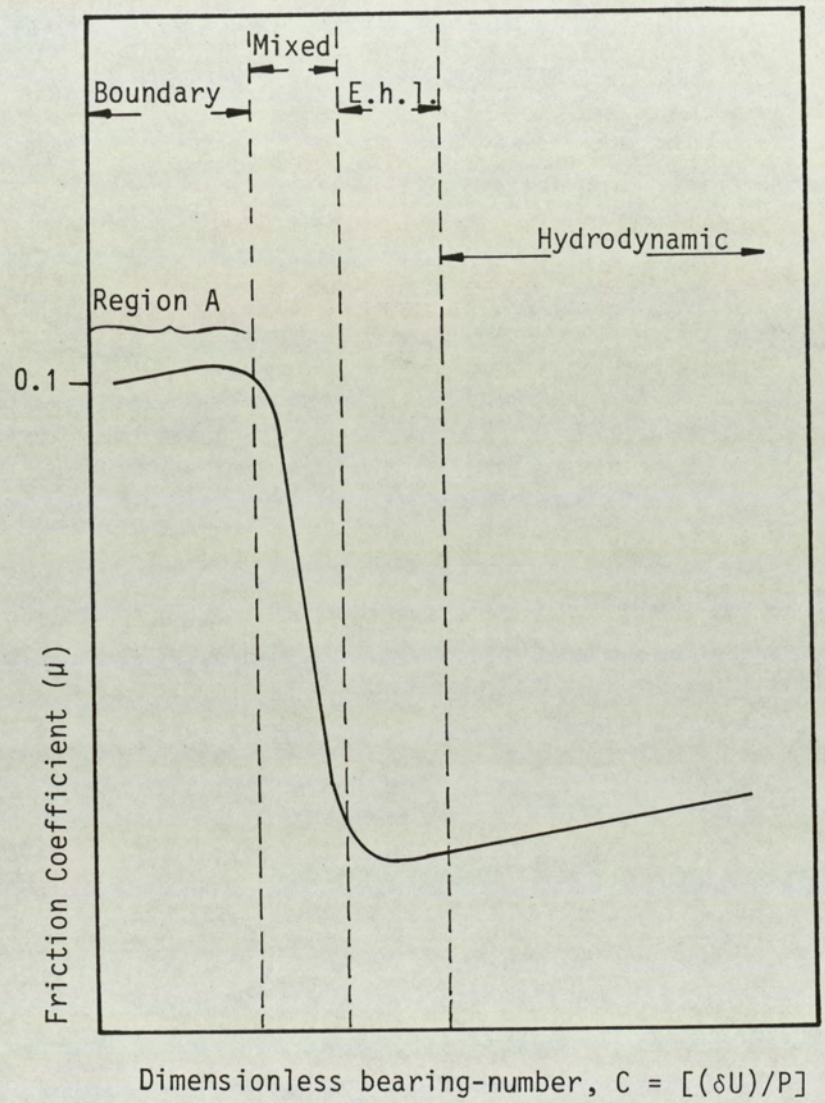

Figure 1.2 Classical Stribeck Curve.

In this type of lubrication, the thickness of the surface film formed by physical and chemical reaction between the used lubricant and the surfaces, is usually regarded as being small in comparison with the total surface roughness of both sliding pairs. Such a kind of lubrication occurs in gears, in rolling contact bearing cages, in journal bearings during starting and stopping, in numerous sliding mechanisms in reciprocating engines, and at the top and bottom of the stroke in the piston pump.

1.6 Additives

A lubricating oil additive can be any material which when added to the mineral oil (usually in small proportions) improves some of the existing properties of that oil or imparts new properties not originally present in it.

1.6:1 Antiwear additives

The antiwear additive is normally most effective under boundary lubrication. Under conditions of boundary lubrication and moderately loaded sliding contacts, it is accepted that an oil film exists between the surfaces but intermittent penetration of this film by surface asperities does occur. The antiwear additive probably functions by reacting with the metal asperities to form films which aid the oil film to reduce intermetallic contact and wear.

1.6:2 Extreme pressure additives

For moderately loaded sliding contacts an elastohydrodynamic lubrication film exists between the sliding surfaces. If pressure increases and viscosity decreases the degree of metallic contact will increase. This results in an increase in both surface and contact temperature with subsequent increases in lubricant temperatures which further reduces viscosity. The overall effect of this is to push the system from elastohydrodynamic lubrication to a mixed or boundary lubrication mode. Further increases in pressure once in the boundary region lead to desorption of the boundary protective molecules from the surface and exposure of metal. Under these conditions extreme pressure lubricants containing S, P or Cl interact with the surface to produce easily sheared films, resulting in very high wear, but preventing welding (seizure).

Bowden and Ridler[11] studied the sliding of one body on another where most of the work done against the frictional force opposing the motion is liberated as heat between the sliding surfaces. This study, also, high-lighted the fact that high temperatures are reached at the points of contact of sliding metals, a significant aspect in understanding the role of lubrication. Bowden and Ridler found in this study that one cause of the breakdown of the lubricant film is the high temperature reached by the contacting sliding surfaces.

As the load and temperature at the contact are increased to a certain level it may not be possible to maintain a film and breakdown will take place accompanied by a dramatic increase in temperature and wear which may lead to welding of the moving surfaces in the absence of additives. To raise the limit, additives have to be added to the

lubricant. Additives can be materials which, when added to the mineral oil, improve the efficiency of that oil and impart new characteristics to it, thereby greatly widening the possibility of protective film formation. The most common additives are sulphur, phosphorous and chlorine. These additives react chemically with the metal surfaces forming a protective[12] chloride, phosphide or sulphide film of low shear strength which keeps the metal surfaces apart - see, for example, Forbes[13]. Davey[14] found that sulphur additives are active in forming an iron sulphide film, in extreme pressure conditions.

Prutton, Turnbull and Dlouhy[15] have also studied the mechanism of action of organic chlorine and sulphur compounds in extreme pressure lubrication. They suggest that possible mechanisms for the reaction of sulphur bearing additives with iron are, direct reaction with the sulphur additive to yield iron sulphide, or the dissociation of sulphur additive to either H_2S or sulphur followed by reaction with iron. They suggested the mechanism of the reaction of organic sulphides with iron may take place by the following formula

$$R_2S_x + Fe \rightarrow FeS + R_2\ S_{x-1}$$

The reaction of iron with organic sulphur compounds has also been studied by Hamilton and Woods[16]. They concluded that the overall reaction of an aliphatic disulphide can be presented as follows:-

$$RSSR + 2Fe\ (\text{or } Fe^{++} + 4e) \rightarrow 2FeS + \text{hydrocarbon (RR?)}$$

Davey and Edwards[17] suggested the following mechanism operates in the extreme pressure condition of some disulphides:

$$R - S - S - R + Fe \rightarrow Fe{:}S \begin{matrix} \diagup R \\ \diagdown S - R \end{matrix}$$

The above-mentioned equation represents an adsorbed layer formed under mild loading conditions. The formation of iron mercaptide is represented by the following equation

$$Fe{:}S \begin{matrix} \diagup R \\ \diagdown S - R \end{matrix} \rightarrow Fe\ (S - R)_2$$

This equation represents the lubrication in conditions approaching extreme pressure. As loading is increased, the mercaptide film would break down, under very severe loading, forming ferrous sulphide and organic sulphide, as shown below:

$$Fe\ (S - R)_2 \rightarrow FeS + R - S - R$$

Godfrey[18] found, from SAE extreme pressure tests carried out with mineral oil containing a sulphur additive, that the major compound was Fe_3O_4 or similar to a spinel. Minor constituents were FeS, FeO, and an "iron carbide".

Greenhill[19] found that FeS films were not very good lubricants on their own. Sakurai, Ikeda and Okabe[20] reported that iron sulphide films appeared to absorb polar compounds more actively than iron oxide where the following possible mechanism may take place:

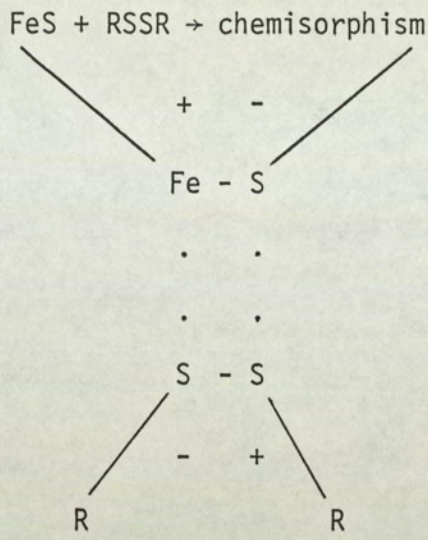

Interaction of chlorine additives with iron have been studied by many researchers. Prutton, Turnbull, and Dlouhy[15] deduced the following mechanism under mild or slowly applied loads, for the interaction of organic chlorine compounds with iron:

$$R_yCl_x + Fe \rightarrow FeCl_2 + RCl_2 + R_yCl_{x-2}$$

They summarized their work as follows:- "In general, iron sulphide films from active sulphur additives form much more rapidly than ferrous chloride films from active chlorine additives at temperatures above 200°C". Investigations on the joint action of active sulphur and active chlorine additives were also made. These investigations have revealed that active chlorine and sulphur additives in extreme pressure conditions exhibited high load-carrying capacity compared with their static corrosion process[21]. Also, it has been found that ferrous chloride is formed in large amounts, much more than would be formed by the action of the chlorine additive by itself[15].

Work has been particularly devoted to studying the mechanisms of action of some other additives in extreme pressure conditions, such as zinc dialkyl dithiophosphate and tricresylphosphate. Loeser, Wiquist and Twiss[22-25] studied the action of zinc dithiophosphate. They found that the mechanism of additive interaction seemed to be "related to chemical reactions of additive decomposition products with the metal surfaces to form tightly-bound solid films which reduce damage under extreme pressure conditions". In 1959 Bennett[26] also studied a surface effect associated with lubricants containing zinc dialkyl dithiophosphate (ZDP). He suggested that ZDP can increase the small-scale roughnesses due to the reaction of ZDP decomposition products with the metal surface.

Allum and Forbes[27] in their investigation involving metal dialkyl-dithiophosphates have shown that the nature of the alkyl group has a very small effect on both extreme pressure and anti wear properties. The anti wear region, is normally defined from the wear rate versus load curve for a standard Four ball machine test (this is discussed in detail in Chapter 2) and is a regime where measured wear scars are of similar diameters to those given by the Hertze line which represents the diameter of the areas under static loading condition.

Coy and Quinn[28] concluded that the zinc dithiophosphates are essentially anti wear additives as assessed by the four-ball machine.

Regarding the mechanism of the additive tricresyl phosphate (TCP), Godfrey[29] showed that when a lubricant containing TCP was used in experiments involving steel on steel, the iron phosphates ($Fe\ PO_4$ and $Fe\ PO_4\ 2H_2O$) appeared in the lubricated film.

1.7 The Use of Physical Analytical Techniques in Lubrication Research

Physical analytical techniques have been widely used in tribological research. In 1962 Godfrey[18] used several methods of analysis to study the chemical changes in steel surfaces during extreme pressure lubrication. He analysed the specimens by X-ray diffraction, electron diffraction, emission spectrography, proton scattering, chemical spot tests and volumetric analysis. He concluded that iron oxides, carbide and silicon in addition to iron sulphide, were present in the surface film. Using proton scattering, Godfrey measured the amount of oxygen in the worn surfaces. Also, he found that "Iron sulphides are a minor constituent, but necessary for the high load-carrying capacity".

Allum and Forbes[30] used electron probe microanalysis to examine the wear scars obtained with a sulphur additive in 4-ball extreme pressure tests. They found that the quantity of sulphur increases and the quantity of oxygen decreases with the increasing extreme pressure activity. Also, they found that the distribution of sulphur in the wear scar was irregular and was present to a depth of several microns.

Analyses of worn surfaces have been carried out by scanning electron microscopy. Such analyses have been conducted by Cziettos and Kirnchke[31], Coy and Quinn[32] and Brainard and Buckley[33].

X-ray diffraction techniques have been used to investigate elements and compounds present in the surface film or debris. An unconventional glancing-angle X-ray diffraction film technique was used, following the approach of Isherwood and Quinn[34] and Coy and Quinn[28,32].

1.8 Present Work

Considerable work has been done in studying the mechanism of extreme pressure additives, mainly on metallic materials, such as EN31 steel. Also many investigations have been carried out studying the worn surfaces by using various physical techniques. The most relevant of this work was carried out by Coy and Quinn[28,32].

The main objectives of the present work are:

(i) To study the wear behaviour of stainless steel (martensitic AISI 420) under extreme pressure conditions, and to compare it with high carbon chrome steel (SAE 52100), taking into account the influence of chromium, in particular, throughout this investigation.

(ii) To examine the combination of both materials in the wear tests conducted under similar anti wear and extreme pressure conditions, including the dissimilarity of those materials used in the wear tests.

(iii) To investigate the influence of both anti wear and extreme pressure conditions on the microstructures of the stationary worn surfaces of both materials. This is an attempt to clarify the metallurgical aspect of the wear scar subsurface, in respect of which little attention has been paid by previous investigations.

In this work three sulphur additives, Sulphur (S), Dibenzyl Dissulphide (DBDS) and Diphenyl Disulphide (DPDS), in addition to Risella 32 were used in wear tests carried out by the four-ball machine. Each additive was blended in Risella 32 and used in wear tests conducted with two materials (i) high carbon chrome steel (SAE 52100); (ii) Martensitic stainless steel (AISI 420).

Afterwards, three physical techniques were applied to analyse the surface films in the wear scars produced under anti wear and extreme pressure conditions. Electron probe microanalysis (EPMA) was used to investigate the distribution and concentration of elements present at the surface films. Scanning Electron Microscopy (SEM) was used to identify elements present at the surface films and the topography of the wear scars. Also, microstructures of both materials were studied by SEM in locations just under the scar and in the bulk of the specimens. These investigations were associated with the X-ray diffraction analysis.

CHAPTER 2

2. EXPERIMENTAL DETAILS

2.1 The Four-Ball Machine

The four-ball machine was first employed by Boerlage[35] in 1933, for testing of extreme pressure lubricants. It is now a standard tribology test rig, widely used as a lubrication bench tester. It is also used as a wear tester, by measuring the diameter of the wear scar formed on the stationary balls, at both light and heavy applied loads. The machine is also useful in studying the thicknesses of films of lubricants formed under boundary and extreme pressure lubrication conditions. The main advantages of this apparatus are:

a) Its ease of use and ruggedness.

b) A high constant load is obtainable using a convenient set of weights.

c) It can be used to evaluate wearing, seizing and welding over a considerable range of applied loads.

In spite of using the crude method of increasing the applied load in steps until seizure occurs, the seizure loads of lubricants in the presence of different additives may, nevertheless, be readily determined.

The principle of the wear test in this machine is based on the sliding of a metallic ball on three stationary metallic balls. A drive shaft is used which is free to rotate about a vertical axis, at a constant speed of 1500 r.p.m. A vertical load is applied to the revolving ball, by exerting pressure on the underlying stationary balls by means of

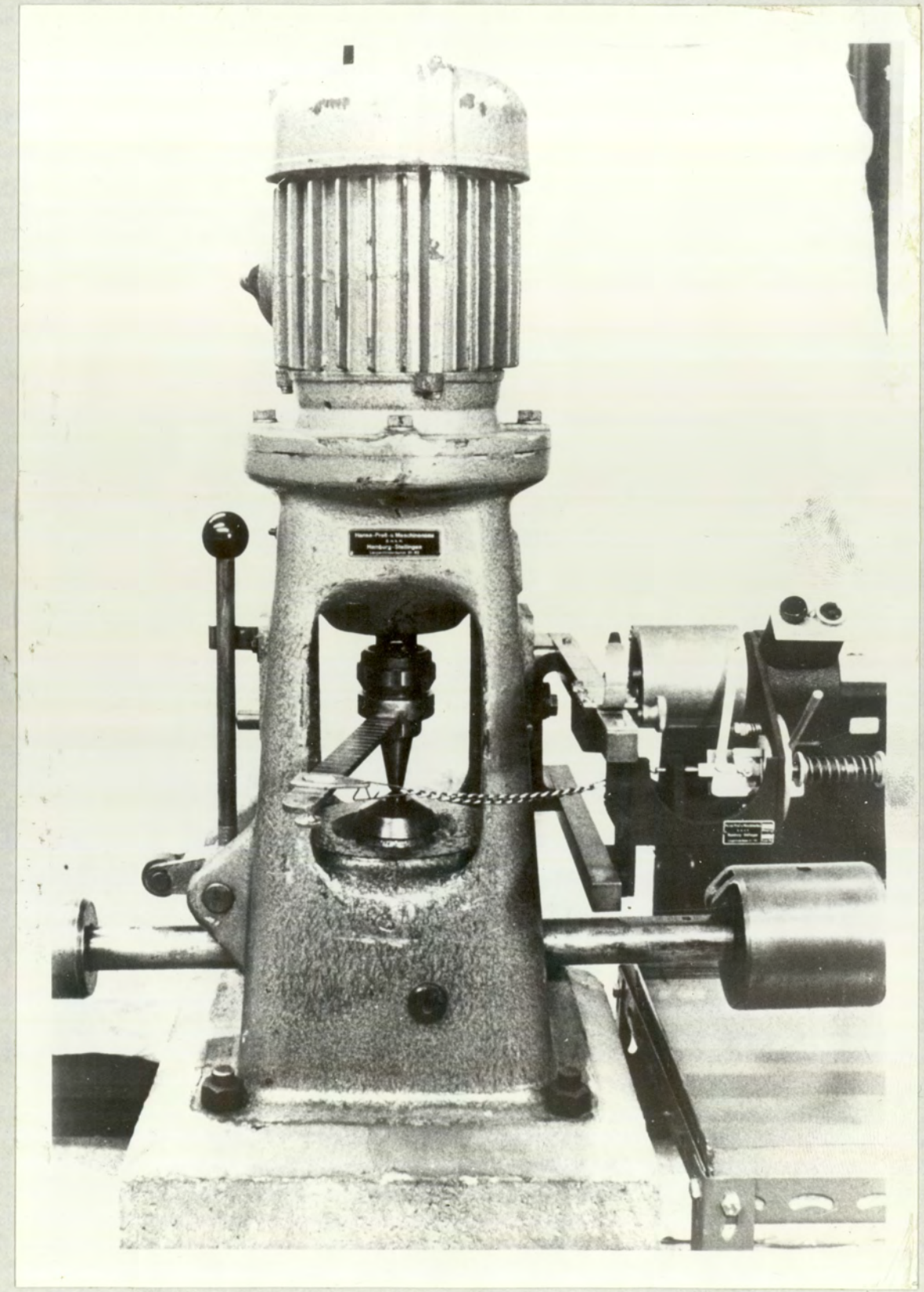

Figure 2.1 Four-ball machine.

weights on a suitable load arm. This load arm is initially balanced so as to exert zero load; the applied load can be increased by sliding a weight along the load arm, typically in steps of 100 or 200 N.

2.1:1 Four-ball geometry

The wear test in the four-ball machine was first associated with the four-ball geometry, in which the four balls form an equilateral tetrahedron. The three lower balls form a three point cradle contact, so that the forth rotating ball can slide on them.

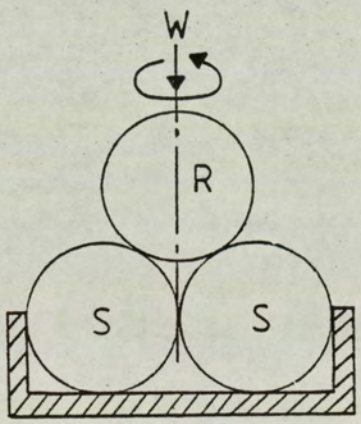

Rotating ball (R)

Stationary ball (S)

Figure 2.2 Four-ball geometry.

2.1:2 A one-ball on three rollers geometry

Clearly, wear tests can be carried out by using a four-ball geometry. A one-ball on three rollers geometry is, however, more convenient in practice if subsequent examination of the specimen is to be carried out in the electron probe microanalyser.

Difficulties arise when using 0.5 in. diameter balls since they are inconvenient in size and the curvature of the surface poses focussing problems. Moreover, rollers are easier to mount, so as to make accurate taper sections through wear scar.

In this geometry the rollers are placed in three slots in a holder, which has to be locked solidly by a circular ring. The holder must be designed in such a way that the flat faces of the rollers are orientated such that the top rotating ball can rest on them and slide at the centres of their faces, as shown in Fig. (2.3).

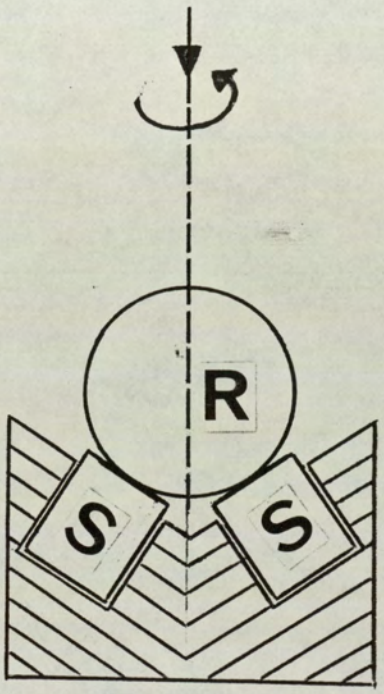

Rotating ball (R)

Stationary roller (S)

Figure 2.3 A one-ball on three rollers geometry used as a modification of the four-ball machine.

2.2 The Wear Tests

The top metallic ball is clamped in the drive shaft. The top ball is spun on three balls or rollers, tighly locked together in a holder containing the lubricant to be tested. Wear tests are conducted over a range of loads, usually applied from 100 to 1000 N in steps of 100 N and from 1000 N in steps of 200 N.

After the wear test was completed, a small cap could be seen to be worn off each of the three stationary balls or rollers producing a circular wear scar on them. Such wear scar diameters were measured using a travelling microscope and a typical log-log plot of the mean wear scar diameter (mm) as a function of increasing applied load (N) is shown in Figure 2.4. Note that three distinct wear regions can be recognized:

The region AB is called the anti wear (A.W.) region. The wear scars diameter in this region are slightly larger than those given by the Hertz line, which represents the diameter of the contact area under static loading conditions (elastic deformation).

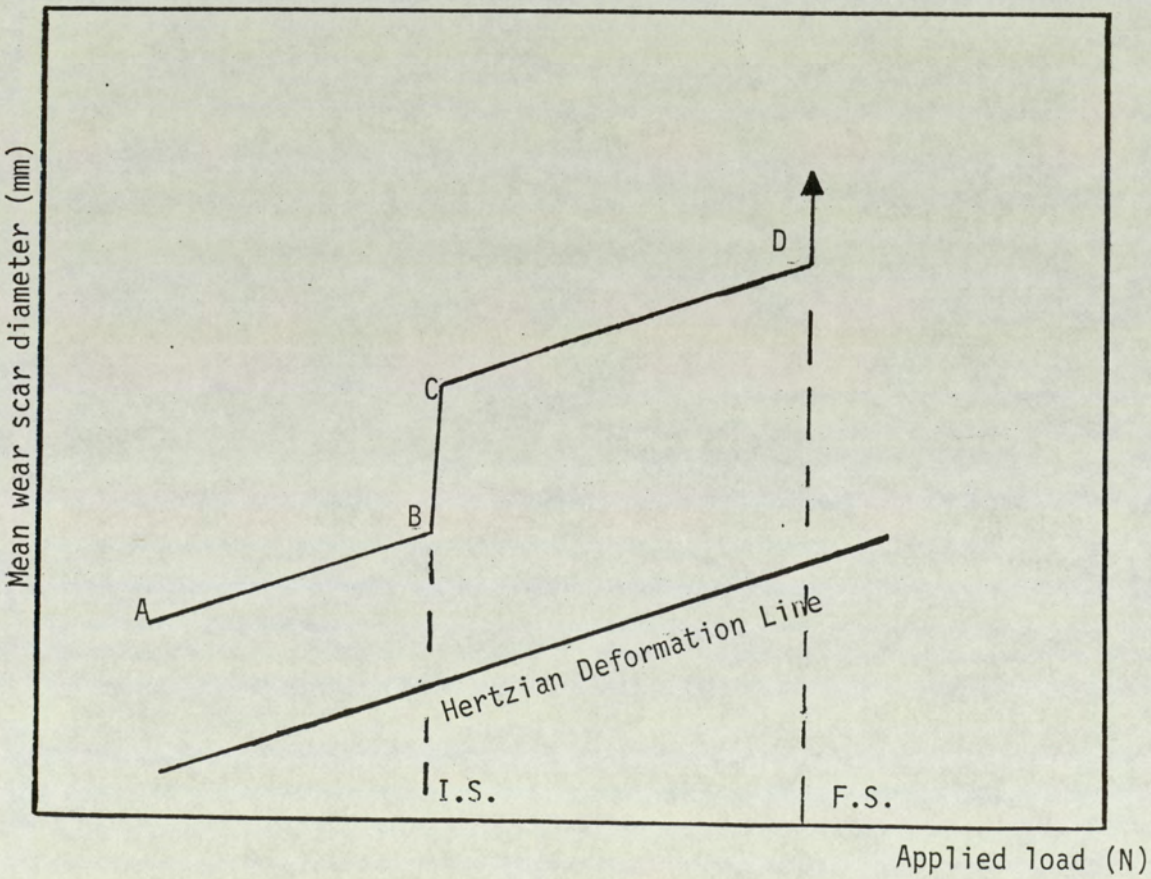

Figure 2.4 A typical wear behaviour of ball bearings in a "shell four-ball" test rig.

The region BC is called the initial seizure (I.S.) region. In this region a sudden increase in the measured wear scar diameter is noticed, due to the rapid increase in wear. This phenomenon is recognized practically by a squeaky sound of the sliding parts and could be caused by a momentary breakdown of the lubricating film which separates the two surfaces involved.

The region CD is called the extreme pressure (E.P.) region. It is distinguished by a high load and the high friction involved in the wear process. This results in producing rough and large wear scars on the three stationary bodies. As the applied loads are increased, the bulk lubricant tends to break down due to the very high pressure imposed on the contact areas.

The major part of the A.W. region is in the boundary lubrication regime and the low wear in this region is due to the adsorption of long chain hydrocarbon molecules on opposing surfaces. As pressure increases temperature at the contact will increase due to the greater dissipation of energy, and boundary molecules will desorb leading to asperity contact and to initial seizure. At these high temperatures/pressures the E P additives break down and release free sulphur which interacts with the metal surface to form an easily sheared film and hence produce the E P region. This continues until the rate of production of FeS etc. is less than the rate of removal. Then true metal-metal contact occurs and this leads to final seizure (F.S.). In the (F.S.) the metal between the rubbing surfaces (the four balls) welds together.

2.3 The Hertzian Diameters

Hertzian diameters can be plotted for both four-ball and one-ball on three rollers geometries in form of a graph of mean wear scar diameter (mm) as a function of applied load (N). The following equation was used to calculate the Hertzian diameters[36]

$$D = 2 \times 1.109 \left[\frac{1}{2} \left\{ \frac{NR_1R_2}{R_1+R_2} \left(\frac{E_1+E_2}{E_1 \times E_2} \right) \right\} \right]^{\frac{1}{3}} \qquad \ldots (1)$$

where N = normal load = 0.408P

P = applied load on the four-ball machine

R_1 = radius of the rotating body

R_2 = radius of the stationary body

E_1 = Young Modulus of the rotating body

E_2 = Young Modulus of the stationary body.

In fact, equation (1) is applied to compute the diameter of the area of contact between two spherical bodies where their radii are different and their elastic properties are not the same.

As $E_1 = E_2 = E = 2.125 \times 10^4$ kg/mm^2[37]

$R_1 = R_2 = R = 6.35$ mm therefore equation (1) can be written as follows:

$$\boxed{D_{Ball} = 2 \times 1.109 \left(\frac{NR}{2E}\right)^{\frac{1}{3}}} \qquad \ldots (2)$$

When $R_2 = \infty$, which is the case where the upper ball is placed on a flat body, equation (1) takes the form

$$D_{Roller} = 2 \times 1.109 \left(\frac{NR_1}{E}\right)^{\frac{1}{3}} \quad \ldots (E_1 = E_2 = E) \qquad \ldots (3)$$

Using the above-mentioned values the Hertzian diameters are:

$$D_{Ball} = 8.73 \times 10^{-1}\ p^{\frac{1}{3}} \qquad \ldots (4)$$

$$D_{(SAE\ 52100\ steel\ roller)} = 11.00 \times 10^{-2}\ p^{\frac{1}{3}} \qquad \ldots (5)$$

2.4 Cleaning and Experimental Wear Procedures

All removable parts of the four-ball machine, balls and rollers were carefully washed in a cleaning liquid (SPB2) and then cleaned by a vapour-bath. After cooling to room temperature, they were ready for use.

The top ball was put in a cup-shaped recess in the end face of the drive shaft. Three clean balls or rollers were clamped in the holder. The lubricant to be tested, was poured in the cup of the holder. A known load was applied.

Each test was performed for a one minute run only. After each series of wear tests, the removable parts were cleaned and prepared for the next wear test. Worn balls or rollers were cleaned and stored for subsequent physical analysis.

2.5 Material

The objectives of the study were to examine the mechanisms of the E P additive interaction with steels of two different chromium

compositions. The commercial additives DBDS and DPDS were chosen since they had been used in previous investigation of this type (Coy and Quinn[28]) and were readily available. The E P action of the additives is thought to be strongly associated with the release of free sulphur, hence elemental sulphur was included in the investigation in order to test this hypothesis. Chromium content of steel is similarly thought to influence A W and E P behaviour and hence material was chosen to give a range of Cr contents. The choice was, however, severely limited by commercial availability of specimens in their received forms i.e. balls and rollers, the SAE 52100 steel and AISI 420 stainless steel.

2.5:1 Martensitic stainless steel balls (AISI 420)

420 AISI stainless steel balls, supplied by Dick Bearings Limited, were used in the wear tests. The chemical composition of the above-mentioned balls was:

Element	Percentage
C	0.15 max
Mn	1.00 max
P	0.04 max
S	0.30 max
Si	1.00 max
Cr	12.00-14.00
Fe	Balance

Table 2.1 Chemical composition of martensitic stainless steel AISI 420. The balls were 0.5 (12.7 mm) diameter.

This material showed a minimum hardness of 617 HV.

2.5:2 High carbon chrome steel (SAE 52100) balls and roller

These balls and rollers were also supplied by Dick Bearing Limited. They had the following composition:

Element	Percentage
Carbon	0.90-1.10%
Silicon	0.10-0.35%
Manganese	0.30-0.50%
Chromium	1.30-1.60%
Nickel	0.35% max
Molybdenum	0.8% max
Sulphur	0.40% max
Phosphorous	0.40% max
Iron	Balance

Table 2.2 Chemical composition of the high carbon chrome steel (SAE 52100)

This material showed a minimum hardness of 800 HV.

All balls were 0.5 in. (12.7 mm) diameter and all rollers were $\frac{1}{4}$ $\frac{1}{4}$ in. (6.35 mm) x in. (6.35 mm)

2.6 Lubricant and Additives

2.6:1 Lubricant: Risella 32 (R32)

The base oil used throughout the experiments was Risella 32 (R32), obtained from Shell Research Limited. This oil has been specially refined to reduce the level of sulphur compounds.

The following are the properties of R32:

Appearance	Clear
Colour (ASTM)	0.0
Specific gravity at $60^{o}F$	0.881
Dynamic viscosity ($\times 10^{-3}$ Nsm^{-2}) at $30^{o}C$	62.37 at 100° 5.09
Pressure coefficient ($\times 10^{-9}$ $m^{2}N^{-1}$)	28.50 at 100° 18.5
Viscosity index	89
Neutralisation values (mg KOH/gm)	<0.05
Pour point (°F)	-20
Sulphur content	<0.01
Aromatic content (% wt)	7.53

Table 2.3 Properties of Risella 32 (SPL 382/75)

2.6:2 Sulphur additives

Elemental sulphur dissolved in oil has been used as a chemically reactive additive for many years. About 2% of sulphur in oil gives the highest load-carrying capacity of any soluble oil blend, subject to the

extreme pressure lubrication. However, the high rates of wear and deleterious effects of the sulphur on the oil and metal are usually intolerable at this concentration.

For this reason, 0.25% by weight of sulphur was dissolved, by heating, in the mineral oil R32. This lubricant was used in wear tests which were carried out using the four-ball machine, with high carbon (SAE 52100) steel balls and rollers, and also with martensitic stainless steel (AISI 420) balls.

Dibenzyl Disulphide (DBDS) and Diphenyl Disulphide (DPDS) were also used as additives. The chemical structure and other properties of the additives are given below.

Dibenzyl Disulphide (DBDS) $C_{14}H_{14}S_2$ Structure

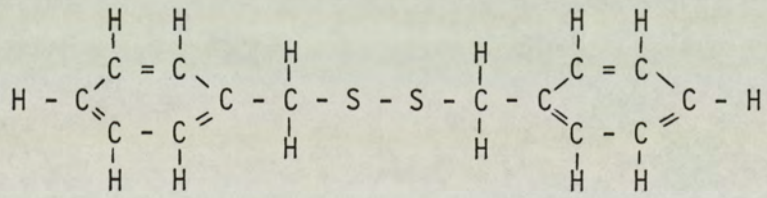

This compound has a molecular weight of 246.4, and is supplied by Shell Research Ltd. 1.00% by weight of DBDS was used at a concentration of about 0.25% weight sulphur.

Diphenyl Disulphide (DPDS), $C_{12}H_{10}S_2$, Structure

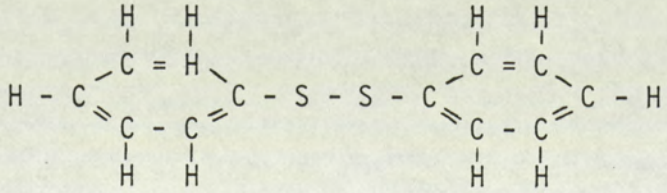

This compound has a molecular weight of 218.3, and is also supplied by Shell Research Ltd. 0.886% by weight of DPDS was used at a concentration of 0.25% weight of sulphur.

CHAPTER 3

RESULTS OBTAINED WITH THE FOUR-BALL MACHINE

3.1 The Four-Ball Machine Tests

Wear tests were carried out on two steels (high carbon chrome steel, SAE 52100, and martensitic stainless steel (AISI 420), both mentioned in Section 2.4). Four combinations of materials were used in these tests, namely:-

(1) Rotating high carbon chrome steel ball (SAE 52100) on three similar stationary steel balls.

(2) Rotating high carbon chrome steel ball (SAE 52100) on three stationary martensitic stainless steel balls (AISI 420).

(3) Rotating martensitic stainless steel ball (AISI 420) on three similar stationary stainless steel balls.

(4) Rotating martensitic stainless steel balls (AISI 420) on three stationary high carbon chrome steel balls (SAE 52100).

The above-mentioned wear tests were carried out with the lubricant Risella 32. The wear tests were then repeated with a further three lubricants, in which three different kinds of sulphur additives were blended in with Risella 32. Each wear test was run for one minute. Several wear tests were conducted with the lubricant Risella 32 (mentioned in Section 2.5) with material combination Number 1. The wear tests were carried out at increasing applied loads, until the final seizure had taken place. The wear tests were then repeated with the other three material combinations mentioned above.

In a similar way, the wear tests were then repeated with the three additive lubricants (S, DBDS and DPDS).

The tribological behaviour of the high carbon steel balls (ASE 52100) and martensitic stainless steel balls (AISI 420) will now be described in terms of the four material combinations.

One experiment was conducted at each load, but the measured wear scar diameters were the result of two readings on each of the three balls i.e. the mean of 6 readings, which should reduce errors due to material or other variations.

3.2 Wear Results Using the Risella Lubricant

Figures 3.1, 3.2, 3.3 and 3.4 show that the final seizure load occured at 1200 N for all, material combinations and R32 has no effect on the final seizure load due to the material differences. The wear scar diameters are much larger than the corresponding Hertzian diameters (see Figure 3.6).

When the three stationary high carbon steel balls (SAE 52100) were replaced by three similar stationary steel rollers, the wear behaviour (Figure 3.5) was similar to that shown in Figure 3.4 where the final seizure load occured at 1000 N.

3.3 Wear Results Using Lubricant R32 Containing Sulphur Additive

In order to investigate the effect of additives, sulphur (0.25% by weight) was blended in with R32 and used in further wear tests. These wear tests were carried out on the following cases of rotation.

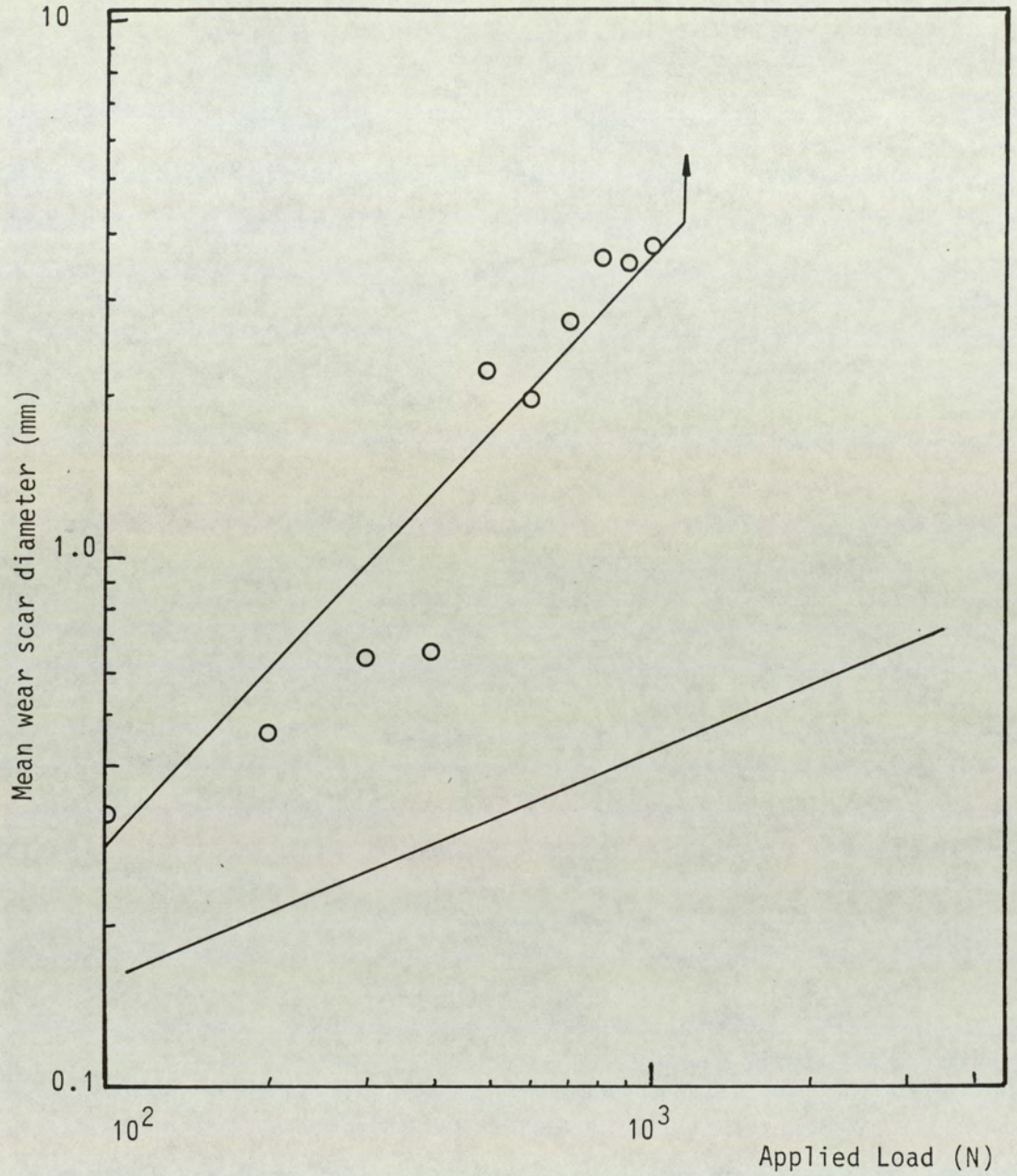

Fig. 3.1 Experimentally measured mean wear scar diameter (mm) as a function of increasing applied load (N).

Lubricant: R32

SAE 52100 steel run on similar stationary steel balls

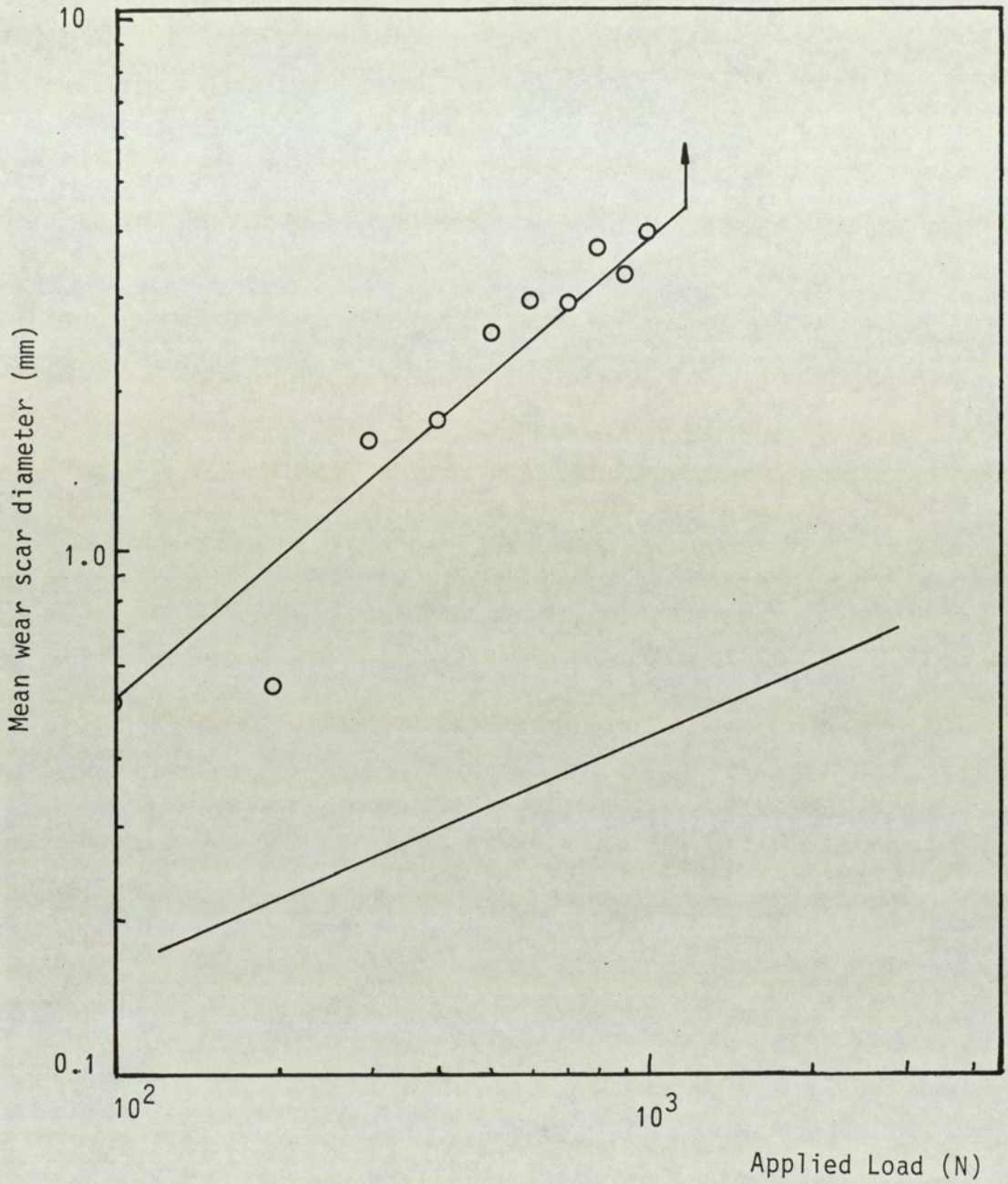

Figure 3.2 Experimentally measured mean wear scar diameter (mm) as a function of applied load (N).
Lubricant: R32
SAE 5200 steel run on AISI 420 stationary stainless steel balls.

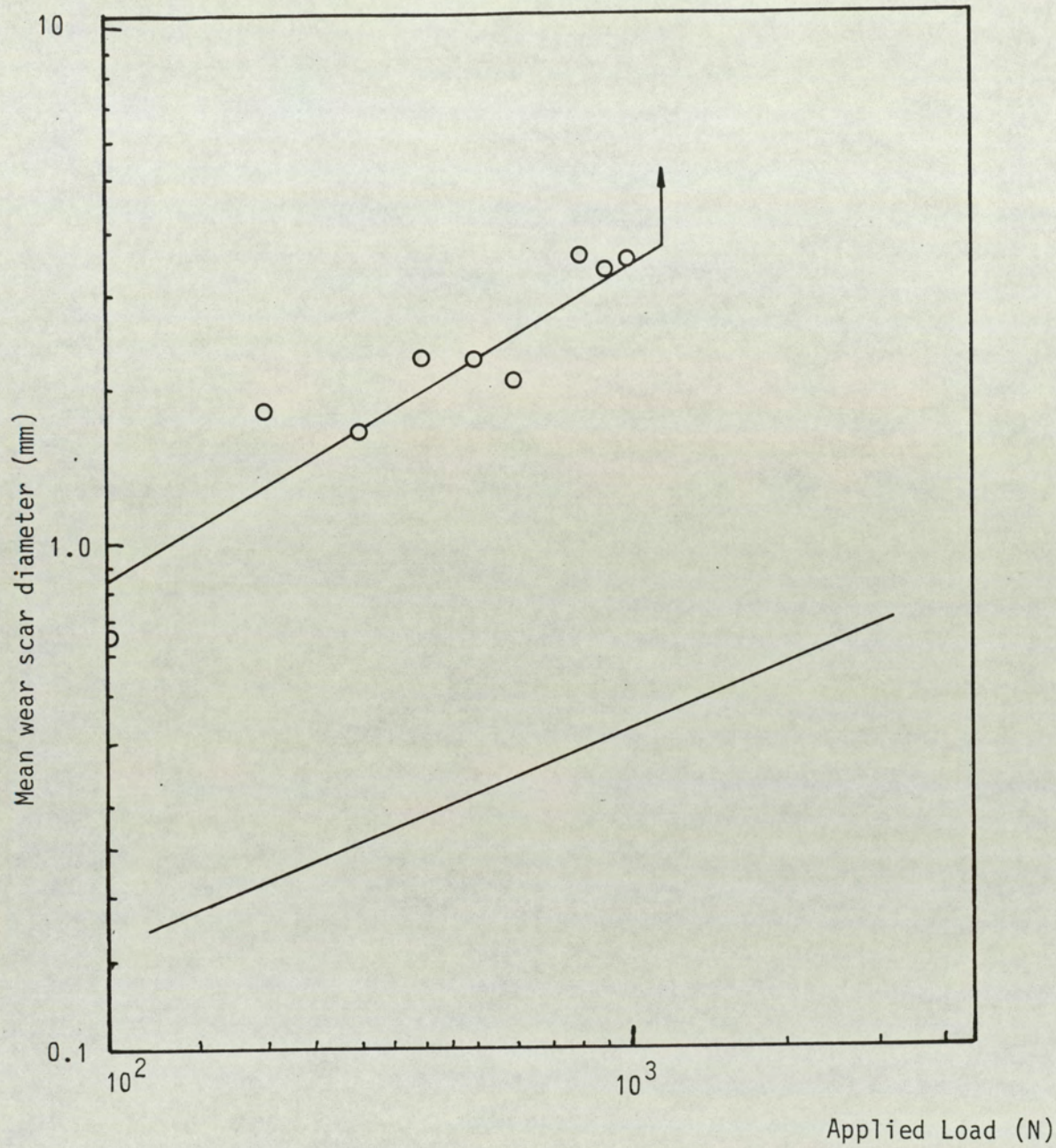

Figure 3.3 Experimentally measured mean wear scar diameter (mm) as a function of applied load (N).

Lubricant: R32

AISI 420 stainless steel run on similar stainless steel balls.

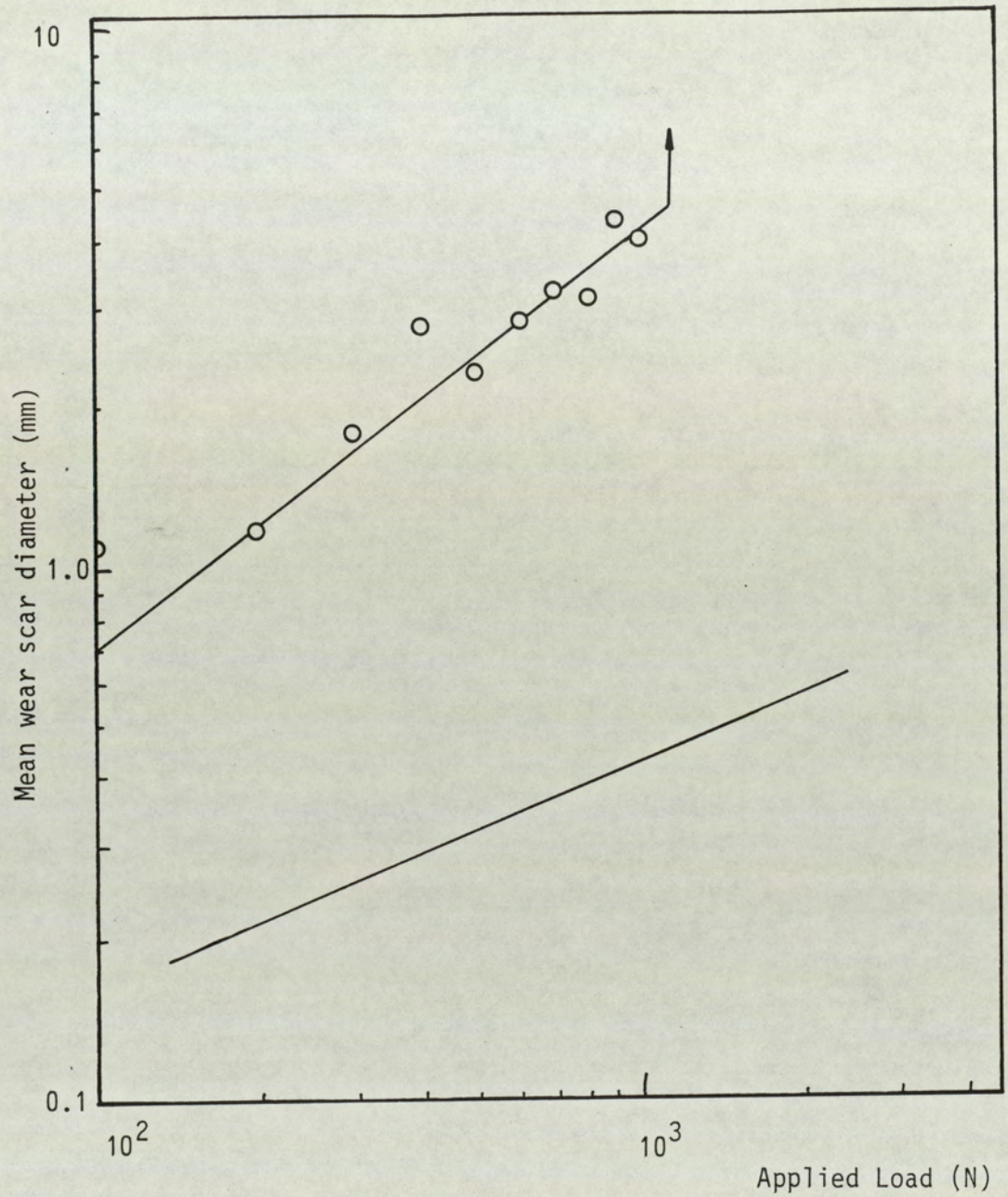

Figure 3.4 Experimentally measured mean wear scar diameter (mm) as a function of applied load (N).

Lubricant: R32

AISI 420 stainless steel run on SAE 52100 steel balls.

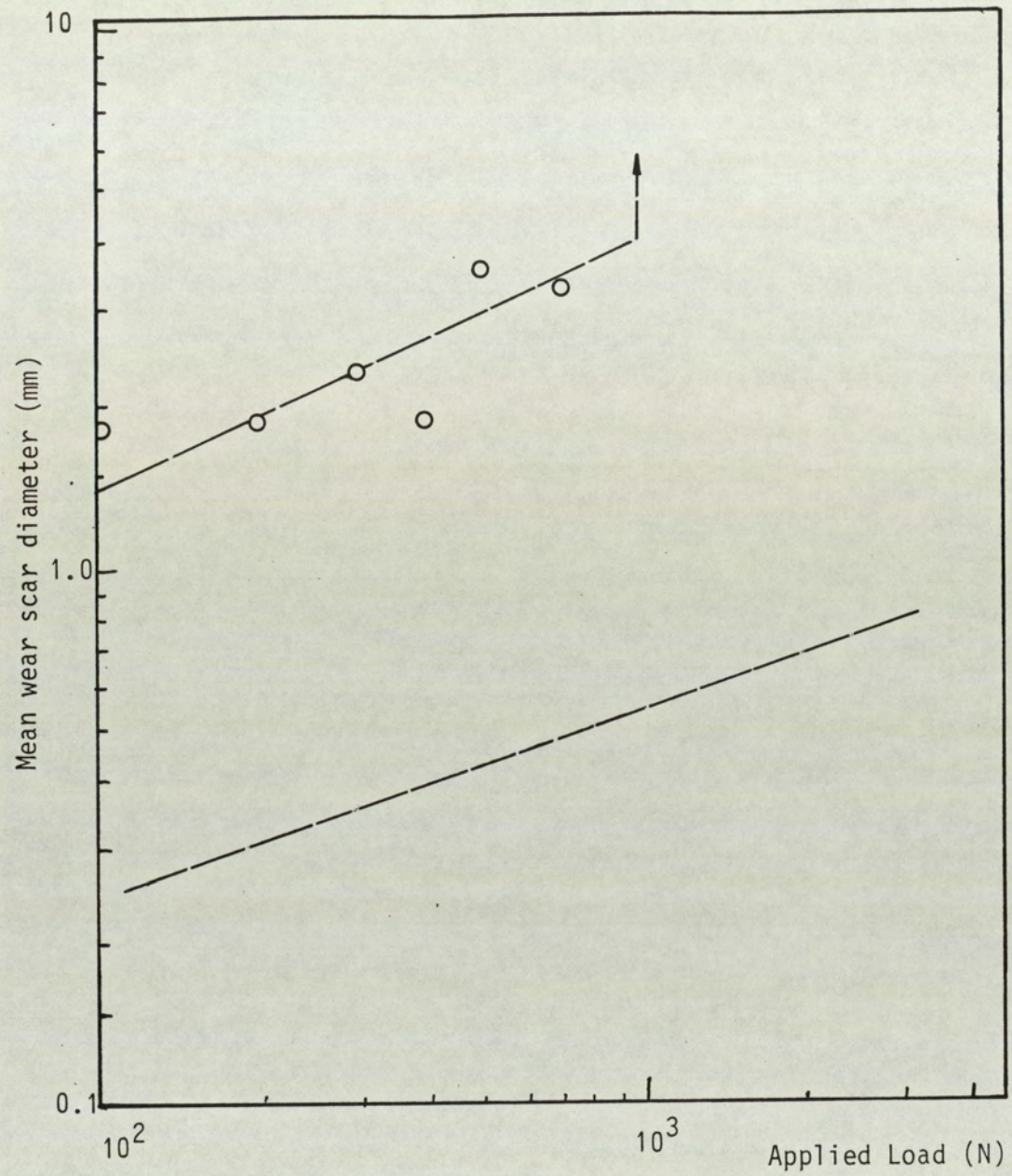

Figure 3.5 Experimentally measured mean wear scar diameter (mm) as a function of applied load (N).

Lubricant: R32

AISI stainless steel run on SAE 52100 steel rollers.

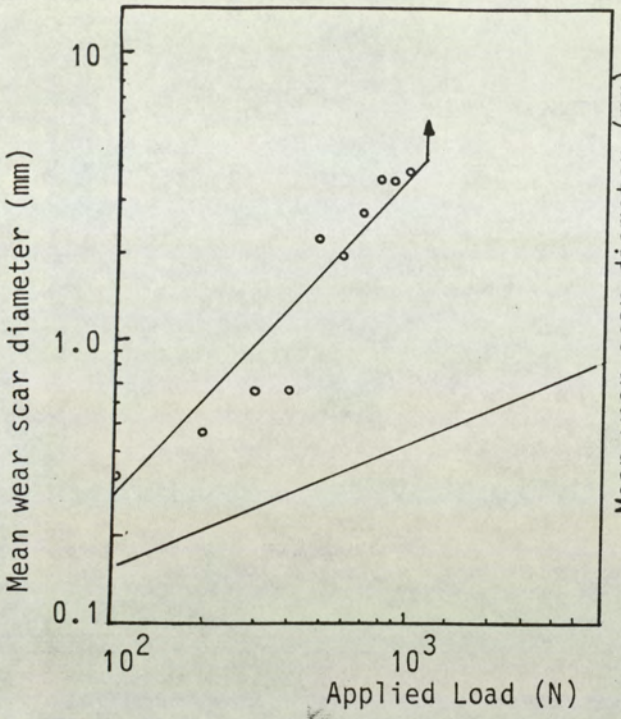

SAE 52100 steel run on similar stationary steel balls.

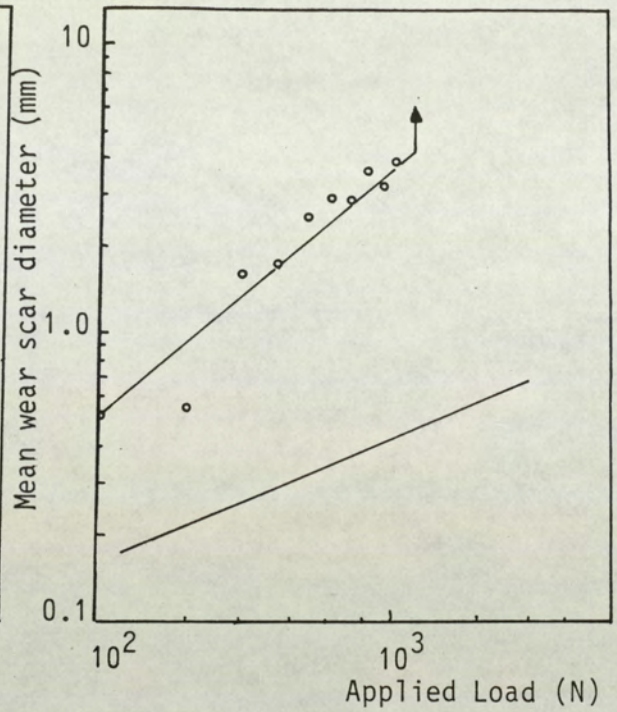

SAE steel run on AISI 420 stationary stainless steel balls.

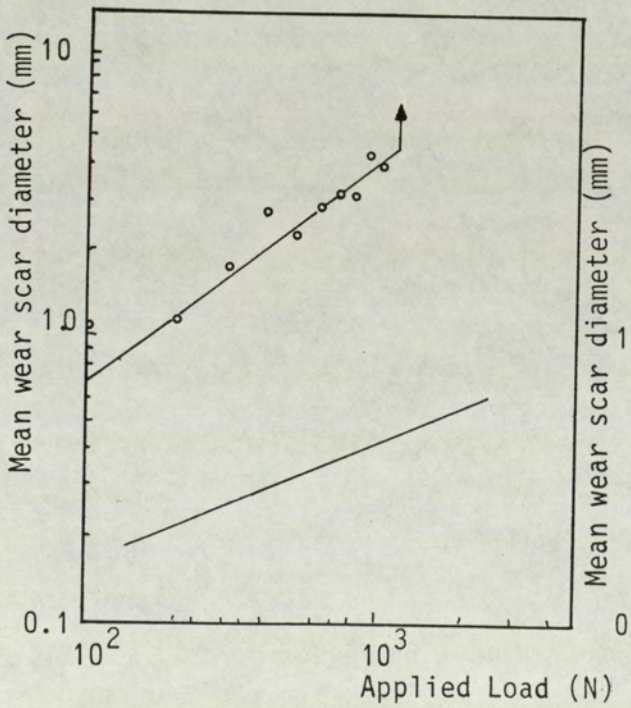

AISI 420 stainless steel run on SAE 52100 steel balls.

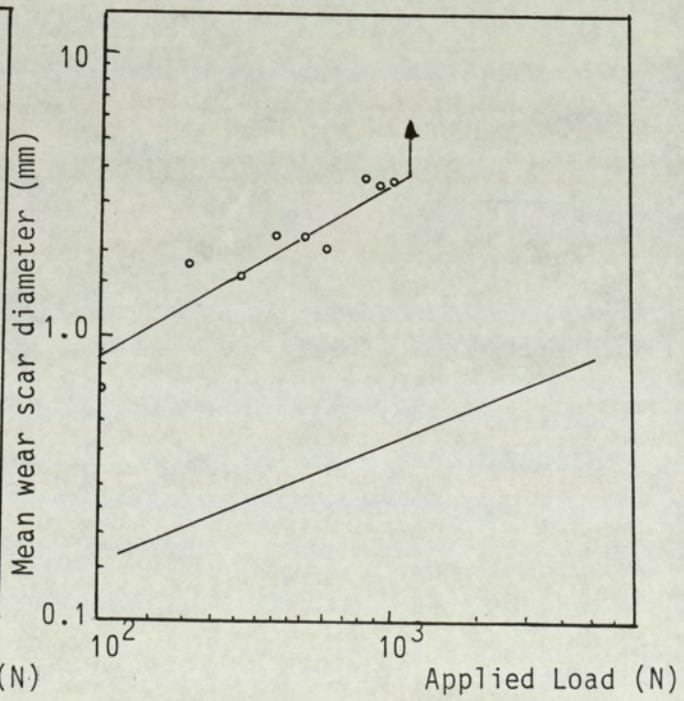

AISI 420 stainless steel run on similar stainless steel balls.

Figure 3.6 Experimentally measured mean wear scar diameters (mm) as a function of applied load (N).

Lubricant: R32

3.3:1 Rotating steel ball (SAE 52100) on three similar stationary balls

Figure 3.7 shows that the initial and final seizures occured at 400 and 4000 N, respectively. The AW region extended between 100 and 400 N, followed by a transition in the mean wear scar diameters which took place between 400 and 600 N. In the antiwear region the mean wear scar diameters varied between 0.35 and 0.5 mm and were slightly larger than the corresponding Hertzian diameters.

3.3:2 Rotating steel ball (SAE 52100) on three stationary stainless steel (AISI balls)

Figure 3.8 shows that the wear behaviour with sulphur was of a different character from that with the 52100 steel running against itself. The initial and final seizure load occurred at 600 and 2000 N, respectively. The AW region extends between 100 and 600 N showing a good AW action. The transition to the EP region appeared between 600 and 800 N. Also Figure 3.8 shows that the mean wear scar diameters in the EP were spread around the EP line and distributed far from those of the corresponding Hertzian diameters. This indicates that wear on the three stationary stainless steel balls had increased with a corresponding reduction in the EP action, due probably to the high chromium concentration in the martensitic stainless steel.

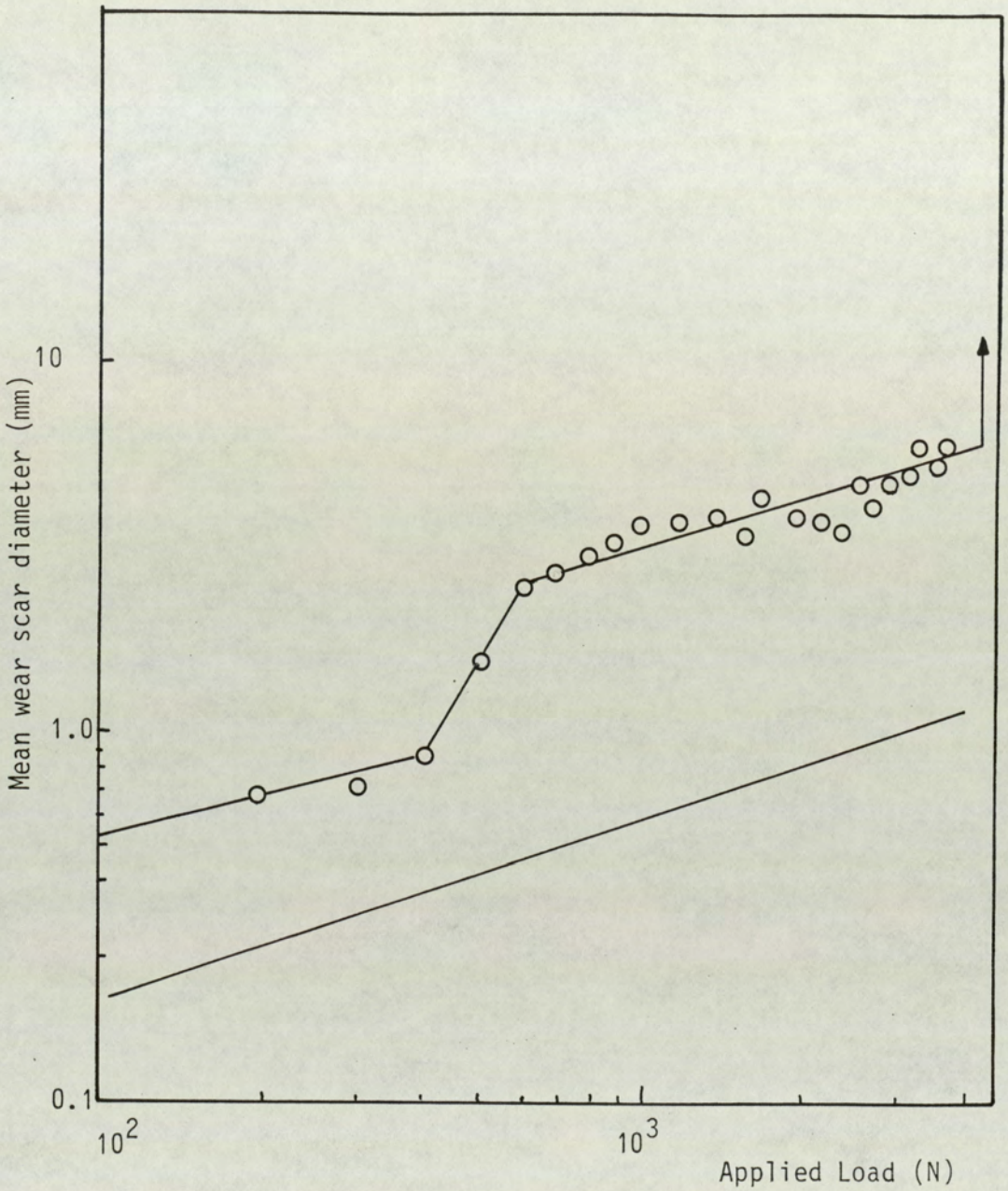

Figure 3.7 Experimentally measured mean wear scar diameter (mm) as a function of applied load (N).
Lubricant: R32 + S 0.25% by weight.
SAE 52100 steel run on similar steel balls.

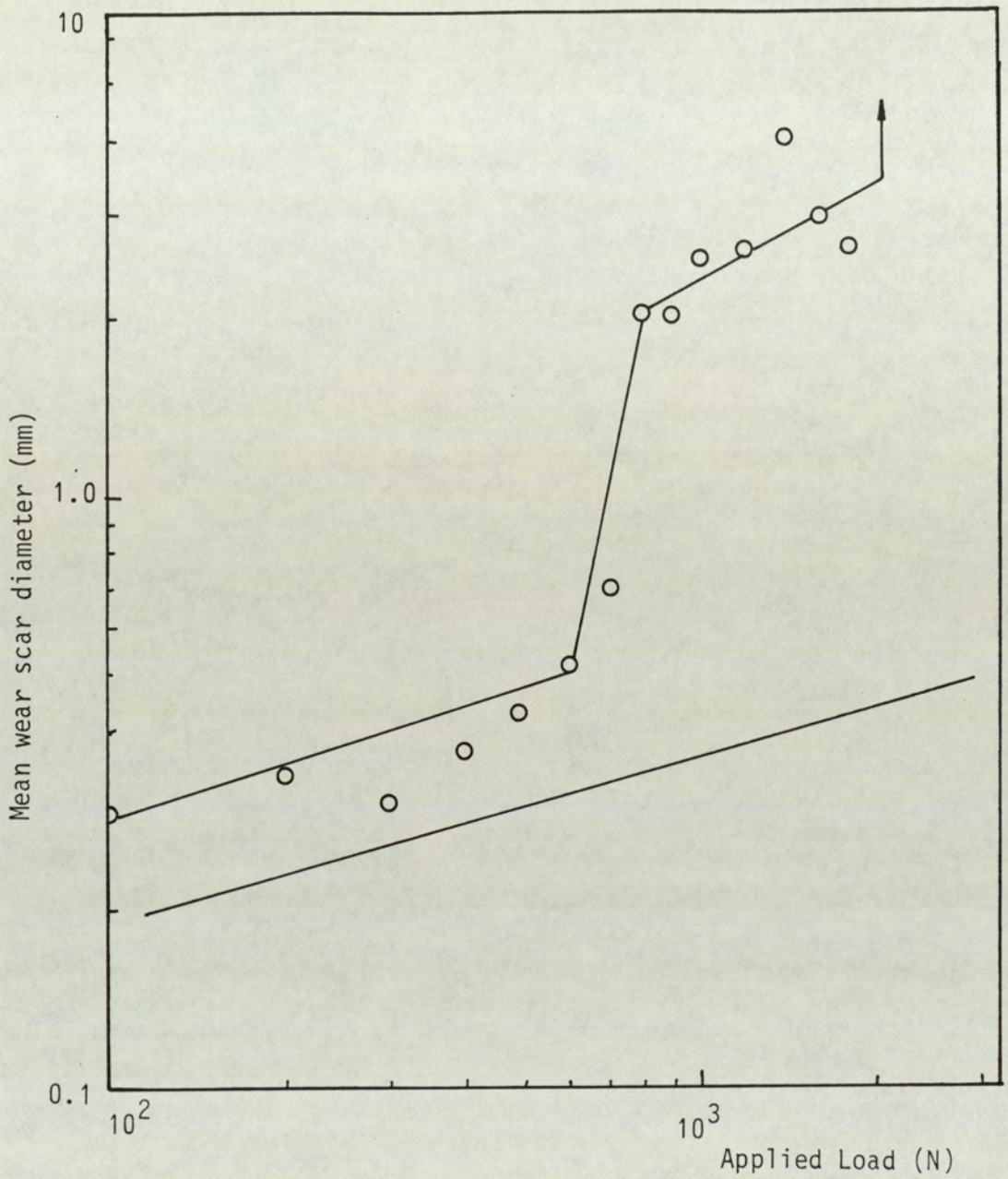

Figure 3.8 Experimentally measured mean wear scar diameter (mm) as a function of applied load (N).
Lubricant: R32 + S 0.25% by weight.
SAE 52100 steel run on AISI 420 stainless steel balls.

3.3:3 Rotating stainless steel ball (AISI 420) on three similar stationary stainless steel balls

The wear tests of this combination show that the onset of the initial seizure was at 200 N (Figure 3.9). The AW region extends between 100 and 200 N, indicating that the AW action was reduced approximately to the half of that observed in Figures 3.7 and 3.8. The E P region cannot be considered a good one, because it compares unfavourably to that observed in Figure 3.7. The wear behaviour of the rotating stainless steel ball against similar stainless steels indicated that the chromium content suppressed both the A W and E P action.

3.3:4 Rotating stainless steel ball (AISI 420) on three stationary steel (SAE 52100) balls or rollers

In Figure 3.10 the initial and final seizure occurred at loads of 300 and 2400 N, respectively.

In general, the wear behaviour is characterized by a poor anti-wear region (extends between 100 and 300 N), and a good E P region.

Figure 3.11 shows that the wear behaviour of the combination of rotating stainless steel ball on three stationary 52100 steel rollers was similar to that observed in Figure 3.10.

The measured mean wear scar diameters in the antiwear region were slightly larger than those of the corresponding Hertzian diameters and smaller than the corresponding ones in Figure 3.10. But the measured mean wear scar diameters in E P were larger than those of the corresponding Hertzian diameters.

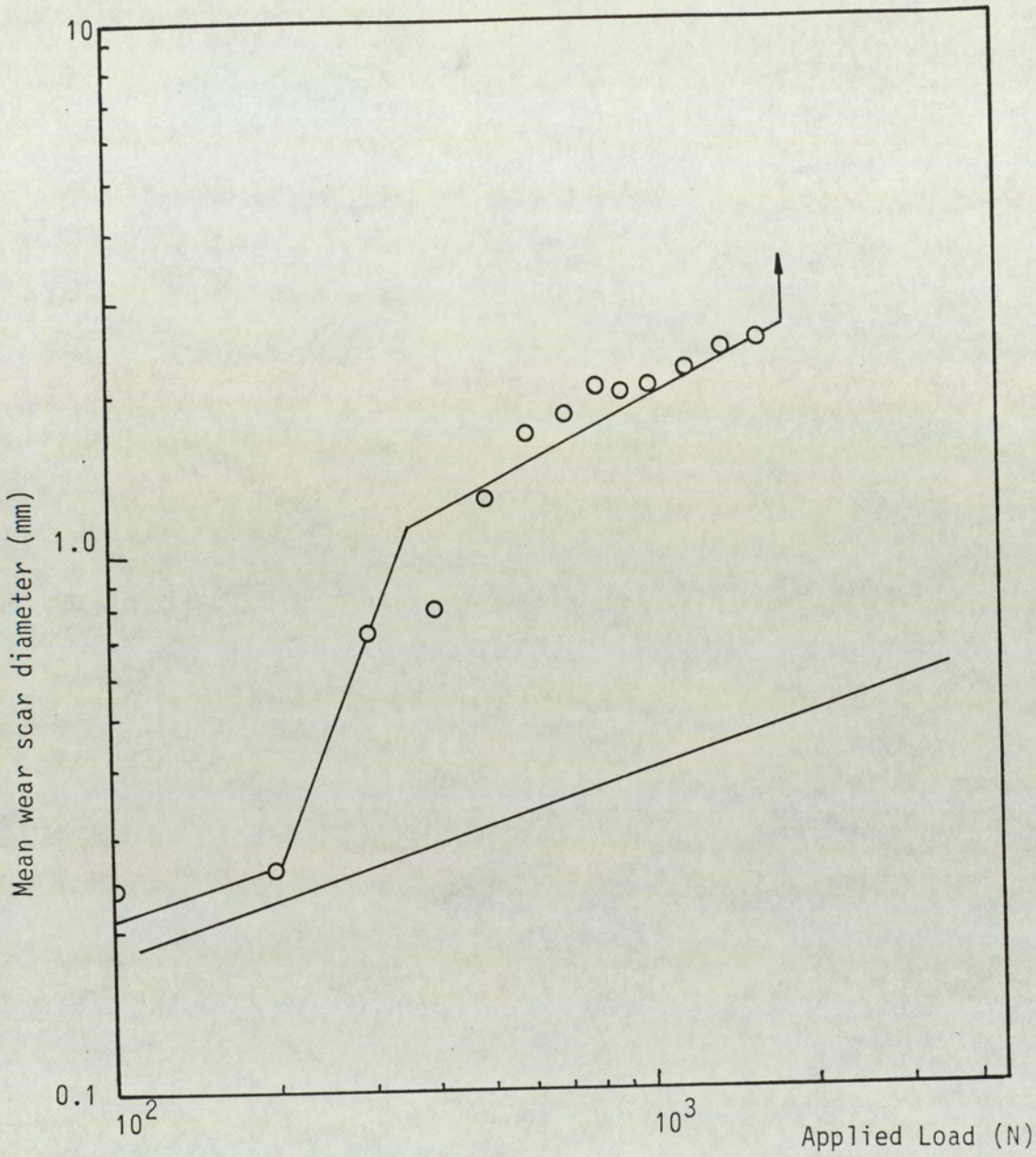

Figure 3.9 Experimentally measured mean wear scar diameter (mm) as a function of applied load (N).
Lubricant: R32 + S 0.25% by weight.
AISI 420 stainless steel run on similar stainless steel balls.

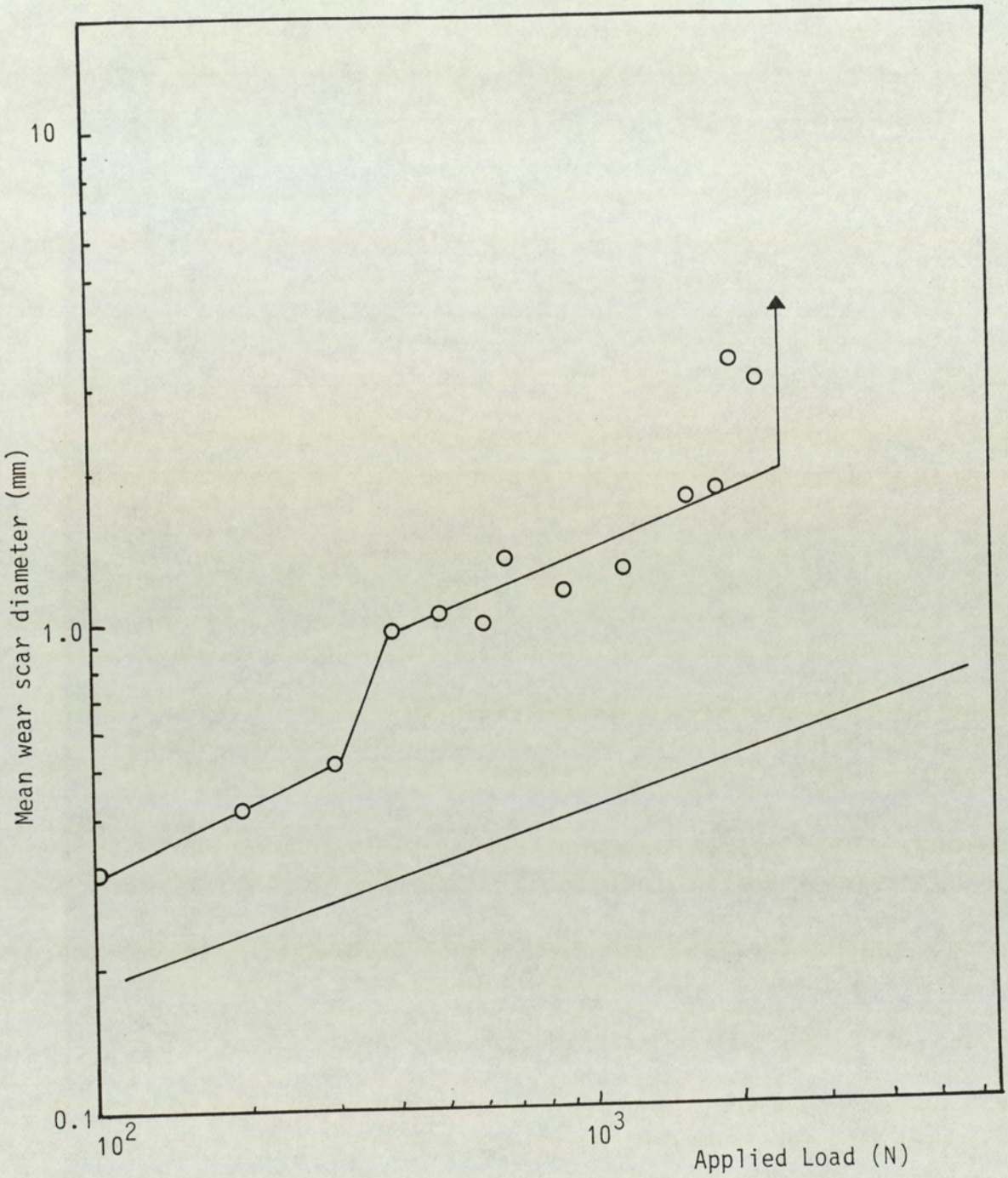

Figure 3.10 Experimentally measured mean wear scar diameter (mm) as a function of applied load (N).
Lubricant: R32 + S 0.25% by weight.
AISI 420 stainless steel run on SAE 52100 steel balls.

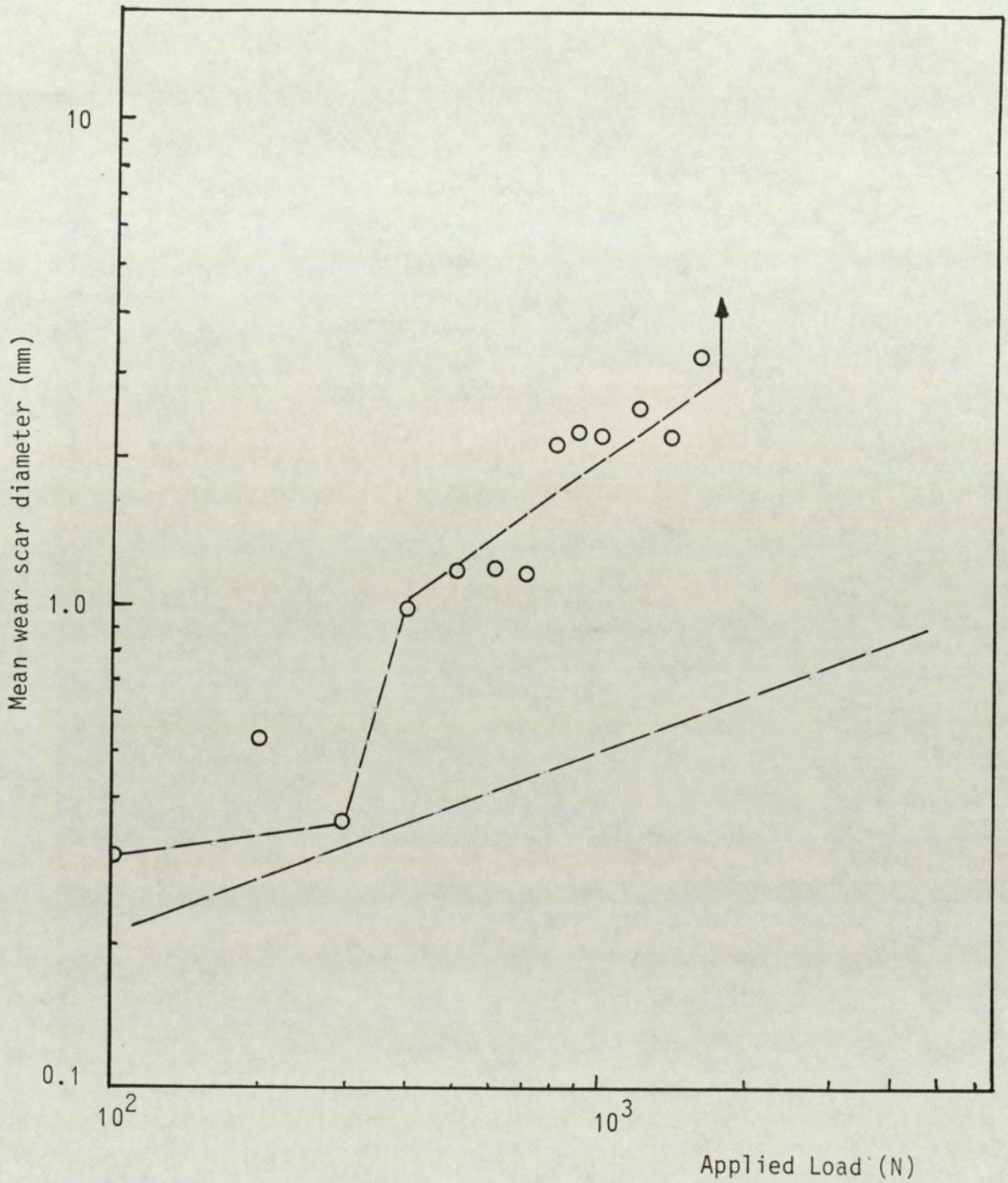

Figure 3.11 Experimentally measured mean wear scar diameter (mm) as a function of applied load (N).
Lubricant: R32 + S 0.25% by weight.
AISI 420 stainless steel run on SAE 52100 steel rollers.

3.3:5 Summarizing remarks

Using Risella 32 containing sulphur additives it has been shown that the wear behaviours of the four combinations of materials are much better than those observed with R32 alone (see Figure 3.12). The A W and E P regions were noticeable, and the load carrying capacity was larger. The improvement of the A W action was very clear when a high carbon steel ball (SAE 52100) was run on three stationary martensitic stainless steel ball (AISI 420). The worst condition occurs when (AISI 420) stainless steel is run against itself.

3.4 Wear Results Using Lubrication R32 Containing Dibenzyl Disulphide (DBDS) Additive

Wear behaviours of both high carbon chrome steel and martensitic stainless steel were studied with R32 containing 1.00% by weight of DBDS additive under the following combinations.

3.4:1 Rotating steel ball (SAE 52100) on three stationary similar steel balls

Figure 3.13 shows that the initial and final seizures occurred at 600 and 2600 N respectively. This additive had shown very good anti-wear behaviour between 100 and 600 N. Also the A W line was parallel to and slightly above the corresponding Hertz line. The E P region extends between 700 and 2600 N, showing quite good E P activity.

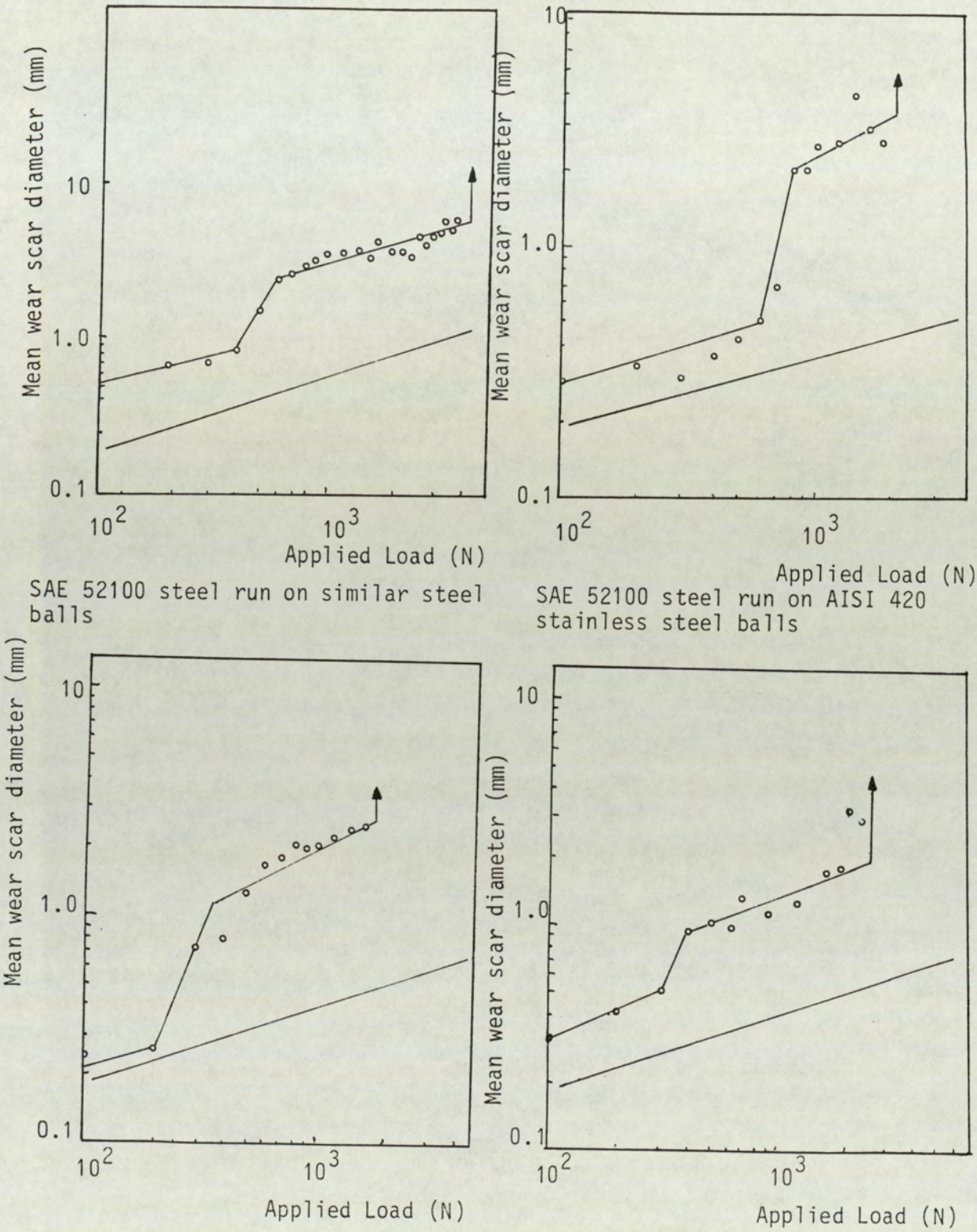

Figure 3.12 Experimentally measured mean wear scar diameter (mm) as a function of applied load (N).

Lubricant: R32 + S 0.25% by weight.

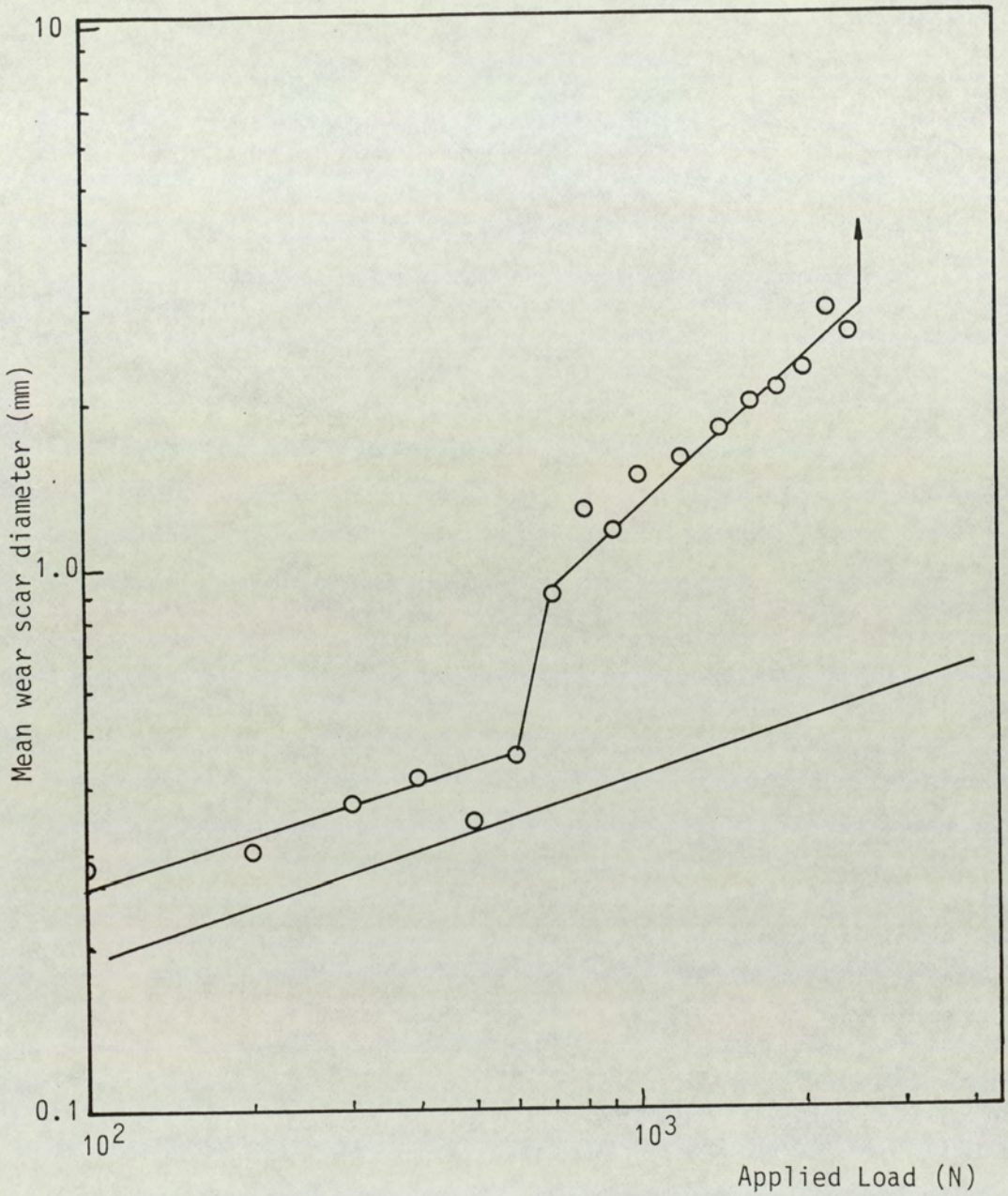

Figure 3.13 Experimentally measured mean wear scar diameter (mm) as a function of applied load (N).
Lubricant: R32 + DBDS 1.00% by weight.
SAE 52100 steel run on similar steel balls.

3.4:2 Rotating steel ball (SAE 52100) on three stationary stainless steel balls (AISI 420)

This combination of steel and stainless steel shows that the initial seizure occurred at 400 N which is 200 N less than that of the the corresponding initial seizure observed in Figure 3.13. Extreme pressure extends between 500 and 2000 N where the final seizure occurred at 2000 N (Figure 3.14) and both AW and EP regions were of a limited extent. This is due to the high chromium content in the three stationary stainless steel balls.

3.4:3 Rotating stainless steel ball on three similar stationary stainless steel balls

The AW was completely suppressed due to the effect of chromium in the rotating and stationary stainless steel balls. As a result of this, the measured mean wear scar diameters were large and varying between 2 and 3 mm (Figure 3.15).

3.4:4 Rotating stainless steel ball (AISI 420) on three stationary steel (SAE 52100) balls or rollers

When the steel balls were involved (see Figure 3.16), the initial seizure took place at 100 N and the EP region extended between load of 200 and 2000 N, exhibiting a good EP activity. The final seizure load occurred at 2000 N and prior to its occurrence the mean wear scar diameter was about

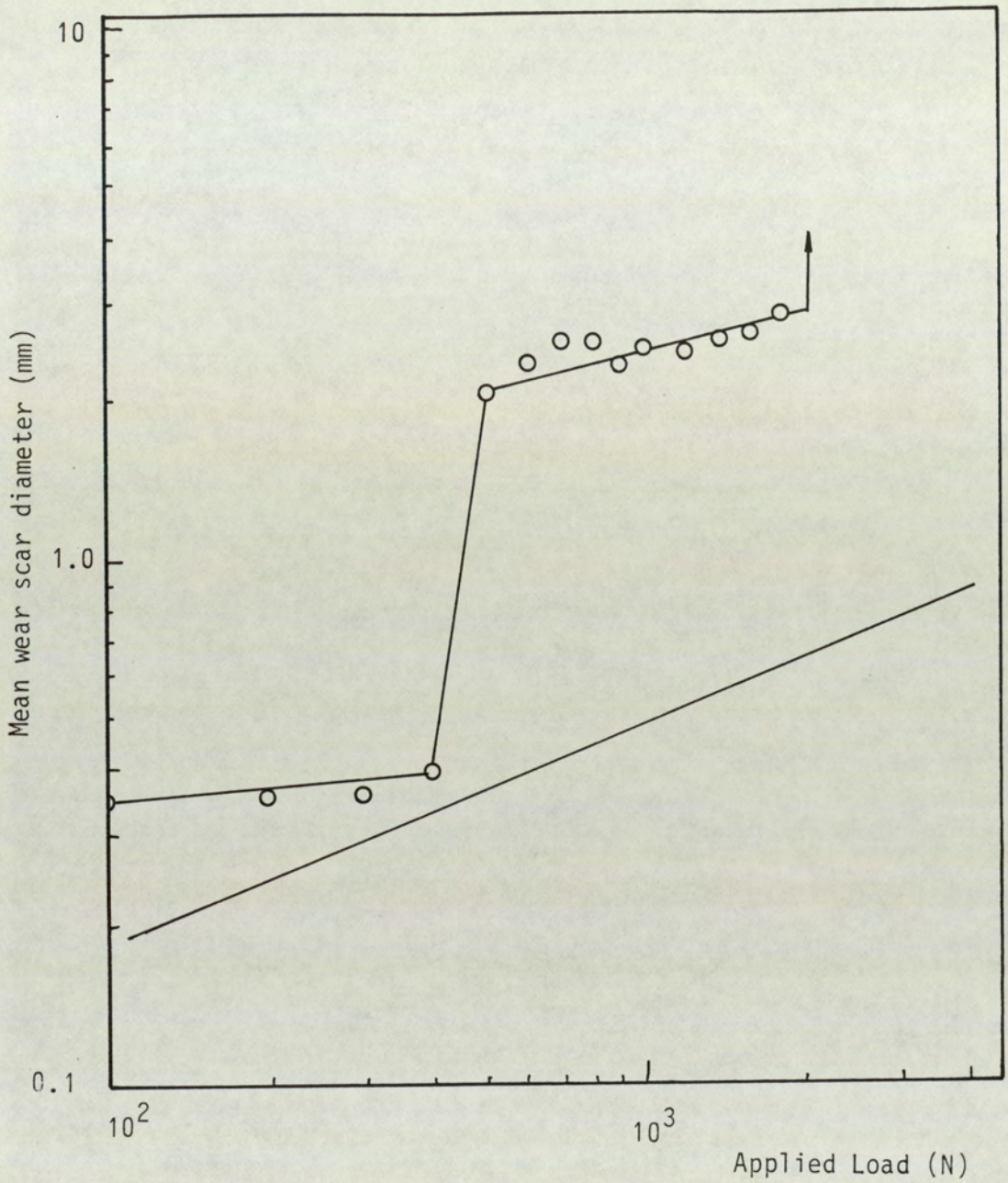

Figure 3.14 Experimentally measured mean wear scar diameter (mm) as a function of applied load (N).
Lubricant: R32 + DBDS 1.00% by weight.
SAE 52100 steel run on AISI 420 stainless steel balls.

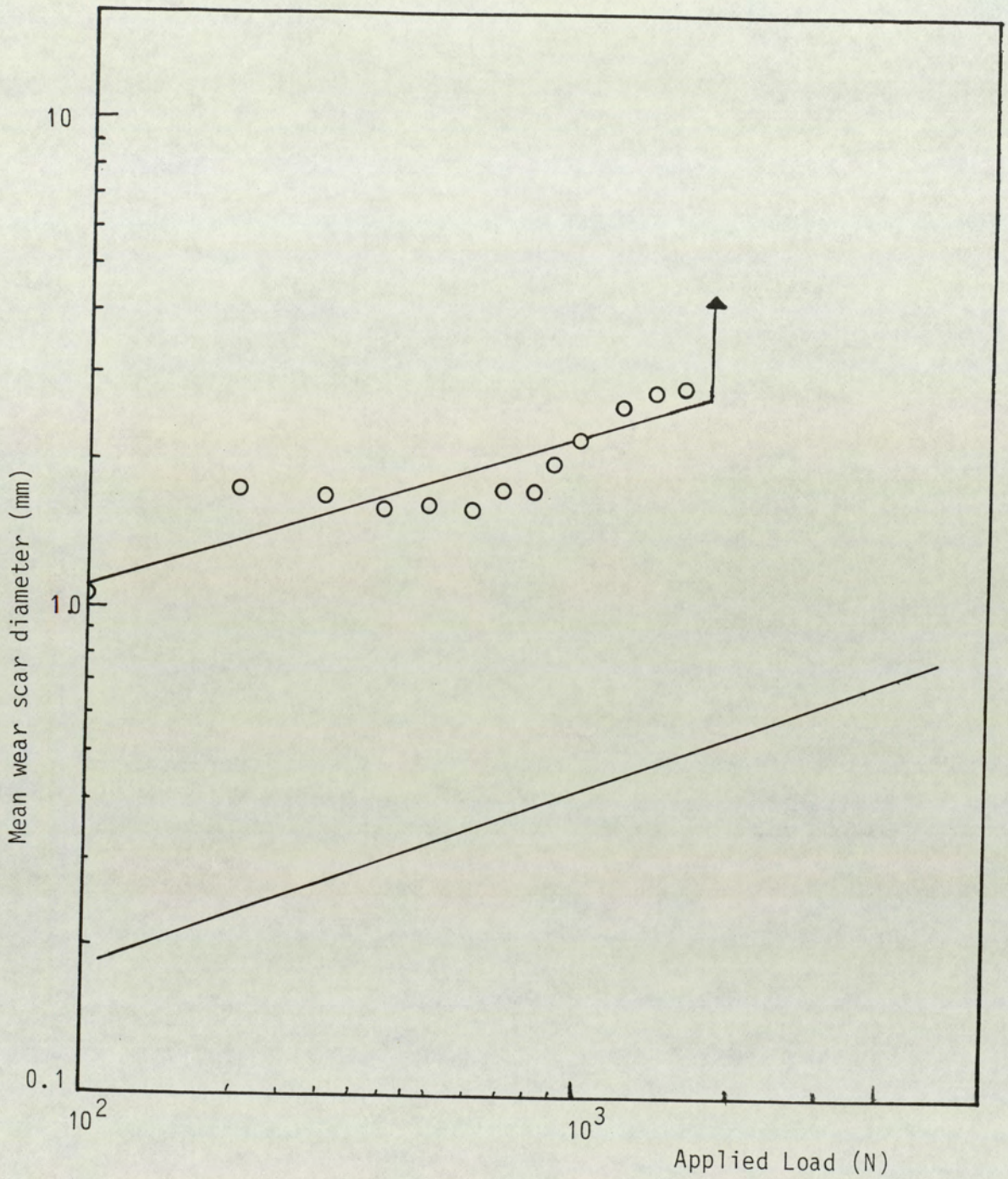

Figure 3.15 Experimentally measured mean wear scar diameter (mm) as a function of applied load (N).
Lubricant: R32 + DBDS 1.00% by weight.
AISI 420 stainless steel run on similar stainless steel ball.

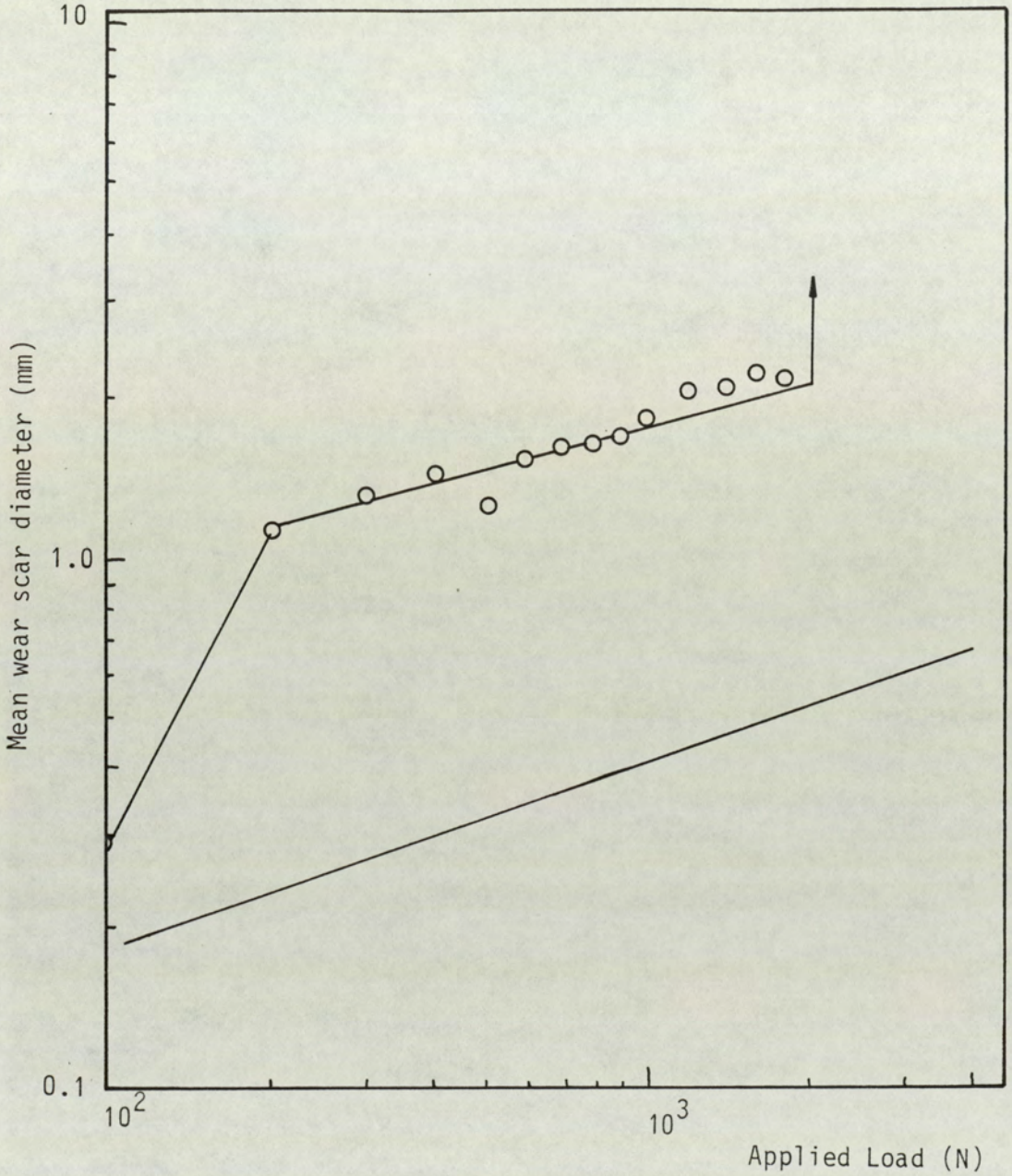

Figure 3.16 Experimentally measured mean wear scar diameter (mm) as a function of applied load (N).
Lubricant: R32 + DBDS 1.00% by weight.
AISI 420 stainless steel run on SAE 52100 steel balls.

2.10 mm which is considerably less than the corresponding value shown in Figure 3.15. This means that the nature of the stationary material does have an effect on the worn surfaces.

Although steel rollers were used instead of the stationary steel balls, the wear behaviour (Figure 3.17) shows little difference from the previous one observed in Figure 3.16. The minor differences were that the final seizure occurred at 1600 N and the EP line is not parallel to the corresponding Hertz line. Also, the measured mean wear scar diameters were, in general, larger than those shown in Figure 3.16.

3.4.5 Summarizing Remarks

In the wear tests carried out with DBDS additive, the antiwear region was remarkably good (see Figure 3.18). The suppression of AW and EP actions were obvious in wear tests involving the stainless steel as a rotating ball (see Table 3.1). The load carrying capacity of DBDS is slightly smaller than the load-carrying capacity of sulphur additive.

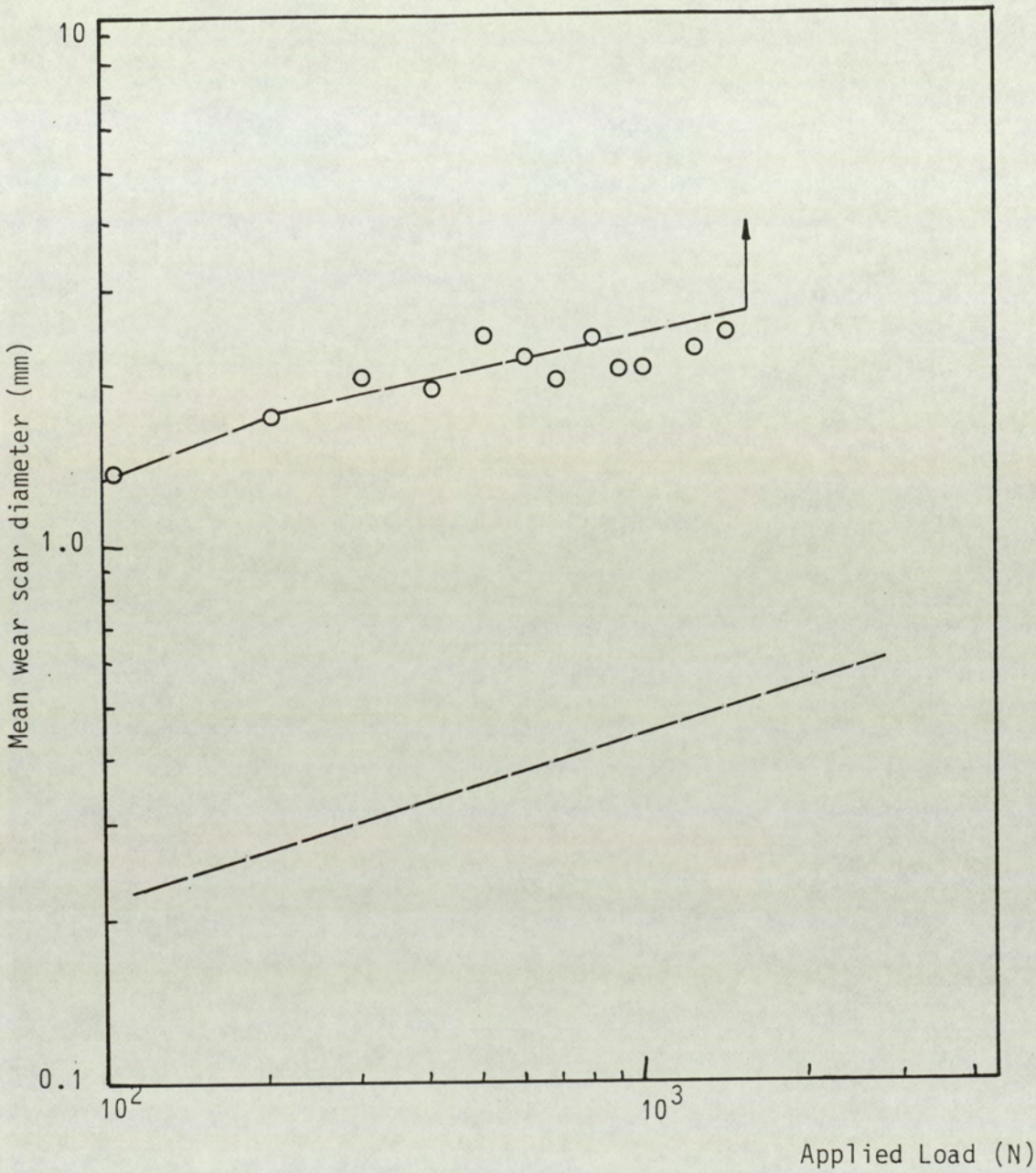

Figure 3.17 Experimentally measured mean wear scar diameter (mm) as a function of applied load (N).
Lubricant: R32 + DBDS 1.00% by weight.
AISI 420 stainless steel run on SAE 52100 steel rollers.

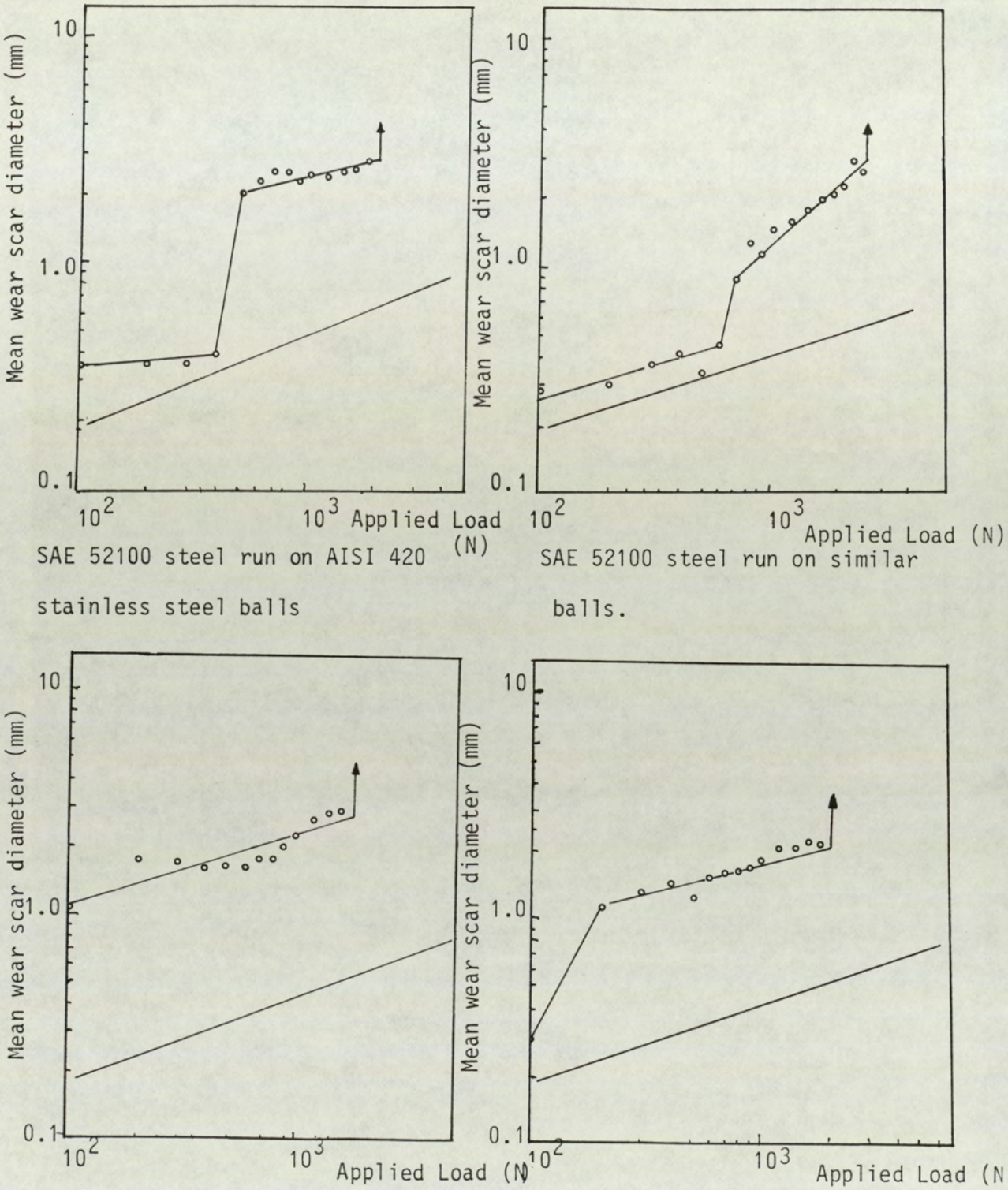

SAE 52100 steel run on AISI 420 stainless steel balls

SAE 52100 steel run on similar balls.

AISI 420 stainless steel run on similar stainless steel ball

AISI 420 stainless steel run on SAE 52100 steel ball.

Figure 3.18 Experimentally measured mean wear scar diameter (mm) as a function of applied load (N).

Lubricant: R32 + DBDS 1.00% by weight.

3.5 Wear Results Using R32 Containing Diphenyl Disulphide (DPDS) Additive

Diphenyl Disulphide additive was investigated with steel and stainless steel materials in the following combinations:-

3.5:1 Rotating steel ball (SAE 52100) on three similar stationary steel balls

Figure 3.19 shows that the initial and final seizures occurred at 700 and 1600 N, respectively. This means that the AW activity was good, while the EP activity was less than the EP activity of DBDS. The AW region extended between loads of 100 and 700 N and its wear scar diameters were slightly larger than that of the corresponding Hertzian diameters. The smallest measured mean wear scar diameter was 0.22 mm under load of 100 N. The transition to the EP region occurred between 700 and 800 N, whereas the measured mean wear scar diameters vary between 0.45 and 1.10 mm.

3.5:2 Rotating steel ball (SAE 52100) on three stationary stainless steel balls (AISI 420)

When the stainless steel was used in stationary balls the wear behaviour (shown in Figure 3.20) showed considerable differences from that observed in Figure 3.19. The AW region was reduced from 700 to 400 N as shown in Figures 3.19 and 3.20 respectively. The EP region extends between loads of 400 and 1400 N and the mean wear scars diameters were large, reaching 5 mm under 1200 N.

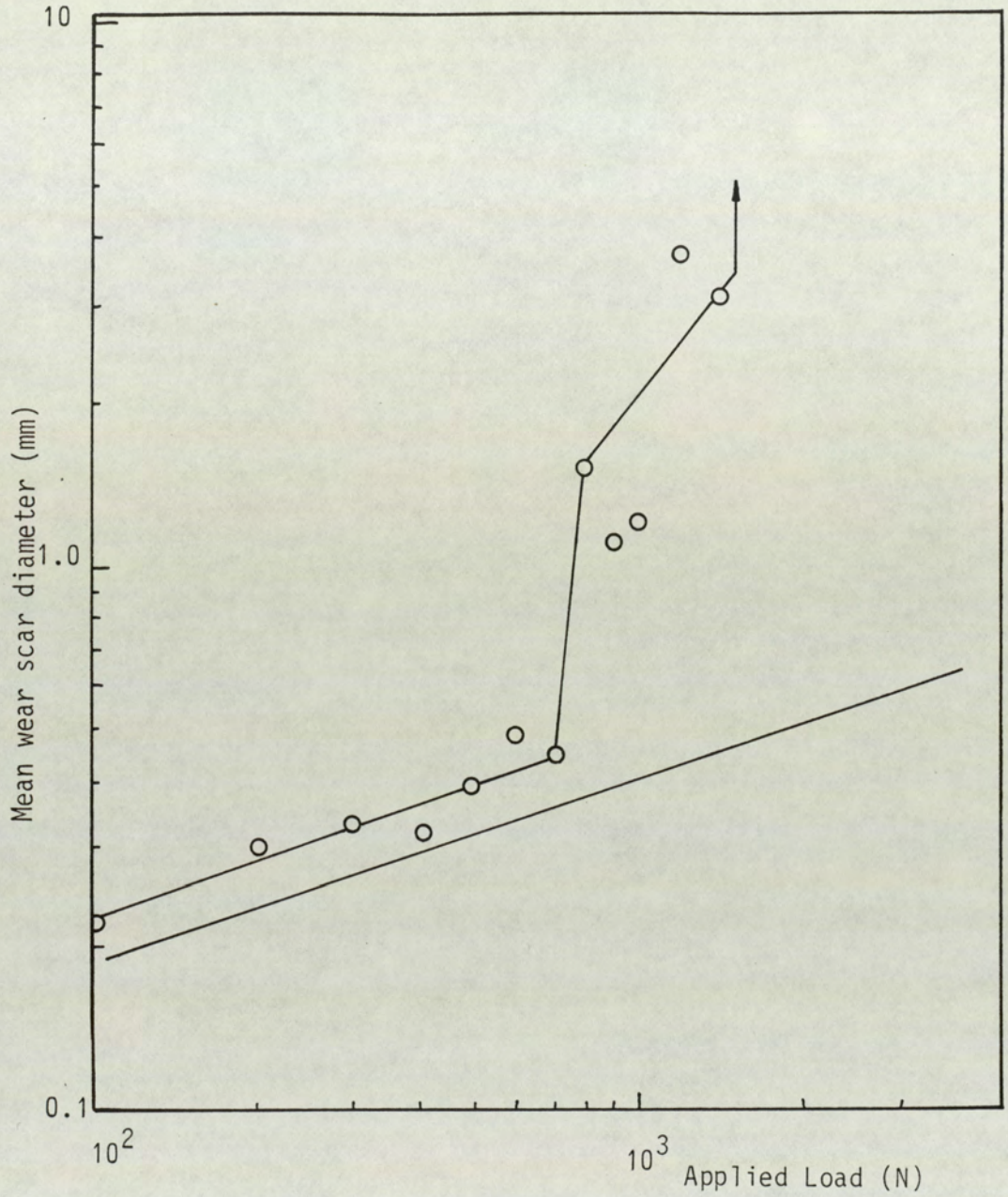

Figure 3.19 Experimentally measured mean wear scar diameter (mm) as a function of applied load (N).
Lubricant: R32 + DPDS 0.886% by weight.
SAE 52100 steel run on similar steel balls.

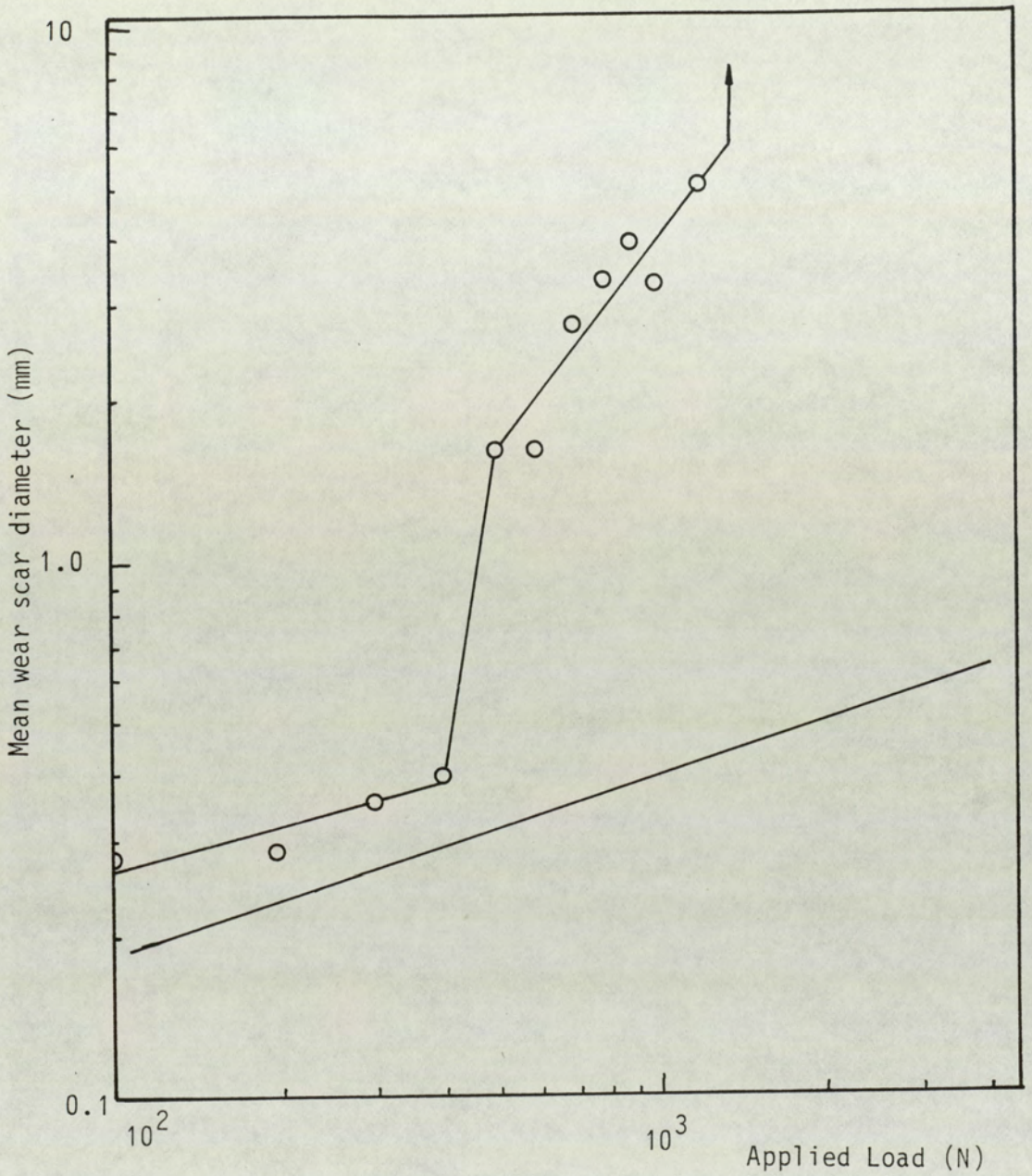

Figure 3.20 Experimentally measured mean wear scar diameter (mm) as a function of applied load (N).
Lubricant: R32 + 0.886% DPDS by weight.
SAE 52100 steel run on AISI 420 stainless steel balls.

3.5:3 Rotating stainless steel ball on three similar stationary stainless steel balls

Both AW and EP regions were observed and the measured mean wear scar diameters were very large in comparison to those measured mean wear scar diameters obtained from a rotating steel ball on similar SAE 52100 steel balls or AISI 420 stainless steel balls. The mean wear scar diameters in the AW region varies between 1.20 and 2.50 mm and between 3.15 and 3.50 mm in the EP region. The initial and final seizures obtained from this combination of materials were at loads of 400 and 1600 N (Figure 3.21) respectively. This means that the AW and EP actions were poor and this could be interpreted as a result of the chromium content in the stainless steel balls.

3.5:4 Rotating stainless steel ball (AISI 420) on three stationary steel (SAE 52100) balls or rollers

The wear behaviour of this combination of materials is characterized by initial and final seizures at loads of 100 and 1400 N, respectively. The AW region was suppressed due to the deleterious effect of chromium in the rotating stainless steel ball, while the EP region was good and extended between 200 and 1600 N (see Figure 3.22).

In Figure 3.23 the AW action was totally suppressed, but the EP action was very good. Note that the EP region extends between loads of 200 and 1600 N.

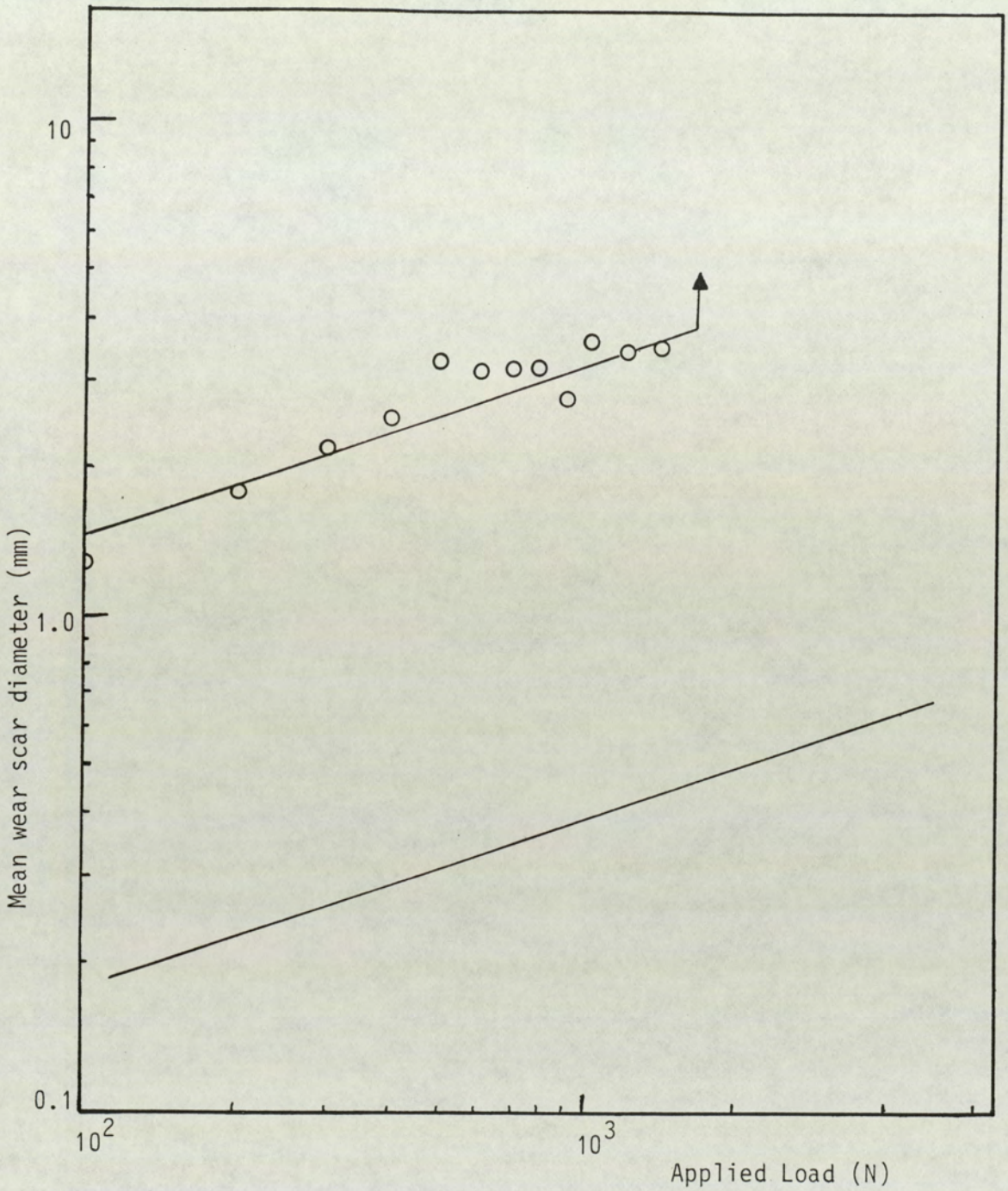

Figure 3.21 Experimentally measured mean wear scar diameter (mm) as a function of applied load (N).
Lubricant: R32 + DPDS 0.886% by weight.
AISI 420 stainless steel run on similar stainless steel balls.

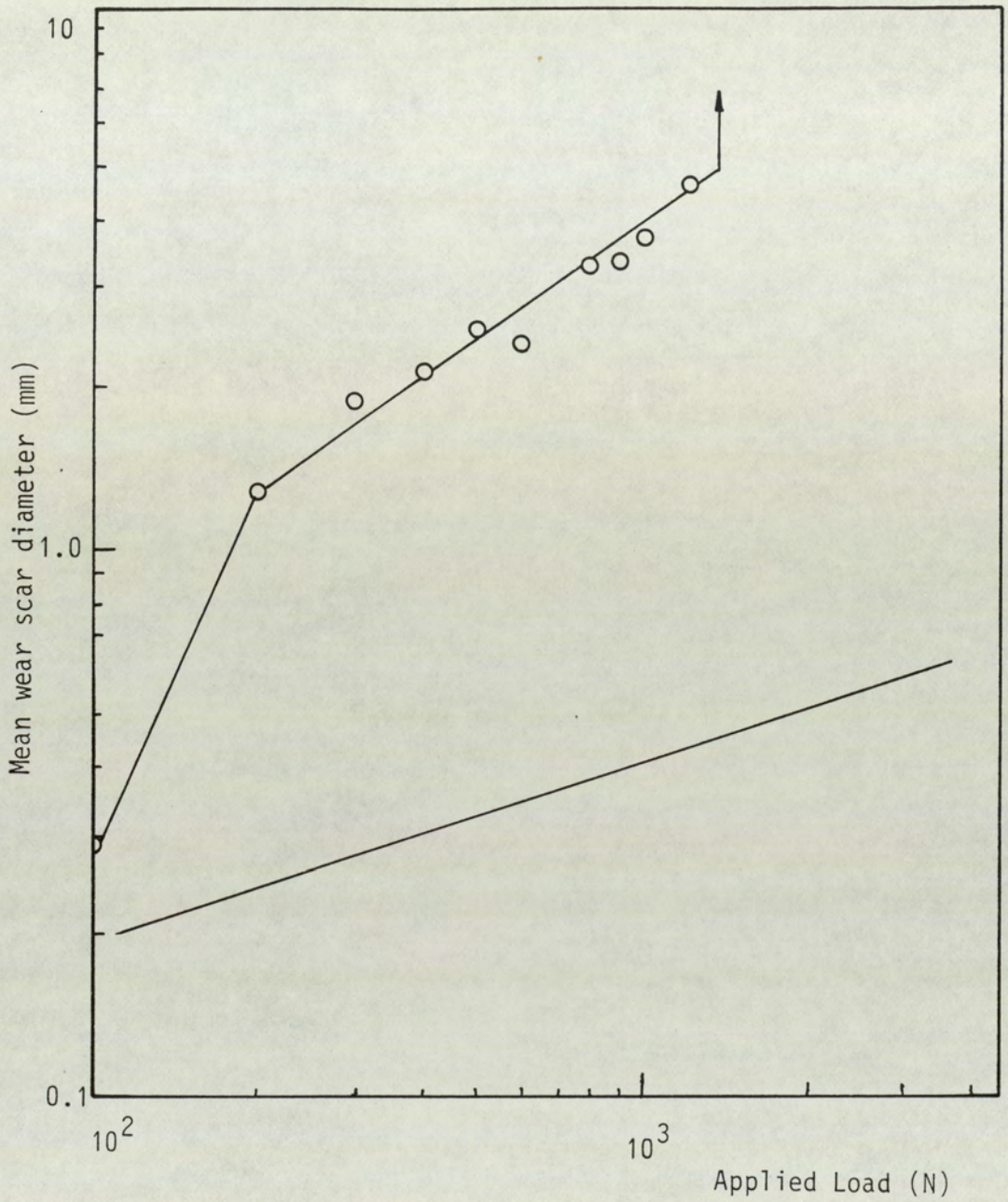

Figure 3.22 Experimentally measured mean wear scar diameter (mm) as a function of applied load (N).

Lubricant: R32 + DPDS 0.886% by weight.

AISI 420 stainless steel run on SAE 52100 steel balls.

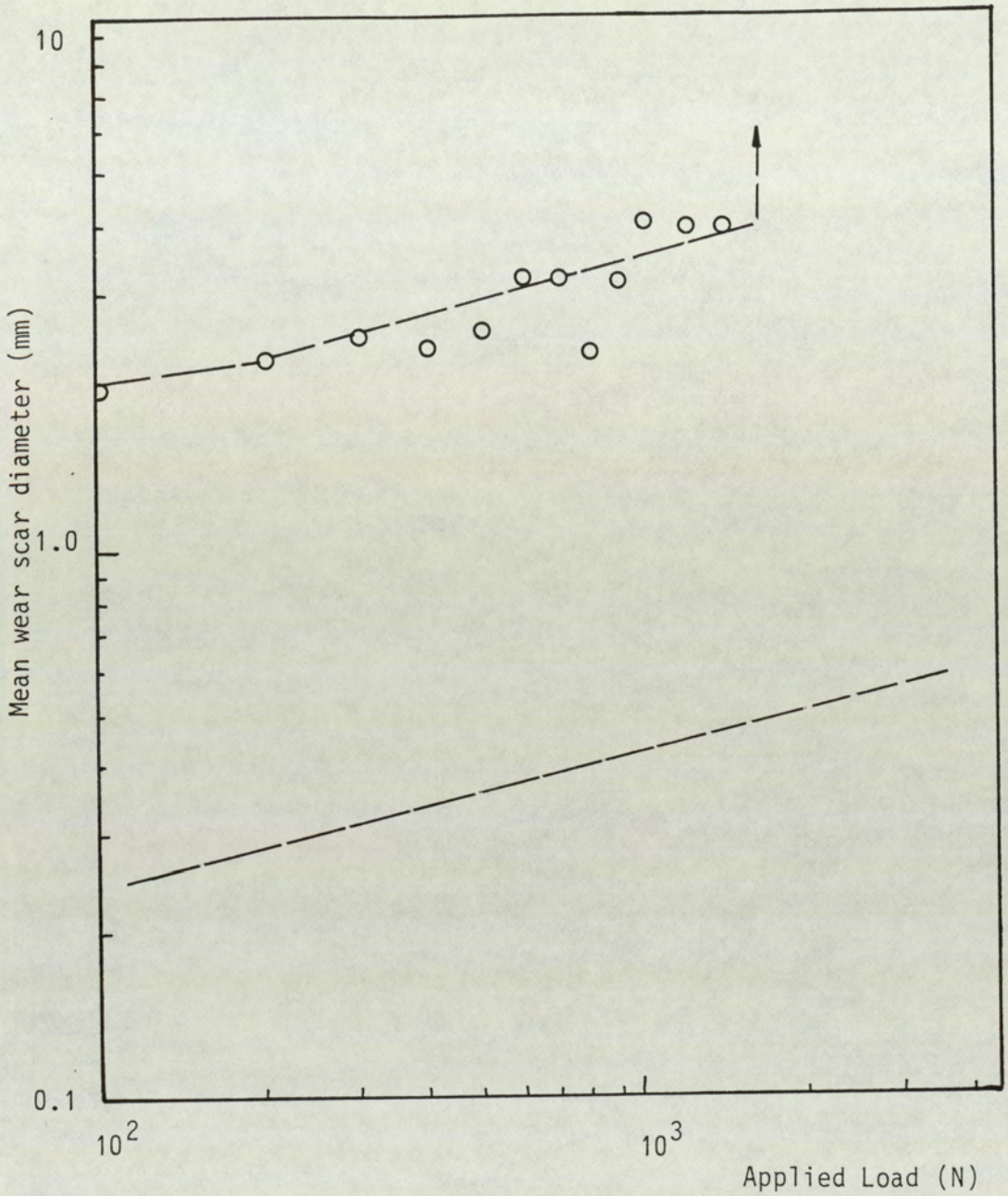

Figure 3.23 Experimentally measured mean wear scar diameter (mm) as a function of applied load (N).
Lubricant: R32 + DPDS 0.886% by weight.
AISI 420 stainless steel run on SAE 52100 steel rollers.

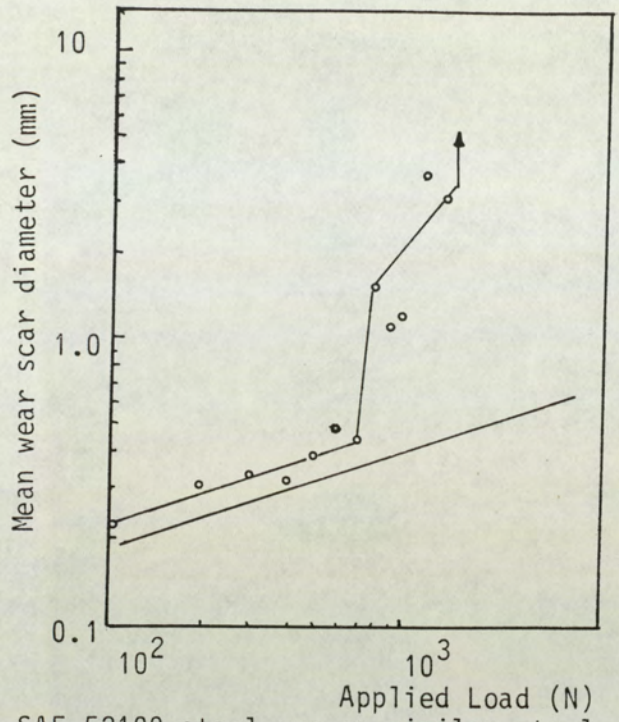

SAE 52100 steel run on similar steel balls.

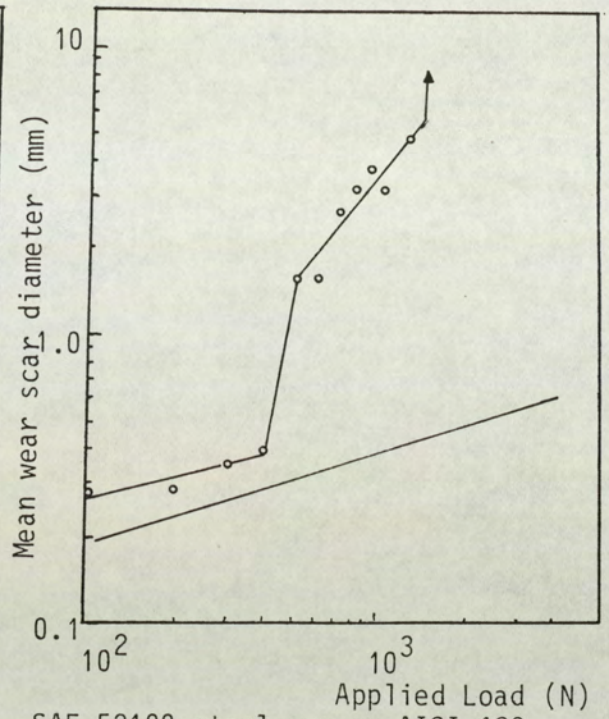

SAE 52100 steel run on AISI 420 stainless steel balls.

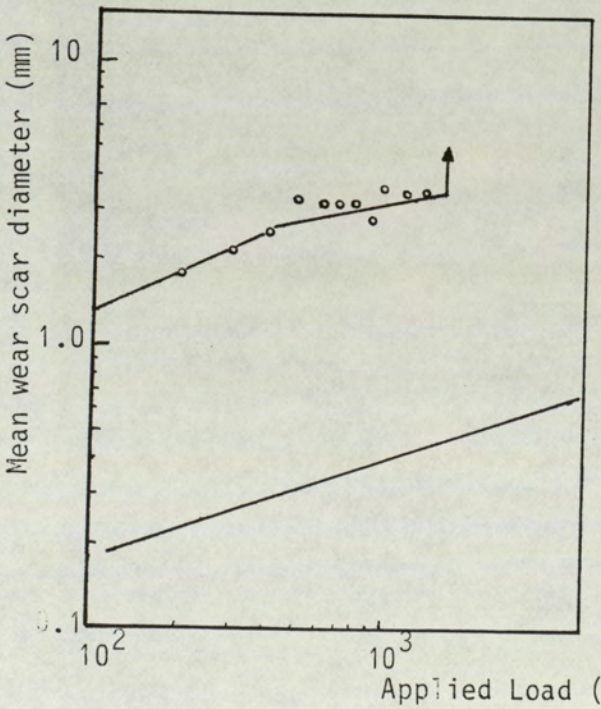

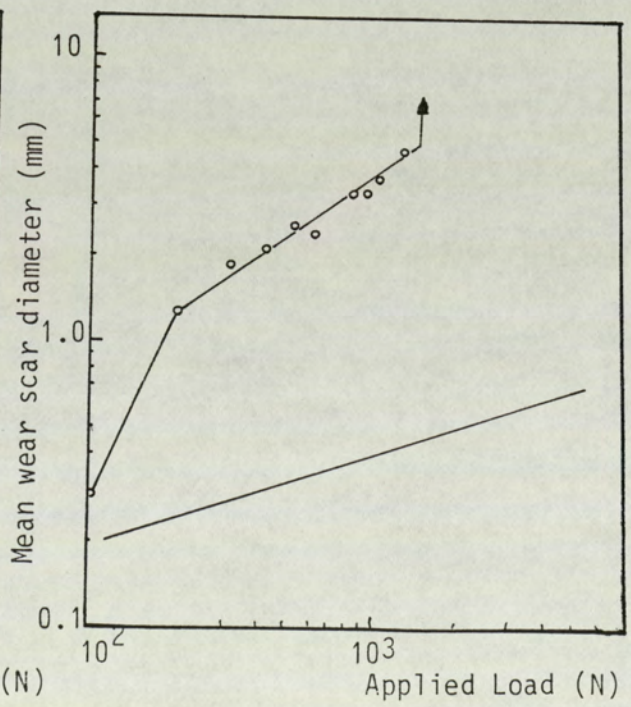

Figure 3.24 Experimentally measured mean wear scar diameter (mm) as a function of applied load (N).

Lubricant: R32 + DPDS 0.886% by weight.

3.5:5 Summarizing remarks

Table 3.1 demonstrates that R32 has no effect on the final seizure load due to the material differences, and the final seizure of any combination does not exceed 1200 N. The use of S, DBDS and DPDS additives has shown that these disulphides exhibit good AW activity where SAE 52100 run on similar steel, while this activity was reduced when AISI 420 stainless steel was involved either in the rotating or stationary balls. This is almost certainly associated with the role of chromium (12-14% in AISI 420 stainless steel). The AW activity of S was less than that shown by the disulphides.

Table 3.1 shows that the wear behaviour from worst to best conditions takes the following order in the four combinations of material.

	Rotating Balls	Stationary Balls
Worst	S/S	S/S
↓	S/S	52100
Best	5200	S/S
	5200	5200

The suppression of the AW region and the reduction of final seizure is greatest when the rotating ball has high Cr content. Also, with all additives including S the chromium content of the material conjunction has some effect in suppression in both initial seizure and final seizure.

All wear tests carried out with DPDS additive under the four combinations of materials showed that the DPDS additive provided less EP action compared with DBDS additive, as shown in Table 3.1. In general, the DBDS additive shows a better wear behaviour than the DPDS additive.

Table 3.1: Showing initial and final seizures of wear tests carried out with the four-ball machine

Lubricant	Steel on steel balls		Steel on stainless steel balls		Stainless steel ball on stainless steel ball		Stainless steel on steel balls and rollers			
	Initial seizure N	Final seizure N	Initial seizure N	Final seizure N	Initial seizure N	Final seizure N	Steel ball		steel rollers	
							I.S.	F.S.	I.S.	F.S
Risella 32		1200		1200		1200		1200		1000
Risella 32 + S 0.25%	400	4000	600	2000	200	1800	300	2400	300	1800
Risella 32 + DBDS 1.0%	600	2600	400	2000	100	1800	100	2000	400	1600
Risella 32 + DPDS 0.886%	700	1600	400	1400	400	1600	100	1400	100	1600

CHAPTER 4

ANALYSIS OF THE WORN SURFACES

The main aim of this chapter is to present the results of the various physical methods of analysis that were used to examine the compositions, structures and topographies formed in the surfaces of wear scars produced on high carbon steel specimens (SAE 52100) and martensitic stainless steel specimens (AISI 420). The analysis of surface films of the wear scars obtained with sulphur, Dibenzyl Disulphide and Diphenyl Disulphide was carried out using electron probe microanalysis, glancing angle X-ray diffraction and scanning electron microscopy. Also, analyses were carried out on the worn surfaces, which were produced under the four cases of rotation mentioned in Section 3.1.

The layout of this chapter will be presented to show that the three above-mentioned techniques can give much more information than the use of any single one in relation to the conditions of extreme pressure lubricants.

4.1 Electron Probe Microanalysis

4.1:1 Introduction

Electron probe microanalysis is an analytical technique used extensively as a research instrument in a wide range of scientific disciplines, including solid state physics, metallurgy, geology, mineralogy and biology.

The electron probe microanalyser gives information about the distribution of the various elements present in a surface and also their relative proportions.

This information can be taken from the electron probe microanalyser on the basis of analysing the X-rays produced from the elements present in the surface of the specimen.

When a beam of electrons with high energies impinges on a solid surface, X-rays are emitted. The X-rays will contain radiation of various frequencies, according to the elements present in the specimen. When an electron beam is focussed onto a particular region of a specimen, one can detect the X-rays that are emitted. By moving the electron probe over the specimen, one can also analyse the specimen point by point. The constituents of the specimen will give rise to a characteristic X-radiation. These X-rays can be analysed using crystal spectrometers (crystals of Gyps m or Lithium Fluoride) and the original elements identified. Also, the concentration of the elements in the specimen can be found according to the intensity of the X-rays emitted from the specimen relative to the intensity of X-rays emitted from standards.

The microanalyser can be considered as consisting of three basic units:

(1) The electron optical system.

(2) Probe orienting system.

(3) An X-ray spectrometer.

The wear scars produced on high carbon steel balls and rollers (SAE 52100) and martensitic stainless steel balls (AISI 420) were analysed using a Cambridge Microscan 5 Electron Probe Microanalyser. An electron

beam 0.3 μm in diameter excites characteristic X-rays from a very small volume of the specimen. Measurement of the X-ray wavelength allows identification of the elements present for all elements with atomic number above boron (i.e. $z > 5$) in the periodical table. Analysis is performed by comparison of X-ray intensities from the specimen with that from pure standards enabling overall accuracies of $\pm 1\frac{1}{2}\%$ and minimum limits of 0.05% for most elements.

For accurate quantative electron probe analyses the specimen and the comparison standard should be smooth, flat and clean so that no change in the X-ray "take-off angle" takes place. As the wear scar surfaces were uneven, this would certainly vary the "take-off angle" and have an effect on the accuracy of the analysis. To overcome this problem the variation of the take-off angle has been largely reduced by taking a number of counts in the wear scar. In addition, absorption, fluorescence and atomic number corrections to the results were made, which can be regarded as improving the overall accuracy of the analysis.

4.1:2 Operating procedures

In the operating procedures of the electron probe microanalysis technique the following conditions were satisfied:

a) The thickness of the specimen was less than 1.00 cm.

b) The specimen had been ultrasonically cleaned and fully dried.

The specimen holder was inserted carefully in the specimen chamber of the probe and observed with the optical system. Bragg angles were adjusted

on the appropriate command units for maximum ratemeter readings. All the elements (S, Cr and Fe) were measured and then repeated for the standards (Peaks and Backgrounds). All specimens and standards were focussed optically in focus at the beginning.

4.1:3 Methods of analysis

If one is mainly interested in identifying the presence of certain elements in surfaces relative to particular surface topographical features, then the electron probe microanalyser is the appropriate instrument to use. The methods used in the analysis were:-

(1) A visual display of the element distributions and the topography.

(2) Spot analyses over the wear scar.

(3) A concentration profile for the constituent elements.

In all the analyses a 20 kV accelerating potential was used. The worn surfaces were scanned and a camera was used to record the electron image and the element distributions.

The distribution of elements and the topography of the surface was obtained by scanning the electron beam across fairly large areas of surface. In the quantitative analysis one can analyse the X-rays emitted at a particular spot and then the average of several such spots must be taken. The analyses were conducted at five points over the surface of each wear scar namely, (i) in the centre of the scar and (ii) at four places around it.

The Bragg angle for a particular element was chosen and the crystal in the spectrometer was rotated until the ratemeter indicated maximum counts. Three separate counts of 10 seconds were obtained successively in each spot before the average of these counts were taken. Also counts of the background were obtained successively in each spot before the average of these counts were taken. Also counts of the background were obtained by rotating the crystal off the peak. This was done for the elements sulphur, iron and chromium. In the same way, and under the same conditions, counts were obtained on the standard. Deadtime counts per second (c/s) were obtained for the count-rates in each spot and for the standard. The following formula was applied to obtain the percentage of each element present at the surface of the wear scar (Sulphur, Iron and Chromium).

$$p = \frac{\{\text{peak (c/s)} - \text{background (c/s)} + \text{deadtime (c/s)}\}\ \text{specimen}}{\{\text{peak (c/s)} - \text{background (c/s)} + \text{deadtime (c/s)}\}\ \text{standards}}$$

Then the percentage of elements at the surface of the wear scar were corrected by using a computer programme which accounts for the effects of absorption, fluorescence and atomic number. These analytical procedures were conducted in the same way at selected loads. Graphs of mean element percentages in each wear scar were plotted as a function of applied load (N). Since the sum of the sulphur, iron and chromium contents is almost always below 100%, the difference is due, presumably, to carbon and oxygen. All the analyses of worn surfaces were confined to the detection of sulphur, iron and chromium. Neither carbon nor oxygen contents of the wear scars could be determined directly with the electron probe microanalyser, due to practical difficulties with this particular instrument.

4.1:4 Electron probe microanalysis of the unworn surfaces

To investigate the concentration of iron and chromium in the used balls and rollers, a high carbon steel roller (SAE 52100) was cut parallel to its cylindrical axis and mounted in a conductive carbon powder. The roller's surface was polished and ultrasonically cleaned. Then the specimen was placed in the probe and a line concentration profile was obtained, from the surface to the depth of 0.5 mm, as shown in Figure 4.1. Also a martensitic stainless steel ball (AISI 420) was cut across its diameter. Then the ball was mounted and analysed in the same way, as mentioned above (see Figure 4.2).

Figures 4.1 and 4.2 show that the distribution of Cr was not homogeneous along ½ cm depth, where the highest and lowest values of chromium were 3.49% and 1.12%, respectively in Figure 4.1 while Figure 4.2 shows the chromium's highest and lowest values were 18.83% and 13.58%, respectively. This indicates that the lowest values of the chromium in both figures are the only ones which coincide with the chemical composition of high carbon steel (SAE 52100) and martensitic stainless steel (AISI 420) (see article 2.4).

It is clearly seen in the Table 4.1 that the concentration values of the chromium in the high carbon steel (SAE 52100) was more than three times larger than the lowest chromium concentration value. Also the chromium concentration value was approximately one and a half times bigger than the lowest chromium values in the martensitic stainless steel (AISI 420). This clearly indicates non-homogeneous distribution in both materials.

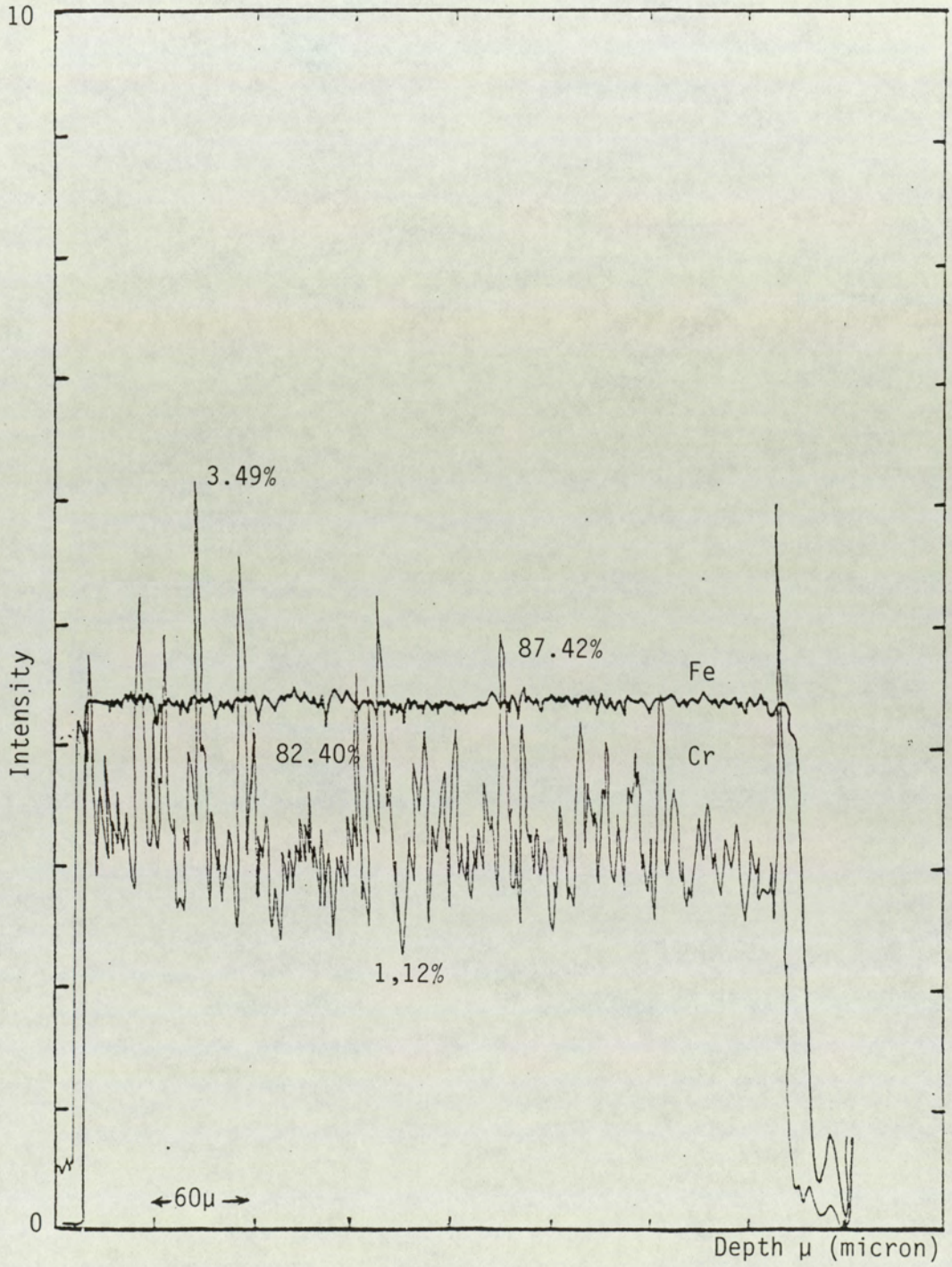

Fig. 4.1 A line concentration profile obtained by the electron probe microanalysis of a high carbon steel specimen SAE 52100. F.S.D.(Fe) = 30 K. F.S.D.(Cr) = 3 K.

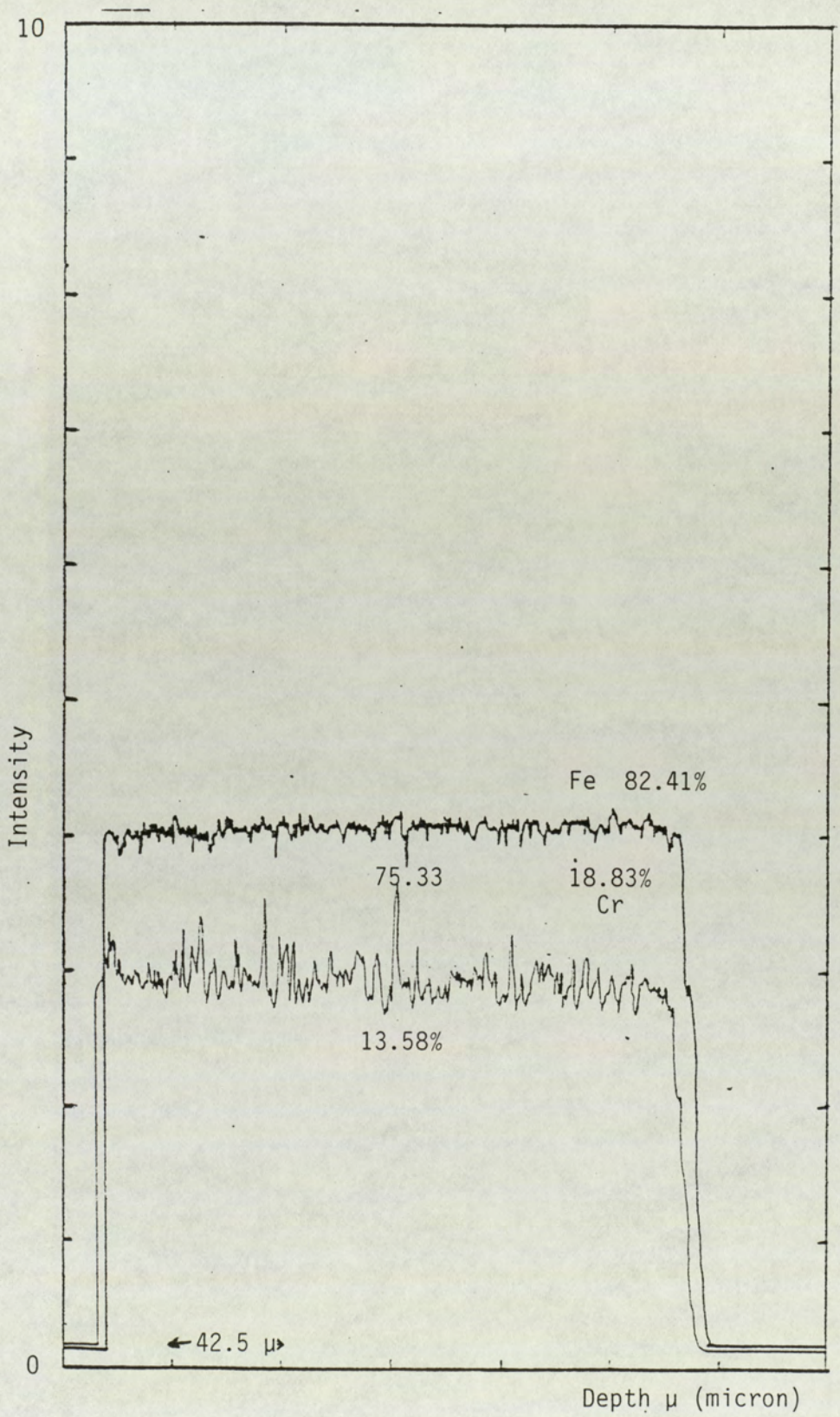

Fig. 4.2 A line concentration profile obtained by the electron probe microanalysis of martensitic stainless steel AISI 420. F.S.D.(Fe) = 30 K, F.S.D.(Cr) = 30 K.

Concentration Values	High carbon chrome steel (SAE 52100)		Martensitic stainless steel (AISI 420)	
	Cr	Fe	Cr	Fe
Lowest Percentage	1.12	82.46	13.58	75.58
Average Percentage	2.04	86.65	15.24	79.98
Highest Percentage	3.44	87.42	18.83	82.41

Table 4.1: Showing the concentration values of chromium and iron along ½ (mm) depth of high carbon chrome steel (SAE 52100) and martensitic stainless steel (AISI 420) obtained by electron probe microanalysis.

4.1:5 Electron probe microanalysis of surfaces worn with the sulphur additives

Several wear scars were obtained from running a high carbon chrome steel ball (SAE 52100) on three similar stationary steel balls. These were analysed by using a spot method. The distribution of sulphur, chromium and iron were analysed within the wear scars, while oxygen and carbon were calculated from the difference of the sum of these intensities and the total signal intensity after allowing for background. The corrected concentrations of these materials in each wear scar formed at applied loads starting at 200 N, in steps of 200 N, up to just before the final seizure load, were plotted in Figures 4.3, 4.4, 4.5 and 4.6. Oxygen and carbon were assumed to be responsible for the difference between 100% and the measured sum of the sulphur, chromium and iron percentages. Figure 4.3 (Figure 4.3 et-sq. are not related to Figures 4.1 or 4.2) shows that the amount of sulphur increases remarkably with increasing load. Between loads

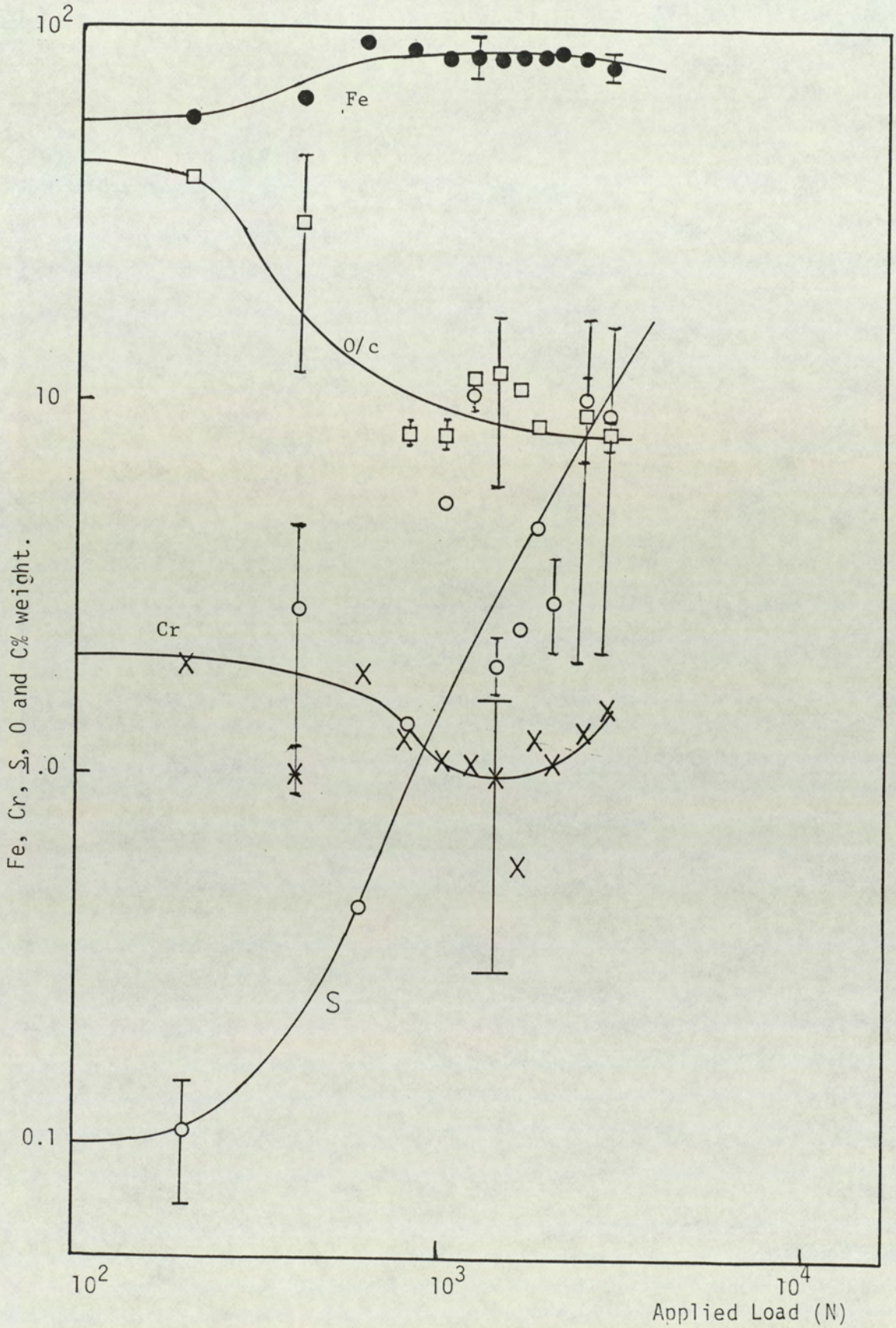

Figure 4.3 Variation of amounts of Fe, Cr, S, O and C in the wear scar with the applied load (N).

Lubricant R32 + 0.25% S.

SAE 52100 steel on 52100 steel.

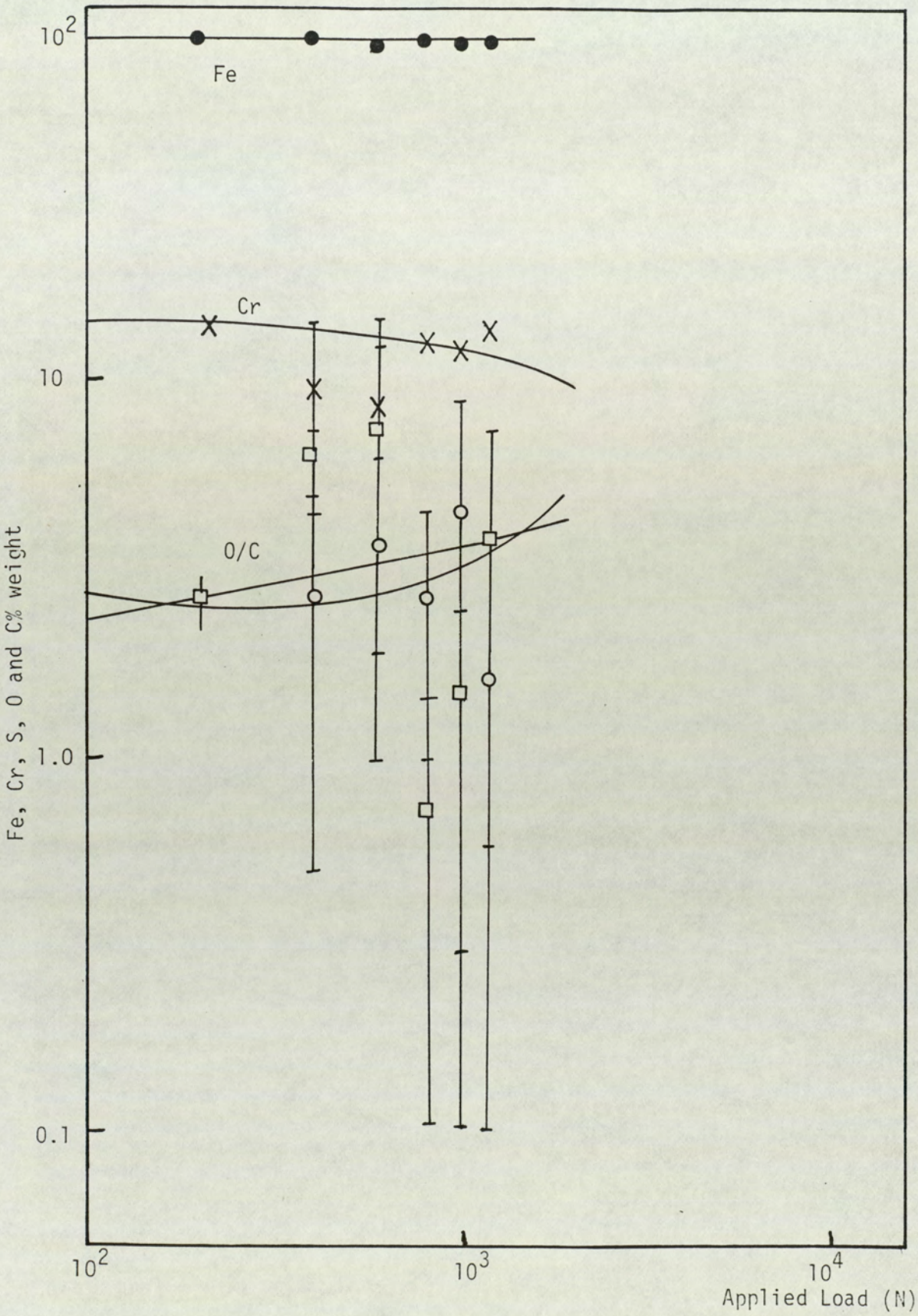

Figure 4.4 Variation of amounts of Fe, Cr, S, O and C in the wear scar with the applied load (N).
Lubricant R32 + 0.25% S.
SAE 52100 steel on AISI 420 stainless steel.

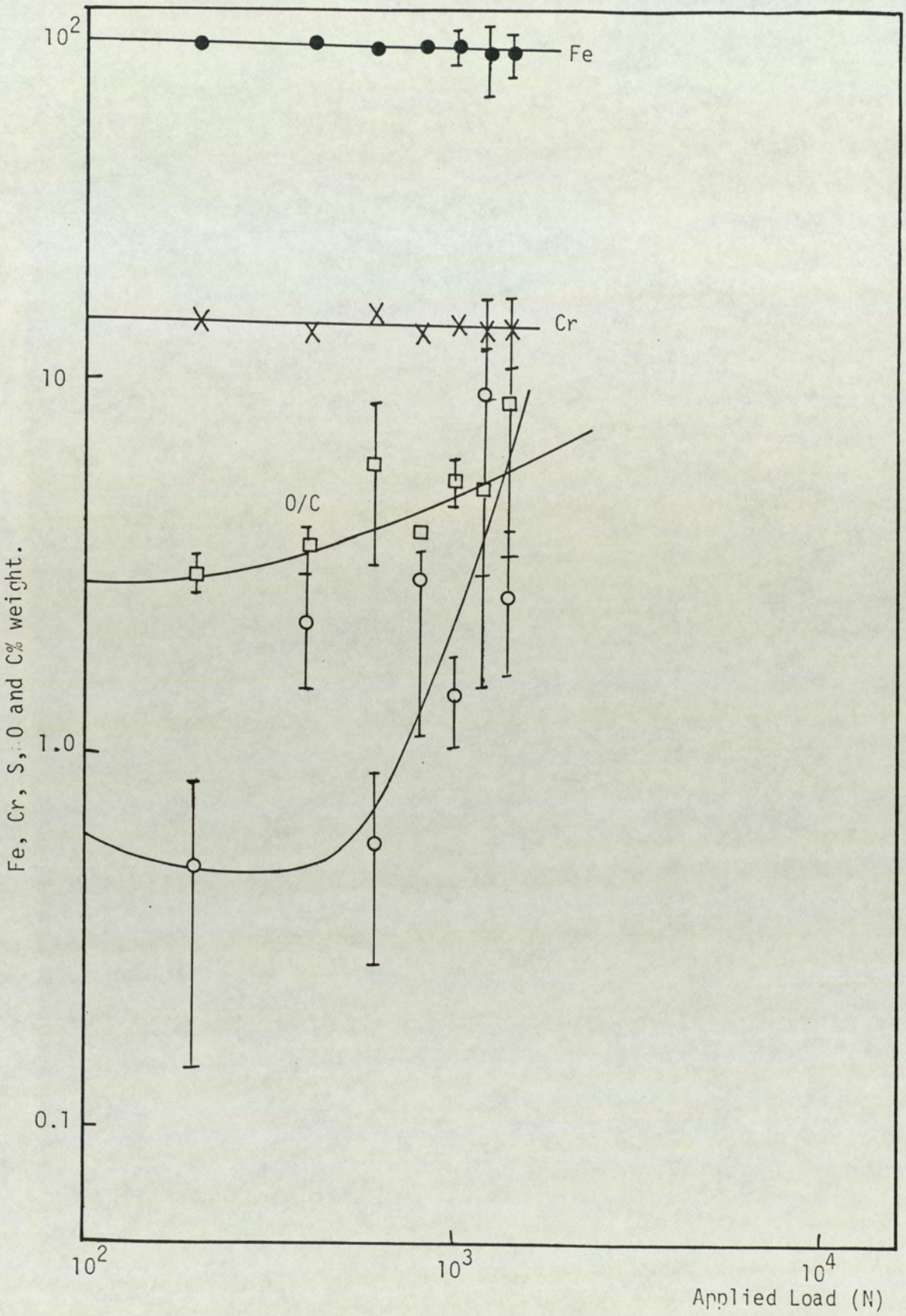

Figure 4.5 Variation of amounts of Fe, Cr, S, O and C in the wear scar with the applied load (N).

Lubricant R32 + 0.25% S.

AISI 420 stainless steel on AISI 420 stainless steel.

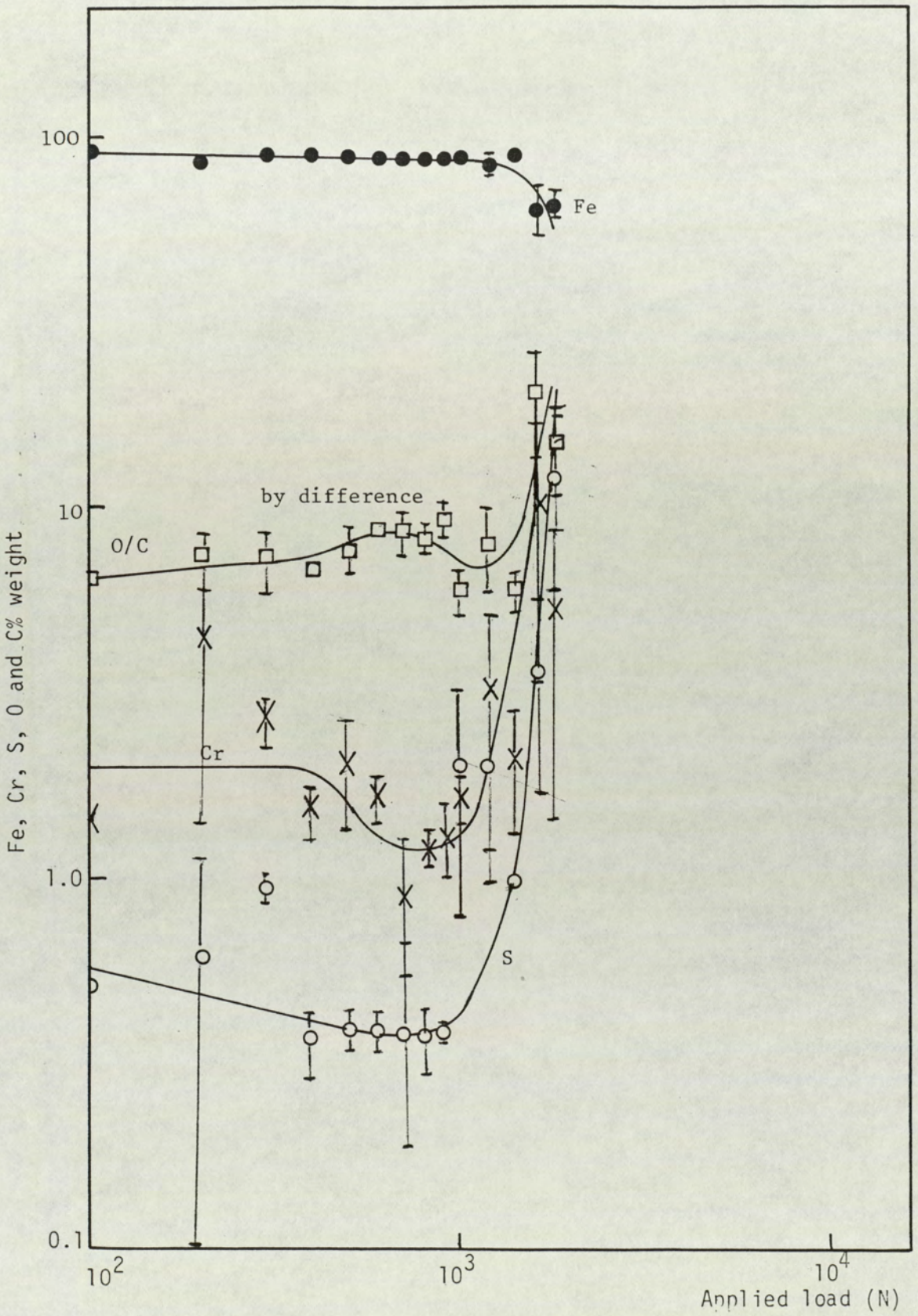

Figure 4.6 Variation of amounts of Fe, Cr, S, O and C in the wear scar with the applied load (N).

Lubricant R32 + 0.25% S.

AISI 420 stainless steel on SAE 52100 steel.

of 100 and 600 N, which represent the AW region, the amount of sulphur was between 0.1 and 0.4% weight, respectively. Sulphur content increased rapidly just after the initial seizure load of 600 N, reaching about 10% weight at 2800 N. In Figure 4.4 the amount of sulphur began to decrease just after 1000 N.

The results of spot analyses of wear scars formed from a rotating martensitic stainless steel ball (AISI 420) on three similar stainless steel balls at loads of 200, 400, 600, 800, 1000, 1200 and 1400 N were plotted in Figure 4.5. These results show that the amount of sulphur increases with increasing load. The minimum and maximum amounts of sulphur, were at 1200 and 200 N respectively. But in Figure 4.6 which shows the element distribution present in wear scars formed under a rotating martensitic stainless steel ball (AISI 420) on three stationary high carbon chrome steel balls (SAE 52100), the amount of sulphur was slowly decreasing around the initial seizure load, reaching its minimum at load 800 N. After this load the amount of sulphur sharply increased, in particular between loads of 1000 and 1800 N, where sulphur content varies between 4.5 and 12%.

The analyses of chromium content in the wear scar, formed under a rotating high carbon chrome steel ball (SAE 52100) on three similar stationary balls indicates that the chromium amount decreases with load reaching its lowest amount at loads of 1000 to 2000 N (see Figure 4.3). The decreasing amount of chromium was noticed at a load of 600 N, just after the initial seizure load. But the amount of chromium started to increase again just after the load of 200 N. However, the highest amount of chromium was seen near the surface of the ball (3.0%) and it was not seen in such amounts in any other wear scar analysed under these conditions.

In the wear scars formed under a rotating high carbon chrome steel ball (SAE 52100) on three stationary martensitic stainless steel balls (AISI 420), the chromium content was around 14% (see Figure 4.4) but it had decreased to its minimum at, and just before, the initial seizure load of 600 N.

In Figure 4.5 the chromium remained at around the same percentage (14%) in the all wear scars analysed under loads of 200, 400, 600, 800, 1000, 1200 and 1400 N.

From an analysis of the wear scars formed under a rotating martensitic stainless steel ball (AISI 420) on three stationary high carbon chrome steel balls (SAE 52100), the chromium was found to be 1.5% at a load of 100 N which was near the surface of the ball, as shown in Figure 4.6. At, and just after, the initial seizure load of 300 N the amount of chromium decreases to between 2.00 and 0.90% and from then onwards increases with increasing load.

Considering Figure 4.3 one can see that the oxygen and carbon content decreases from about 14.00%, at a load of 200 N to 8.5% at a load of 1280 N. Also, the amount of iron in the wear scar formed in the anti-wear region, 80%, was remarkably less than that present in the extreme pressure region, where the amount of iron was 95%.

In Figure 4.4 the highest amount of oxygen and carbon was 7.5% and the chromium content had its lowest value in the wear scar. The iron content varied between 80% and 85%.

When a martensitic stainless steel ball (AISI 420) was run on three similar stainless steel balls, oxygen/carbon concentrations were

found to increase with load as shown in Figure 4.5. But iron varied around 80%, due to the high percentage of chromium present in the wear scars. In Figure 4.6 oxygen and carbon amounts varied between 6.5% and 7.3% in the wear scars formed in the AW region. In the EP region the amounts were between 6% and 12% where a severe wear had taken place. Iron content was high in the wear scars formed under applied loads between 100 and 1000N, but subsequently this content was lost just after 1000 N, reaching about 65% at 1800 N where both sulphur and chromium presence was high, in addition to oxygen and carbon.

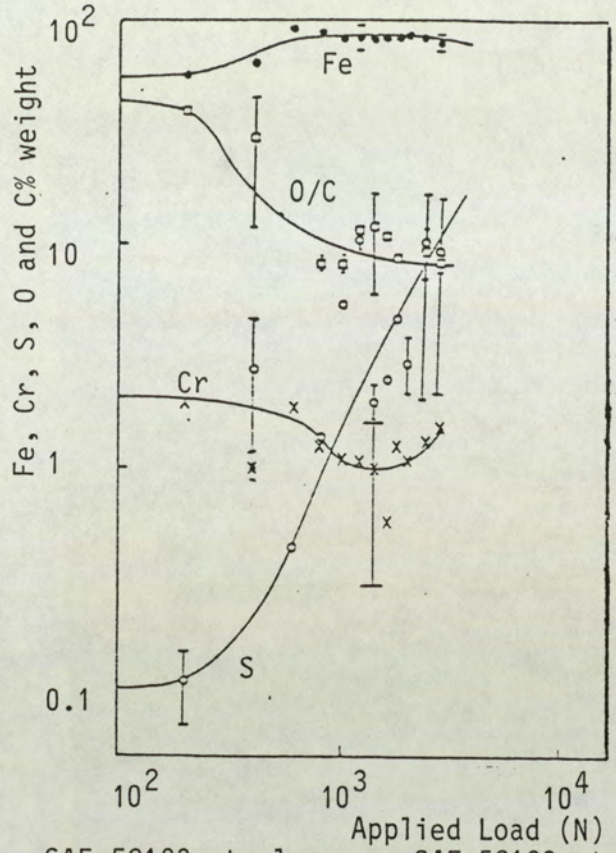

SAE 52100 steel run on SAE 52100 steel.

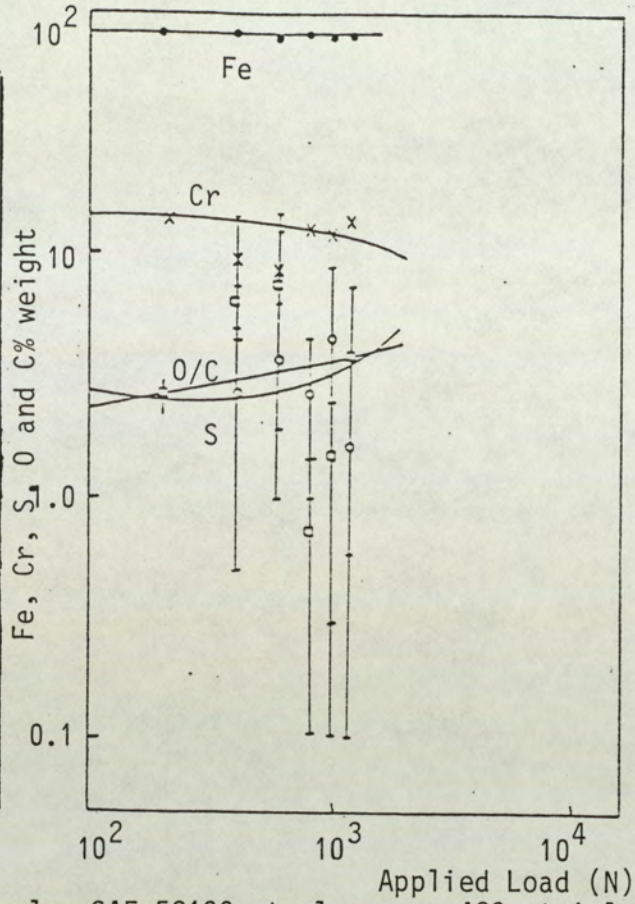

SAE 52100 steel run on 420 stainless steel.

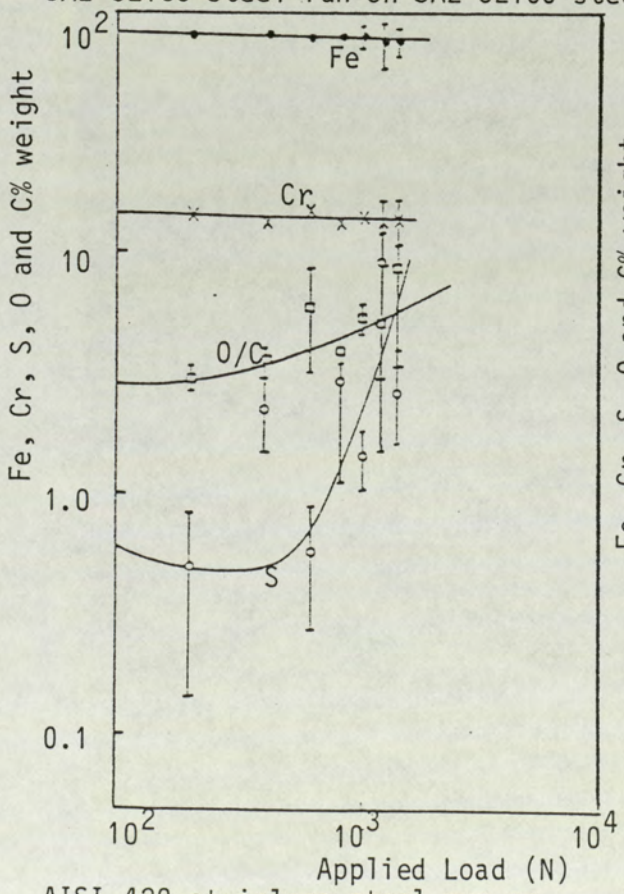

AISI 420 stainless steel run on AISI 420 stainless steel

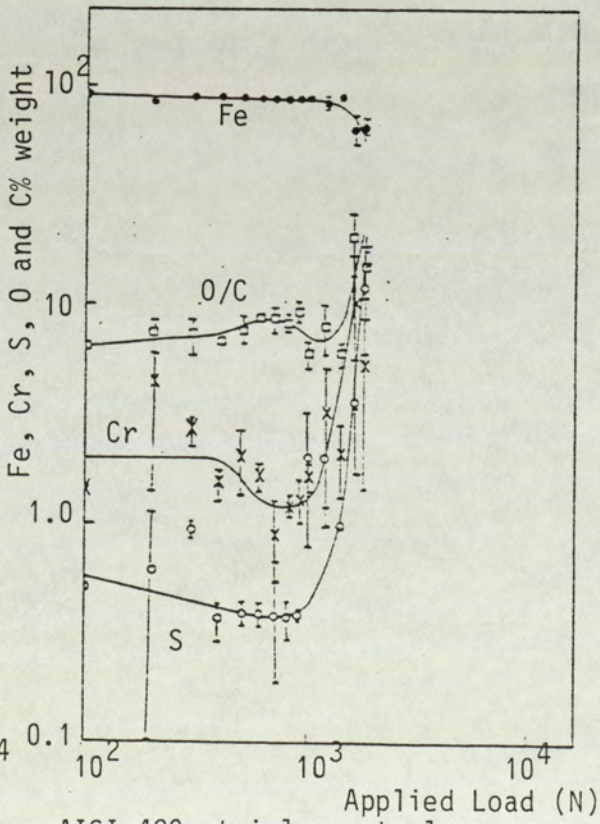

AISI 420 stainless steel run on SAE 52100 steel

Figure 4.7 Variation of amounts of Fe, Cr, S, O and C in the wear scar with the applied load N. Lubricant: R32 + S 0.25%.

4.1:6 Electron probe microanalysis of surfaces worn with Dibenzyl Disulphide (DBDS)

In a similar way, further microprobe analyses were carried out with the four combinations of steels (article 3.1) and the lubricant R32 containing DBDS 1.00% w. In Figure 4.8 the sulphur amounted to nearly 3% in the wear scar of the antiwear region, much higher than shown with the sulphur additive in Figure 4.3. But the amount of sulphur started to decrease just after 400 N. In both Figures 4.8 and 4.9 the sulphur amount was decreasing. However, the general performance of S indicates that content decreases in the anti wear region, with a minimum around the initial seizure load followed by an increase in the EP region.

Looking at Figures 4.10 and 4.11 one can note that the sulphur amounts were increasing with loads. Sulphur content continued to increase, particularly in the extreme pressure region, where martensitic stainless steel (AISI 420) was used as a rotating ball.

In the case of chromium, Figure 4.8 shows that the chromium concentration was about 1.5% regardless of the applied load. Apart from this the amount of chromium started to decrease just after 1000 N. Also, in Figure 3.9 where high carbon chrome steel (SAE 52100) balls were used as stationary ones, the chromium amount was around 14% in the wear scars formed under 200, 400, 600, 800 and 1200 N. However at 1000 N the chromium amount was about 7.7%.

The analysis of chromium concentration in the wear scar formed under the martensitic stainless steel rotating ball shows that the chromium content decreased gradually with the applied load, as shown in Figure 3.10.

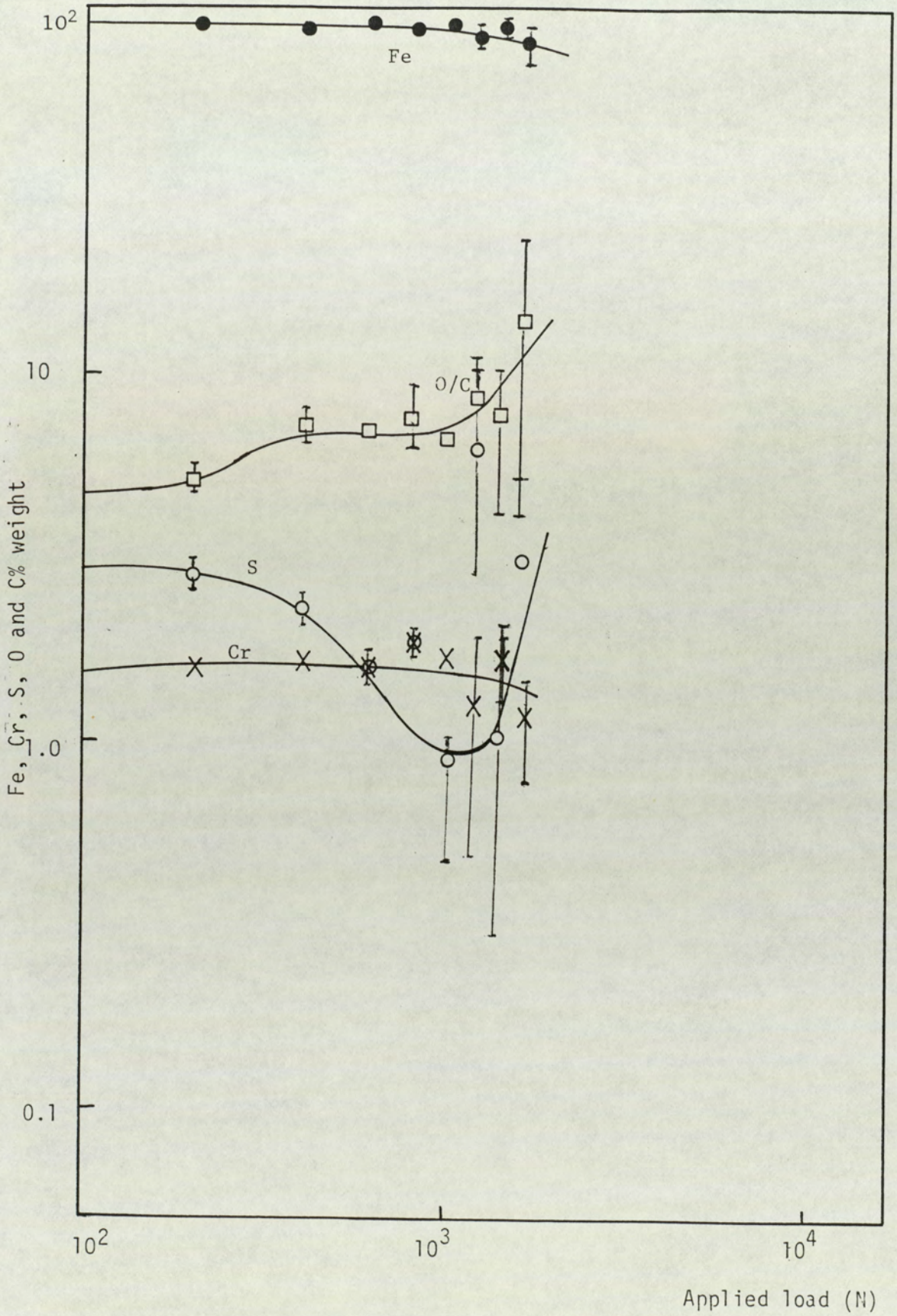

Figure 4.8 Variation of amounts of Fe, Cr, S, O and C in the wear scar with the applied load (N).
Lubricant R32 + 1.00% DBDS
SAE 52100 steel on SAE 52100 steel.

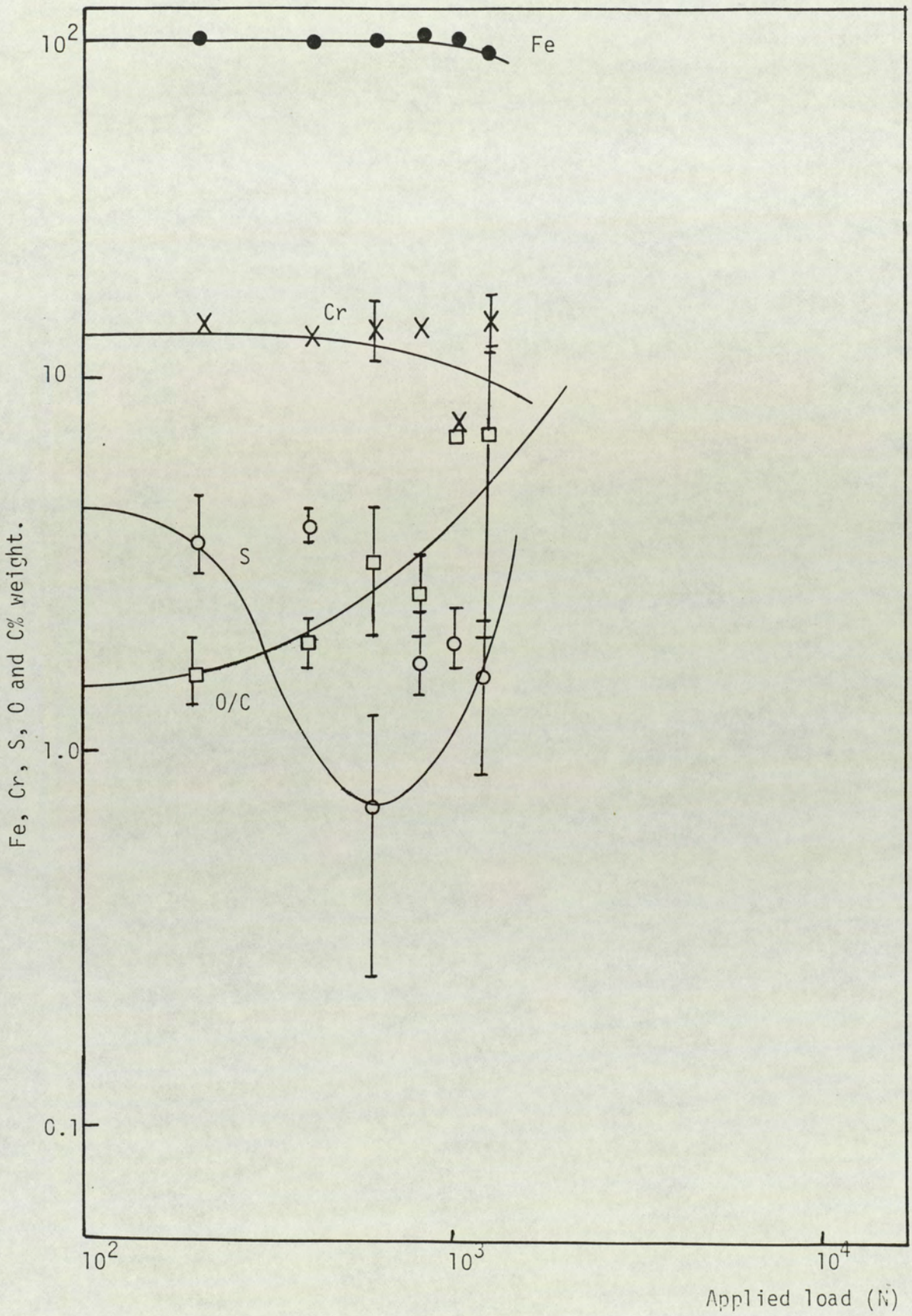

Figure 4.9 Variation of amounts of Fe, Cr, S, O and C in the wear scar with load N.

Lubricant R32 + 1.00% DBDS.

SAE 52100 steel on AISI 420 stainless steel.

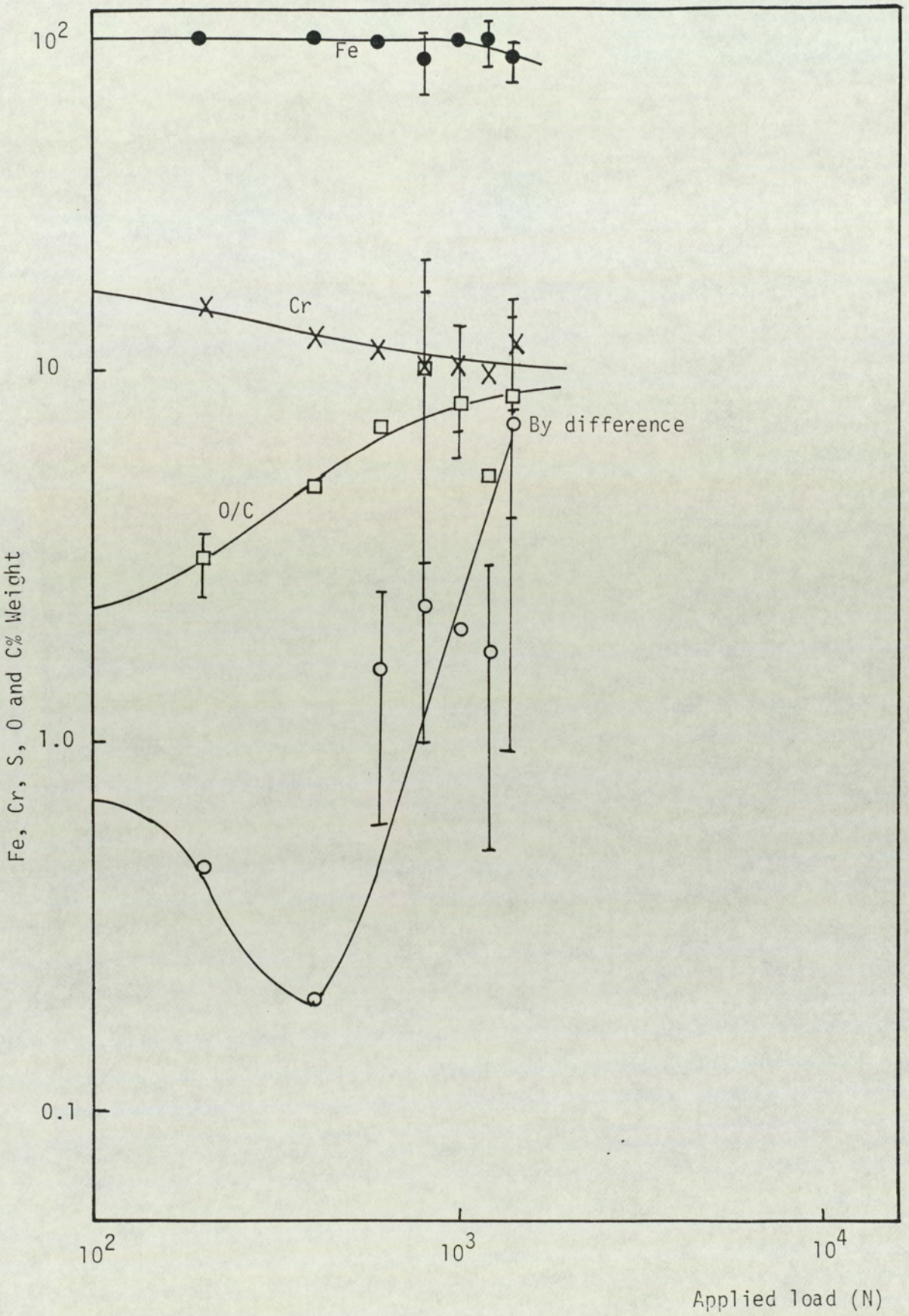

Figure 4.10 Variation of amounts of Fe, Cr, S, O and C in the wear scar with load N.

Lubricant R32 + 1.00% DBDS

AISI 420 stainless steel on AISI 420 stainless steel.

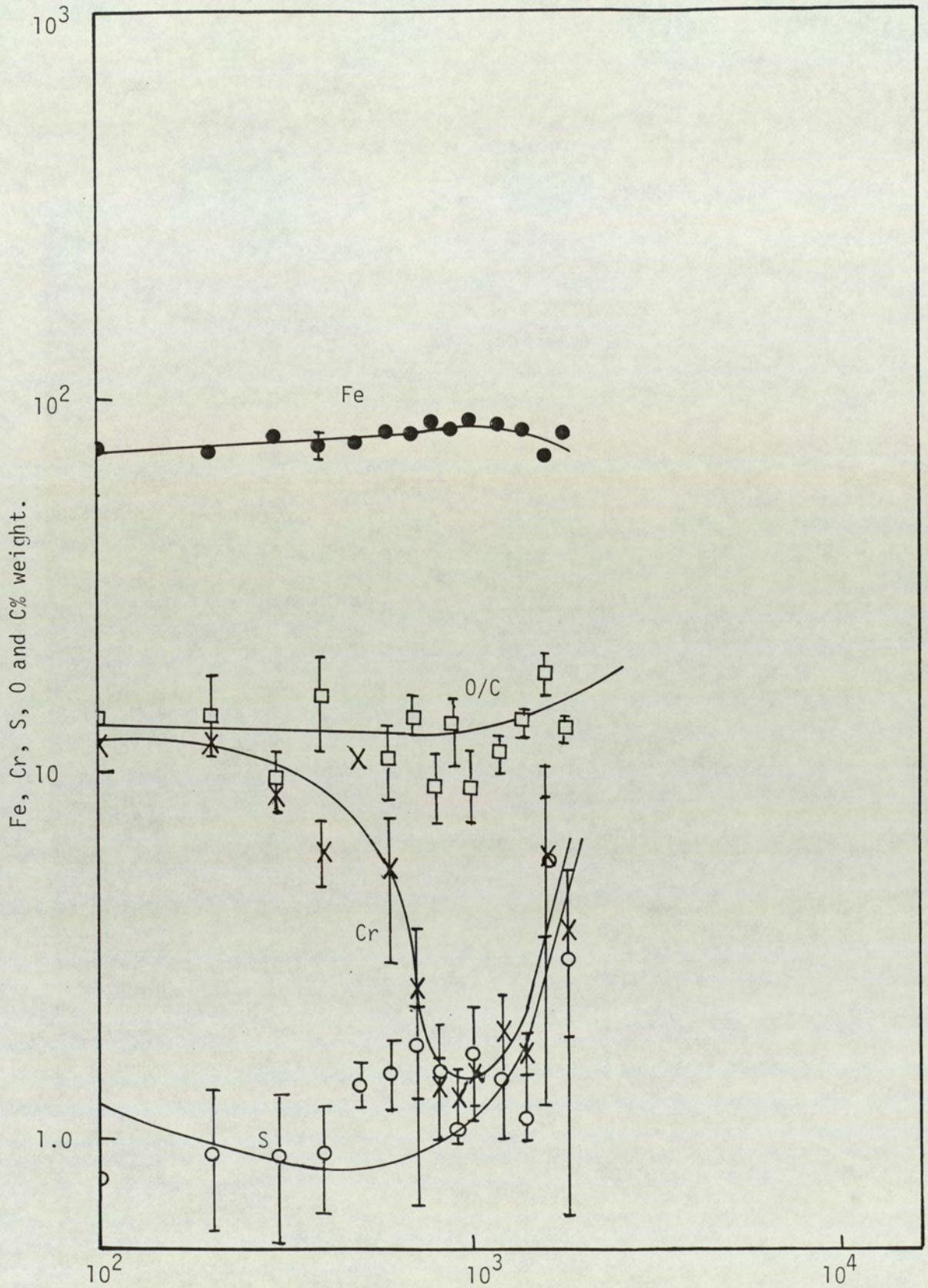

Figure 4.11 Variation of amounts of Fe, Cr, S, O and C in the wear scar with load N.

Lubricant R32 + 1.00% DBDS

AISI 420 stainless steel on SAE 52100 steel.

Also the chromium decreases (see Figure 4.11) just after the initial seizure load 400 N, reachings its minimum amount at around 900 N. The maximum amount of chromium was found in the mean scar formed under small applied loads.

Figures 4.8 and 4.9 show that the amount of iron remained at the same level at loads of 200 up to 1000 N. But this was not so after 1000 N where the amount of iron decreased with the load, regardless of which additive was used, or the kind of rotation. This also can be seen in Figures 4.10 and 4.11 where a martensitic stainless steel ball was involved. as a rotating body in the wear tests carried out with the same additive.

Figure 4.12 shows that oxygen/carbon concentrations generally increased with the applied load, in spite of the combination of high carbon chrome steel and martensitic stainless steel balls.

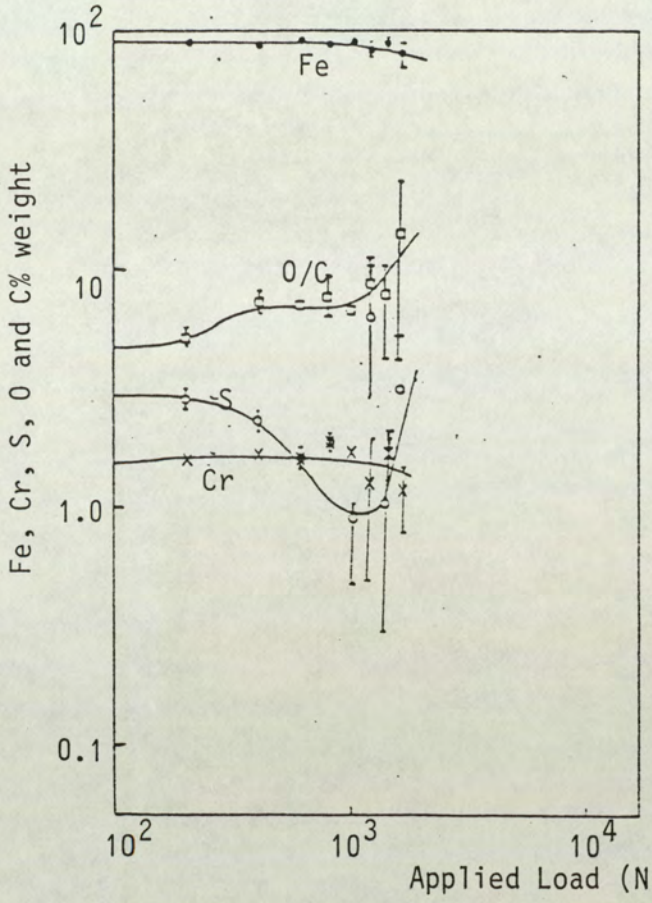

SAE 52100 steel run on SAE 52100 steel.

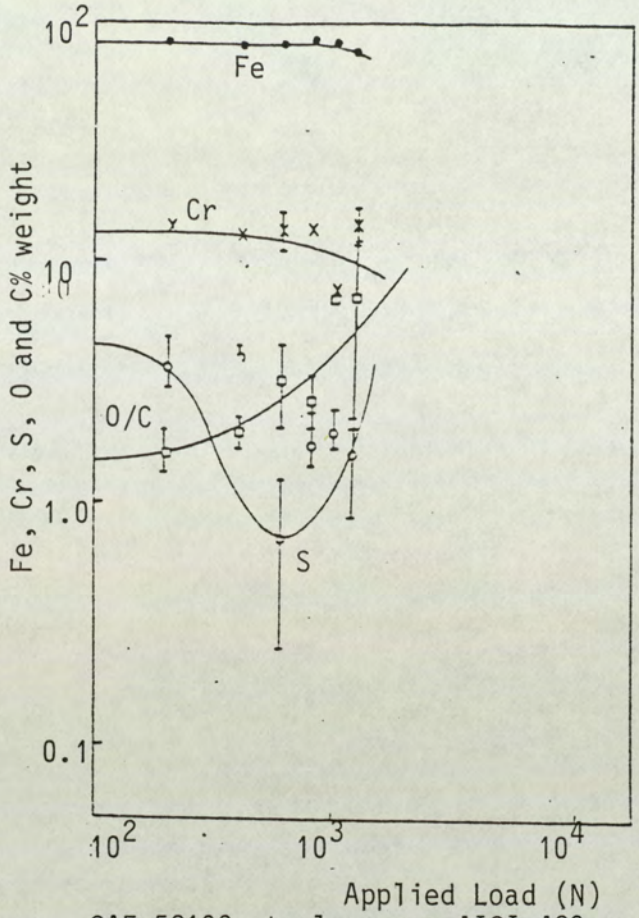

SAE 52100 steel run on AISI 420 stainless steel.

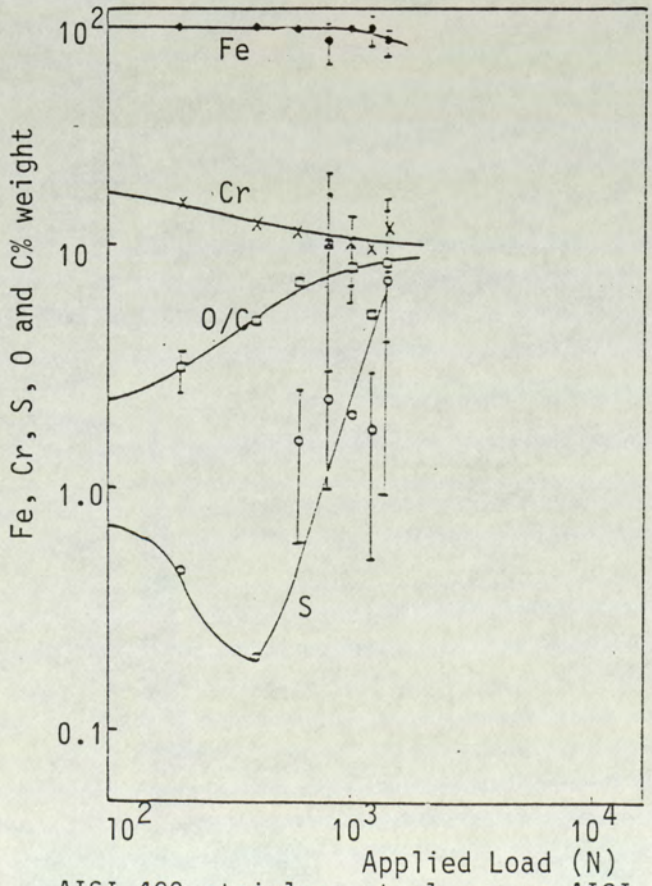

AISI 420 stainless steel run on AISI 420 stainless steel

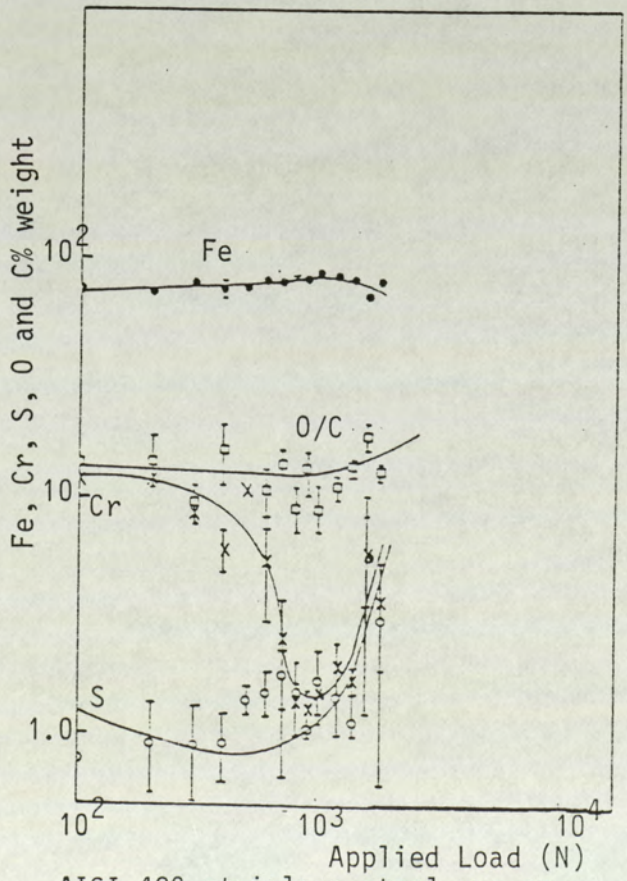

AISI 420 stainless steel run on SAE 52100 steel.

Figure 4.12 Variation of amounts of Fe, Cr, S, O and Cin the wear scar with load N. Lubricant: R32 + 1.00% DBDS.

4.1:7 Electron probe microanalysis of surface worn with Diphenyl Disulphide (DPDS) additive.

The analysis of wear scars formed due to the combinations of high carbon chrome steel (SAE 52100) and martensitic stainless steel (AISI 420) with DPDS additive shows that the amount of sulphur in the wear scar, increased with the applied load, as shown in Figures 4.13, 4.15, and 4.16 whereas in Figure 4.14 the amount of sulphur decreased reaching the minimum amount at the I.S. load and then start to increase with increasing applied load.

In terms of chromium concentration in the wear scars, one can see that the chromium content generally decreases with the increasing applied loads. This is clearly noticed in Figures 4.13 and 4.14 just after 200 N, and in Figures 4.15 and 4.16 just after 400 N where the initial seizure took place.

Analysis carried out regarding iron concentration had shown that there was no remarkable change in the iron content in the wear scar, formed with the increasng applied loads, as shown in Figures 4.13 and 4.14.

In Figure 4.15 the iron content decreases just after 900 N, but increases slightly with applied load varying from 82% up to about 90% (see Figure 3.16).

Oxygen and carbon amounts remained at 10% (Figure 4.13), apart from that found in wear scars formed under 300 N. In Figure 4.14, the oxygen and carbon presence had less content in the wear scar formed under 400, 600 and 800 N than those formed under 200, 1000 and 1200 N.

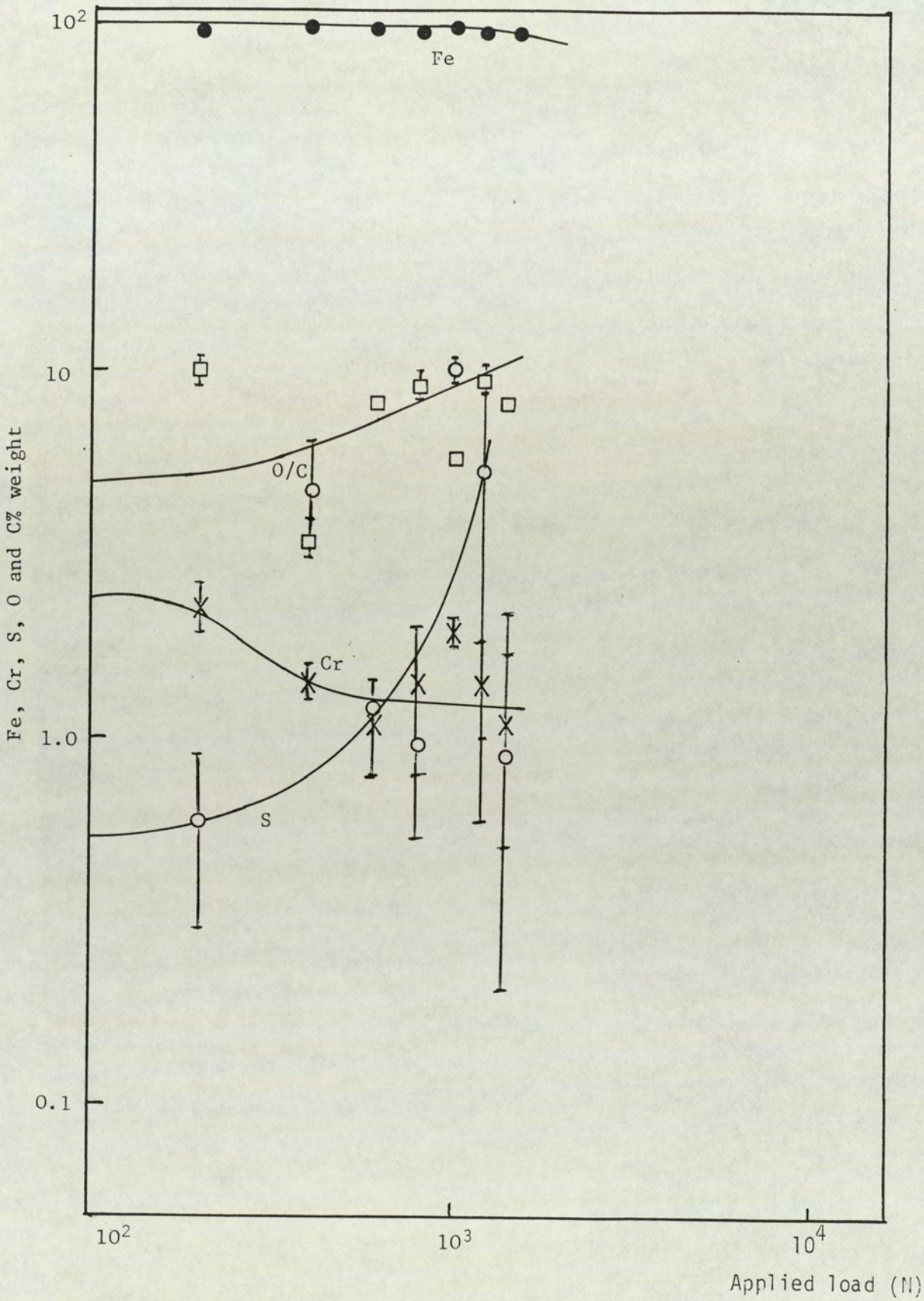

Figure 4.13 Variation of amounts of Fe, Cr, S, O and C in the wear scar with load N.

Lubricant R32 + 0.886% DPDS.

SAE 52100 steel on SAE 52100 steel.

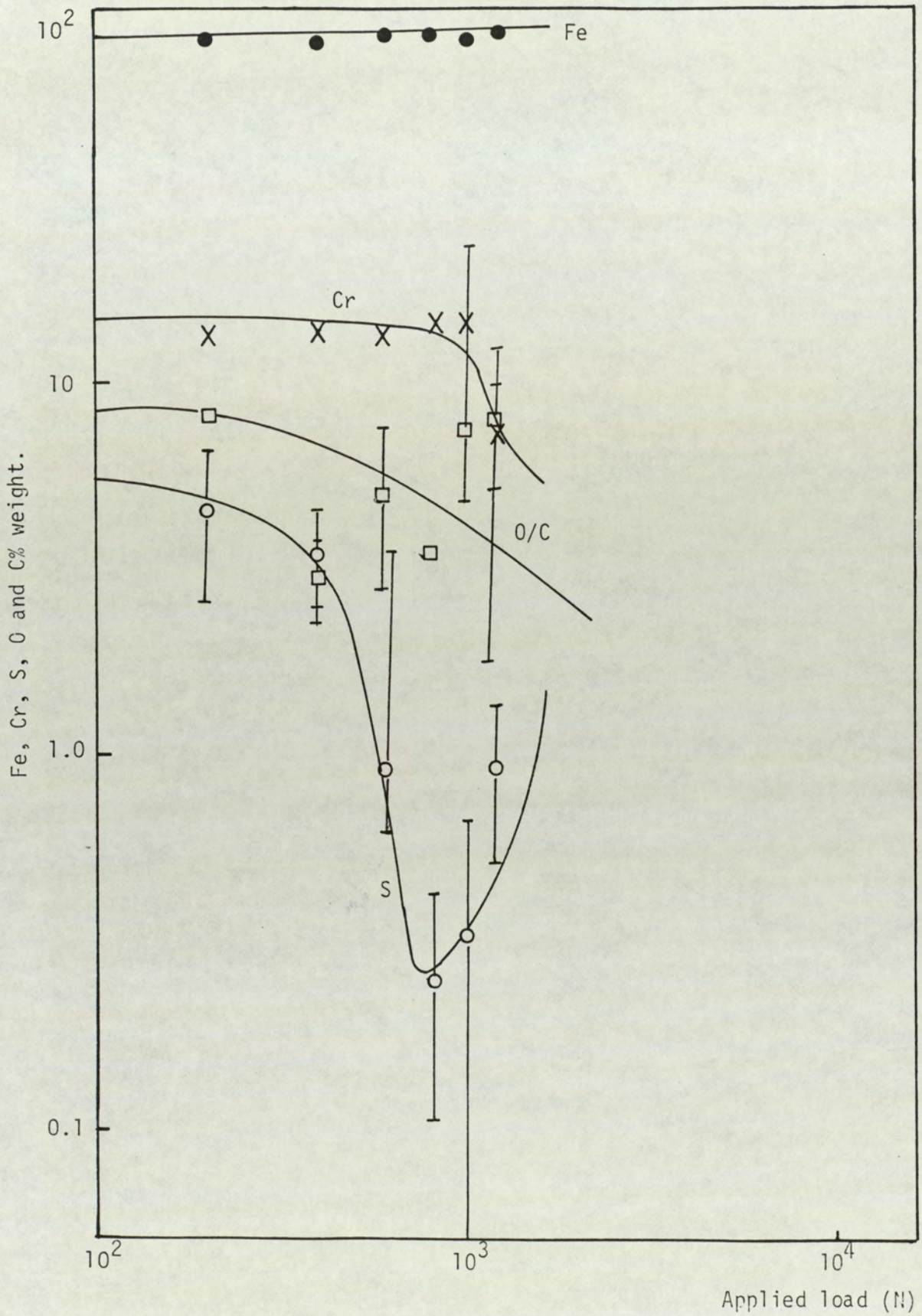

Figure 4.14 Variation of amounts of Fe, Cr, S, O and C in the wear scar with load N.

Lubricant R32 + 0.886% DPDS

SAE 52100 steel on AISI 420 stainless steel.

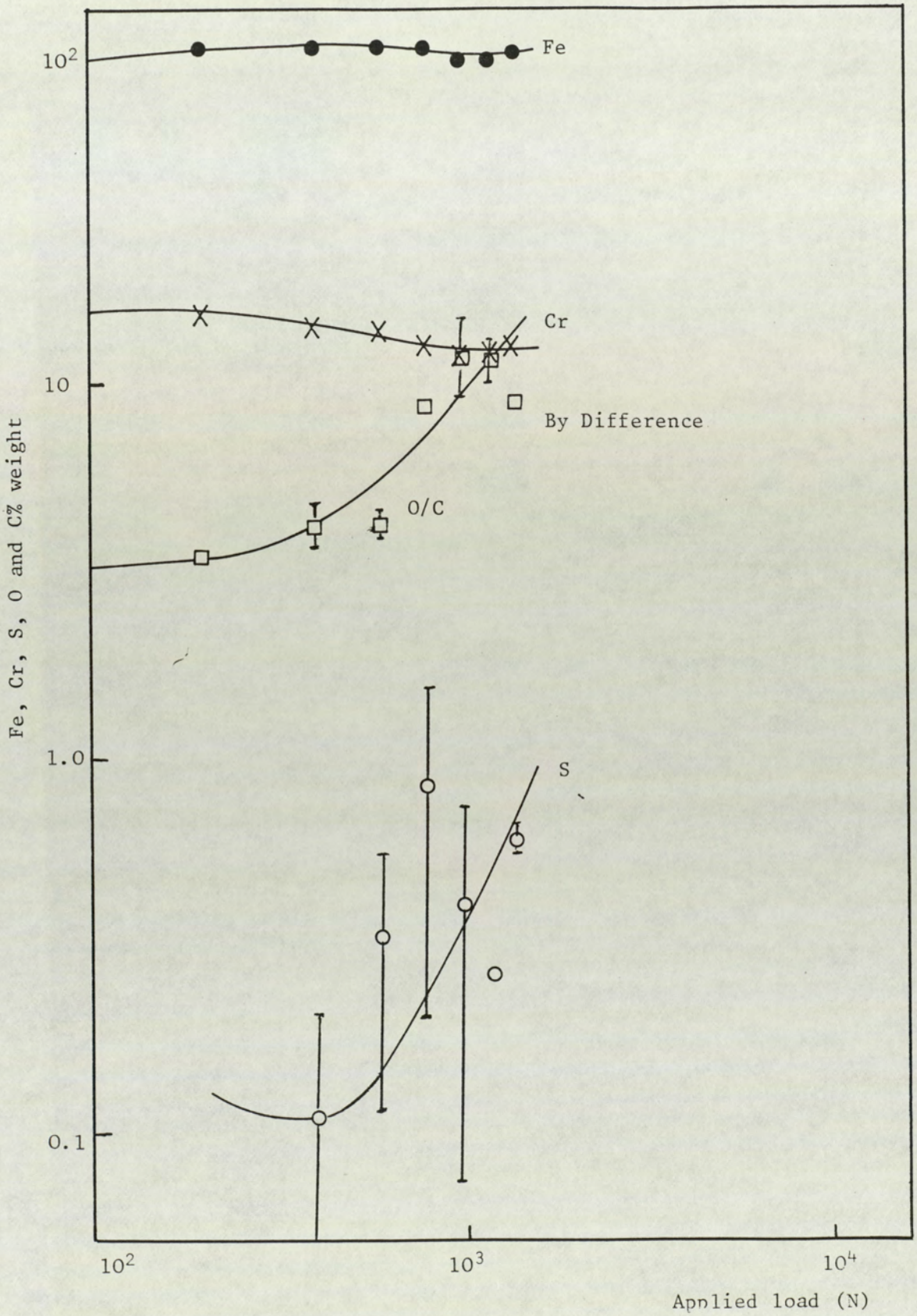

Figure 4.15 Variation of amounts of Fe, Cr, S, O and C in the wear scar with load (N)

Lubricant R32 + 0.886% DPDS

AISI 420 stainless steel on AISI 420 stainless steel

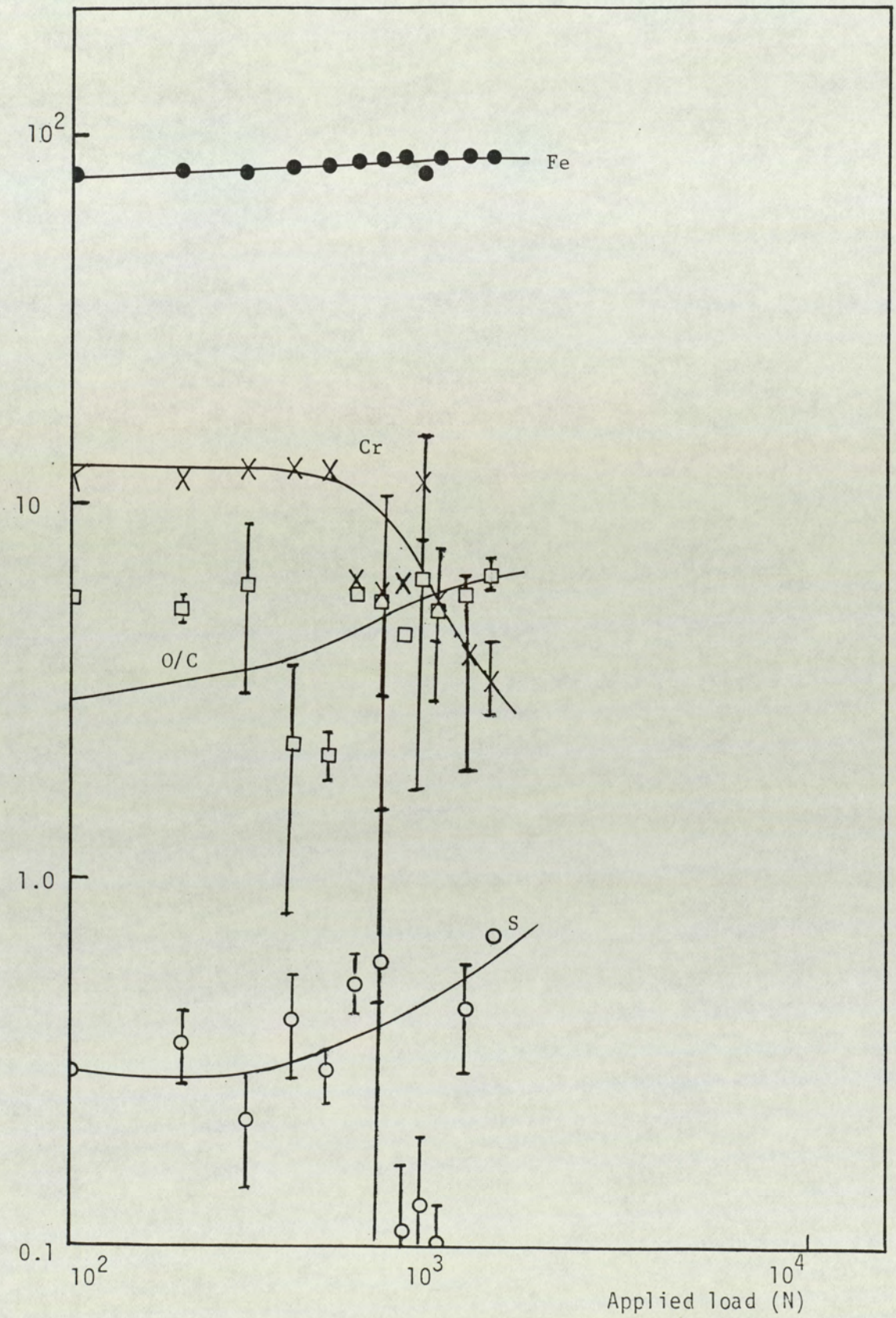

Figure 4.16 Variation of amounts of Fe, Cr, S, O and C in the wear scar with load N.

Lubricant R32 + 0.886% DPDS

AISI 420 stainless steel on SAE 52100 steel.

In Figure 3.15 the lower amount of oxygen and carbon was about 3.3% under 200 N. However, this increases gradually with the increasing applied load, reaching its maximum of 10.15% at 1200 N. Looking at Figure 4.16 the minimum amount of oxygen and carbon was present at 2.2%, in the wear scars formed under the initial seizure load, whereas oxygen and carbon amounts were increasing gradually with the applied loads.

4.1:8 Preliminary discussion on EPMA analysis

The EPMA results obtained by both concentration profile and the spot analyses have shown that chromium distribution is quite different from the iron distribution in both unworn steel and stainless steel materials. chromium distribution was not homogeneous and it varies locally from point to point. In spite of this, the results (shown in Figures 4.1 and 4.2) indicate that the lowest percentages of chromium coicide with the chromium composition of the material. The high percentage of chromium may be interpreted as a result of accumulation of the chromium around its grain boundaries or at the surface in the form of an extremely thin oxide protective layer. The electron probe concentration profile analysis of Cr, S and Fe shows that the distribution of these elements may not be homogeneous in the surface film coating of the wear scar. This is the reason why the average of five different readings was taken. Presumably a high percentage of chromium in the worn surface film corresponds to an average over the chromium in the surface film and in the subsurface material, taking into account that the depth examined was 1-15 μm.

Oxygen and carbon can also be expected in the surface film due to the influence of reactions of the lubricants and sliding materials used.

Clearly iron would have the highest percentage concentration in the surface film due to its major involvement in both rotating and stationary testing pairs.

The constituents of the surface film depend upon the chemical composition of the lubricants and sliding materials. Therefore, the most detectable substances are mainly Fe, Cr, and S. Oxygen/Carbon can be calculated by assuming that any other substances can be neglected.

The EPMA analyses show that the amount of sulphur increases with the increasing applied loads in all wear tests carried out with sulphur additives, despite the use of different combinations of materials. It was noticed that the sulphur percentages decreased slightly with the increasing applied load until the initial seizure load, after which the amount of sulphur began to increase sharply. Sulphur molecules were increasingly adsorbed onto the metal surface, with the increasing temperature.

In Figures 4.6 and 4.8, sulphur concentration decreased partially between 300 N and 1000 N, and then started to increase sharply. In Figures 4.9 and 4.14 the amounts of sulphur decreased to their minimum at the initial seizure loads.

The general tendency of iron was to decrease slightly with the increasing applied loads and especially in the EP region due to the severe wear conditions.

The percentage of oxygen and carbon was related to the presence of Fe, Cr and S. However, their amounts increased with the increasing applied load (see Figure 4.17).

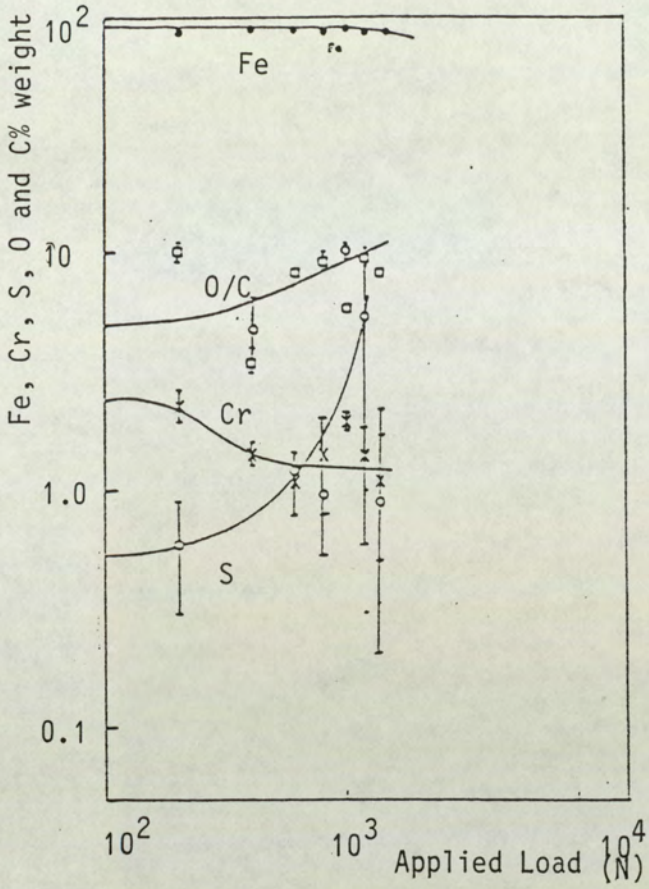

SAE 52100 steel run on SAE 52100 steel.

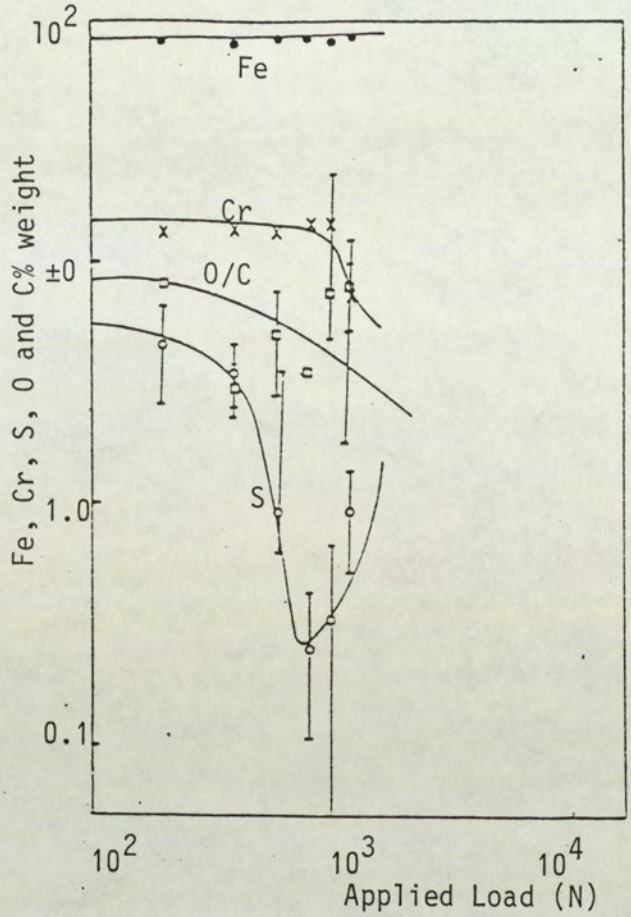

SAE 52100 steel run on 420 stainless steel.

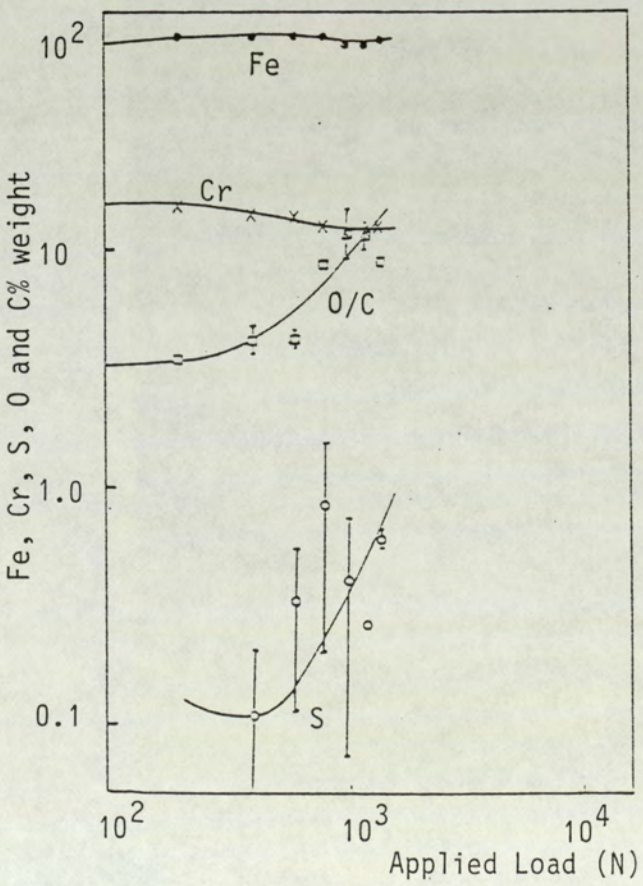

AISI 420 stainless steel run on AISI 420 stainless steel

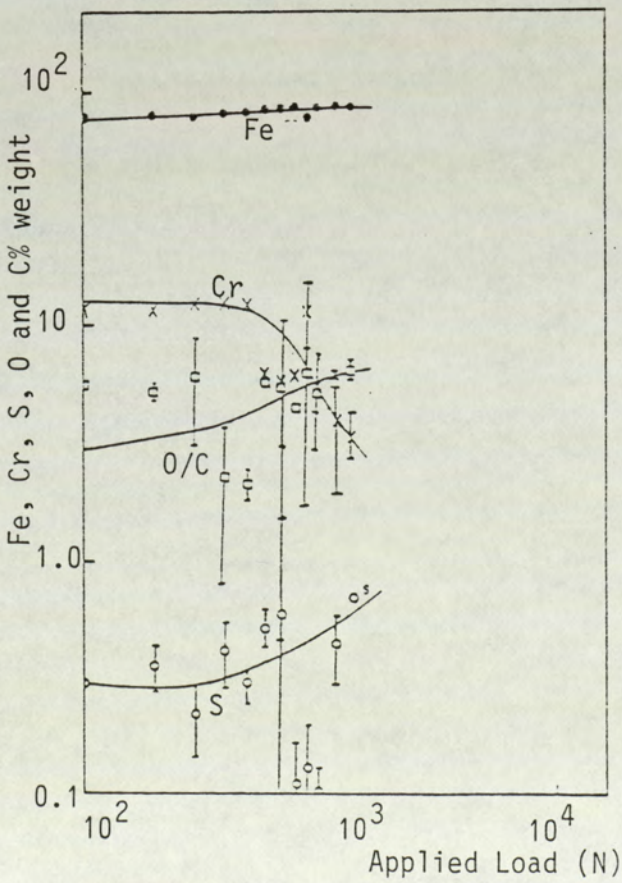

AISI 420 stainless steel run on SAE 52100 steel

Figure 4.17 Variation of amounts of Fe, Cr, S, O and C in the wear scar with load N. Lubricant: R32 + 0.886% DPDS.

It has been noticed that when high carbon chrome steel (SAE 52100) was used in the wear tests for the stationary balls, the percentage of chromium was small (about 1.5%). But this percentage was larger whenever a martensitic stainless steel was used for the rotating ball. This means that there must have been some material transfer occurring.

All oxygen/carbon curves increase with load. One would not expect an increase in carbon because desorption of the hydrocarbon molecules will occur with increase in load. Hence this tells us that some oxides are produced as the load increases. Sulphur is generally decreased at and around the initial seizure load and then increases in the EP region.

The distribution of Cr, in general, decreased with increasing applied load, but Figure 4.6 shows some Cr transfer from the rotating ball to the stationary balls. Also, this kind of transfer can be seen in Figure 4.11.

4.2 X-ray Diffraction

4.2:1 Introduction

X-ray diffraction is a technique widely used for many purposes such as identification and quantitative analysis of elements, compounds and mixtures. X-ray diffraction techniques are concerned with the positions of the diffraction peaks.

The glancing, edge-irradiated, X-ray diffraction technique was used in this X-ray diffraction analysis. This technique was used by Isherwood and Quinn[34], which is particularly relevant to the analysis of surface

structure present in worn surfaces (balls and rollers) where there is no restriction upon specimen geometries. The glancing-angle technique can be used where the specimen is relatively large, provided it has a sharp edge. Balls, or rollers, worn under applied loads were selected, from the antiwear and extreme pressure regions, for the X-ray analysis.

A cylindrical X-ray diffraction camera was used to record the diffraction pattern from the surface of the thin film which covers the wear scar. The camera was designed with a radius of 57.3 mm, which means that the distance between the collimated and transmitted beams must be 180 mm. This will enable us to measure the angle 2θ directly in degrees by measuring the distance in millimeters, as shown schematically in Figure 4.18. Also the camera was designed to take X-ray film of 35 mm width. The cylindrical X-ray diffraction camera is particularly useful for identification, where every element or compound produces a unique pattern.

4.2:2 Operating procedures

The specimen (worn ball or roller) had to be cut off, so that a sharp edge throughout the wear scar could be obtained. The specimen was then placed in the centre of the camera. The wear scar surface was fixed in a position where the collimated, monochromatic X-ray beam impinged on the specimen at a glancing-angle ($2\theta^{o}$), at one extreme edge of the specimen. The diffracted beams were detected on a cylindrical film centered about an axis through the centre of the flat face of the specimen, as shown in Figures 4.19 and 4.20.

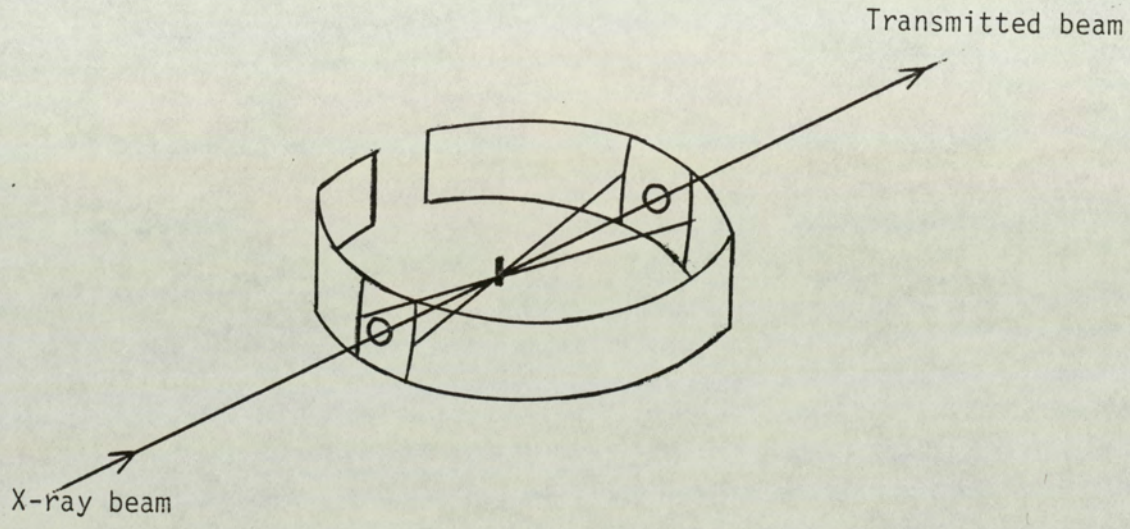

Figure 4.18 A schematic diagram showing how the cylindrical X-ray diffraction technique records diffraction patterns on a photographic film held against the inner surface of a cylindrical camera.

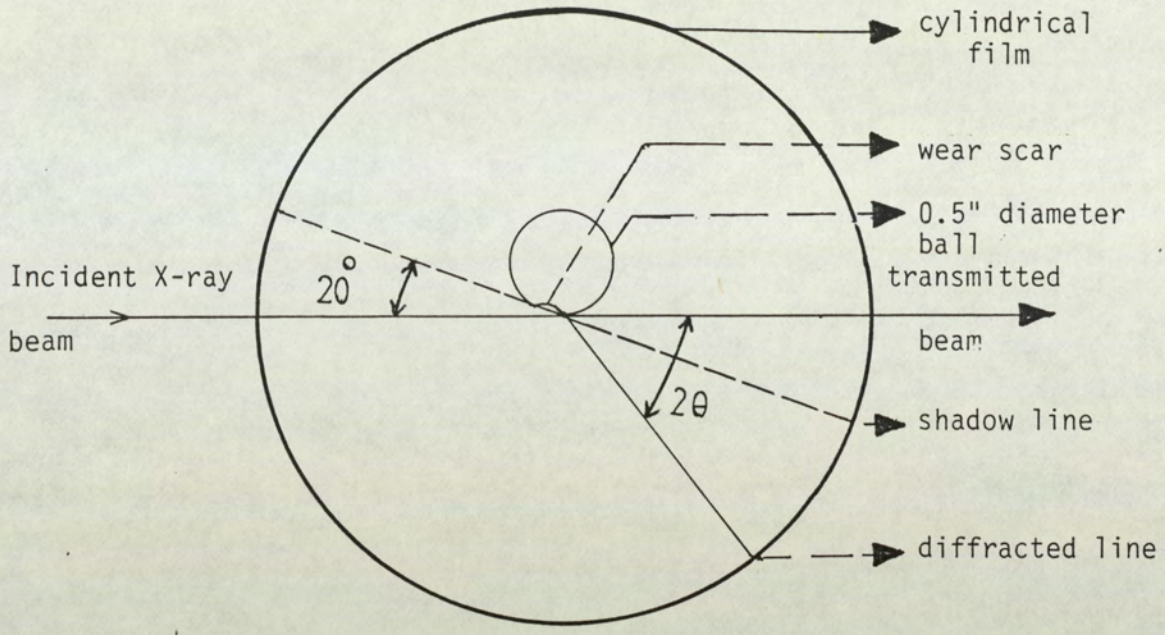

Figure 4.19 Diagram of the glancing-angle X-ray diffraction through a cross-section of a ball bearing wear scar.

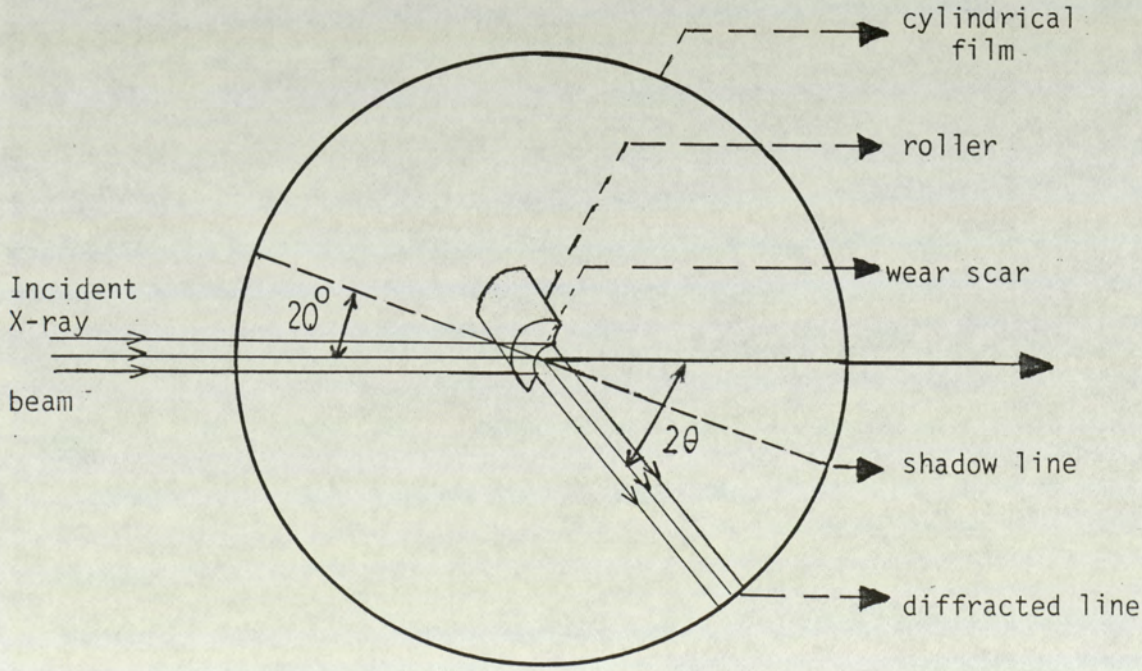

Figure 4.20 Diagram of the glancing-angle X-ray diffraction through a cross-section of a roller wear scar.

The above-mentioned glancing-angle geometry was experimentally chosen in order to record the best diffraction maxima, i.e. line broadening effects due to the exposure of large area of the specimen to the incident X-ray beam were avoided.

The specimen was irradiated by cobalt Kα X-ray so as to obtain a diffraction pattern free from the fluorescent effects of iron with copper radiation. The exposure time required for the irradiation was 30 minutes. Several specimens were selected from the AW and EP regions of each lubricant for each case of rotation, as described in Section 3.1, and were analysed by this technique.

4.2:3 Identification of worn specimens by means of cylindrical X-ray camera

There are two principal requirements for successful identification:

(i) A satisfactory diffraction pattern must be obtained on photographic X-ray film.

(ii) Satisfactory reference data for the compound must be available.

The X-ray photographic film was used to measure 2θ and thence through a simple calculation (the Bragg relation)[38], d (the interplanar spacing) was obtained. All interplanar spacings recorded in the X-ray photographic film were measured and then compared with the interplanar spacings noted in the X-ray powder data file issued by the American Society for Testing and Materials (A.S.T.M.).

The d-values of the strongest lines in the X-ray diffraction pattern to be expected from the specimens were found from the file manual and data-card of (A.S.T.M.) and compared with corresponding lines in the

obtained pattern.

The X-ray diffraction pattern of iron was used as a standard pattern due to the ease of identification of its interplanar spacings. As an additional reference, the X-ray diffraction film of the worn roller formed under the applied load of 400 N with the lubricant R32 containing sulphur additive was used to identify the elements and compounds which existed in other X-ray patterns.

4.2:4 X-ray diffraction analysis of worn surfaces using disulphide additives

This analysis was based on choosing one specimen from each antiwear and extreme pressure region which occurred under each of the lubricants used, and formed under each case of rotation (as mentioned earlier in Section 3.1). Then identifications were carried out on each of the X-ray diffraction films.

(a) X-ray diffraction analysis of surface worn using sulphur additive

Table 4.2 shows that more compounds existed in the wear scar formed under running martensitic stainless steel balls (AISI 420) on three high carbon chrome steel rollers (SAE 52100) these compounds are αFe_2O_3, Fe_3C, $\alpha Fe(Cr)$, Cr_2O_3, Cr_3S_4 and Cr_7C_3.

The analyses of wear scars formed under the EP region revealed that Fe_3C and Cr_7C_3 could possibly be observed in addition to α-Fe and Cr. Also, FeS was found only when the rotating and stationary bodies were of similar material, SAE 52100 steel. The table shows that the presence of

steel 52100 / steel 52100		steel 52100 / stainless steel 420		stainless steel 420 / stainless steel 420		stainless steel 420 / steel 52100	
300 N AW	1400 N EP	300 N AW	1400 N EP	300 N AW	1000 N EP	400 N AW	1200 N EP
αFe	αFe	αFe	αFe	αFe	αFe	αFe	αFe
	αFe_2O_3					αFe_2O_3	
	FeS					γFe_2O_3	
	FeC						
	Fe_3C				Fe_3C	Fe_3C	Fe_3C
						$FeCr_2O_4$	$FeCr_2O_4$
	$\alpha FeCr$		$\alpha FeCr$		$\alpha FeCr$	$\alpha FeCr$	$\alpha FeCr$
Cr	Cr	Cr	Cr	Cr	Cr	Cr	Cr
						Cr_2O_3	
						Cr_3S_4	
			Cr_7C_3		Cr_7C_3	Cr_7C_3	Cr_7C_3

Table 4.2 Showing the possible compositions in wear scars produced under Risella 32 containing sulphur additive by using the glancing-angle X-ray diffraction technique.

other compounds such as Fe_3C, FeCr and Cr_7C_3, in all wear scars analysed from EP regions. FeCr lines were the only lines which could be seen clearly in the unworn surfaces of both SAE 52100 and AISI 420 steels.

(b) X-ray diffraction of surfaces worn under using DBDS additive

Results obtained from the X-ray diffraction patterns show, more or less, the same elements and compounds as were found in the wear scars formed with the sulphur additive. Table 4.3 shows that Fe_3C and Cr_7C_3 were present in the wear scars formed under AW and EP conditions involving martensitic stainless steel (AISI 420) whether it was in rotating or stationary balls. However this was not seen with the high carbon chrome steel balls (SAE 52100).

(c) X-ray diffraction of surfaces worn under using DPDS additive

Analysis of wear scars formed under AW and EP conditions with DPDS additive showed (see Table 4.4) lines due to αFe, Cr in all cases of rotation, similar to those obtained with S and DBDS additives. But the presence of the other elements or compounds was less discernable compared to those Fe_3C, αFeCr and Cr_7O_3 which were obtained under EP conditions (see Table 4.4).

The surface films produced by a rotating martensitic stainless steel ball on steel rollers showed that Fe_3O_4, γ-Fe_2O_3, FeS and CrO_2 are present in the surface films of the EP region. However, Fe_3O_4 and γ-Fe_2O_3 lines were not observed in the surface films produced in the AW region.

SAE 52100 steel / SAE 52100 steel		SAE 52100 steel / AISI 420 stainless steel		AISI 420 stainless steel / AISI 420 stainless steel		AISI 420 stainless steel / SAE 52100 steel	
300 N AW	1400 N EP	300 N AW	1200 N EP	300 N AW	1400 N EP	200 N AW	1400 N EP
αFe	αFe	αFe	αFe	αFe	αFe	αFe	αFe
							Fe_3O_4
						αFe_2O_3	αFe_2O_3
							γFe_2O_3
				FeS			FeS
	FeC						
	Fe_3C		Fe_3C	Fe_3C	Fe_3C	Fe_3C	Fe_3C
			αFeCr	αFeCr	αFeCr		αFeCr
Cr	Cr	Cr	Cr	Cr	Cr		Cr
						Cr_2O_3	CrO_2
			Cr_7C_3	Cr_7C_3	Cr_7C_3	Cr_7C_3	Cr_7C_3

Table 4.3 Showing the possible composition in wear scars produced under DBDS additive by using the glancing-angle X-ray diffraction technique

SAE 52100 steel / SAE 52100 steel		SAE 52100 steel / AISI 420 stainless steel		AISI 420 stainless steel / AISI 420 stainless steel		AISI 420 stainless steel / SAE 52100 steel	
300 N AW	1400 N EP	300 N AW	1000 N EP	300 N AW	1000 N EP	400 N AW	1400 N EP
αFe	αFe	αFe	αFe	αFe	αFe	αFe	αFe
							FeO
			Fe_3O_4				Fe_3O_4
							γFe_2O_3
						FeS	FeS
	FeC						
	Fe_3C				Fe_3C	Fe_3C	Fe_3C
					αFeCr	αFeCr	αFeCr
						CrO_2	CrO_2
Cr	Cr	Cr	Cr	Cr	Cr	Cr	Cr
			Cr_7C_3	Cr_7C_3	Cr_7C_3	Cr_7C_3	Cr_7C_3

Table 4.4 Showing the possible compositions in wear scars produced under DPDS additive by using the glancing-angle X-ray diffraction technique.

4.2:5 Preliminary discussion on X-ray diffraction analyses

X-ray diffraction analyses showed that only αFe and Cr lines were present in all patterns obtained from specimens selected from AW and EP regions, and that Fe and Cr compounds were present in the EP regions.

Whenever martensitic stainless steel (AISI 420) was involved in the wear test, Cr_7C_3 could be seen in the X-ray diffraction patterns of the EP regions. This is perhaps due to the presence of large quantities of chromium carbides in the stainless steel surface.

The X-ray diffraction showed that Cr_7C_3 was less detectable when high carbon steel was involved in the rotating and stationary balls. Iron carbides were observed mainly in the EP regions. This may be due to interaction between hydrocarbon and steel surfaces at these high pressures. The X-ray diffraction analyses showed that the surface film had no detectable amounts of iron and/or chromium oxides in the AW region for any combination apart from rotating stainless steel (AISI 420) against (SAE 52100) steel. In this instance, it was shown that γFe_2O_3 and CrO_2 are formed in the EP regions and Cr_2O_3 in the AW regions.

From these analyses (see Tables 4.2, 4.3 and 4.4) it seems that thick surface films do provide good protection due to the presence of iron oxides and FeS.

4.3 Scanning Electron Microscopy (SEM)

4.3:1 Introduction

The SEM is one of the most important instruments available for the study and analysis of the microstructural characteristics of solid specimens.

The technique has been very useful to tribologists in studies of surface topographies and their relevance to the mechanisms of lubrication, friction and wear. The importance of using SEM arises from its wide range of magnifications, its convenience for studying bulk surfaces, its great depth of focus, and its capability for giving a clear picture of surfaces together with the three dimensional appearance of the specimen. Also, SEM can tell us much about the actual surface and how the surface topography changes throughout the interaction with another surface. Also, the worn surfaces can be studied with this technique without the necessity for taking replicas.

The SEM in its most common form consists of two basic systems with the specimen at the interface. The first system is the electron optical column which provides the scanning electron beam, for illumination of the specimen. The second part of the SEM comprises of a signal collection and display system. By using the X-ray signals the SEM can provide useful information about the elements present at the surface of the specimen.

4.3:2 Methods of analysis

Unworn and worn balls or rollers from wear tests carried out with all used lubricants and under the four cases of rotations were analysed by SEM. The specimens were chosen from both antiwear and extreme pressure regions. This was necessary to study the topography and composition of the surfaces. Also, specimens worn under the same applied loads were chosen to observe the possible change in the stationary balls and rollers which were used in the wear tests. Each specimen was cut off and mounted in a conducting powder, then well polished, cleaned and etched with a suitable reagent (2% Nital for SAE 52100 steel and Vilella's reagent for AISI 420 stainless

steel). The analyses were carried out around the scar and in the bulk of the specimen. X-ray distribution photographs were taken relating to the elements which were present.

4.3:3 Scanning electron microscopy of the unworn specimens

Unworn SAE 52100 balls or rollers and martensitic stainless steel balls (AISI 420) were analysed using the SEM to investigate the elements present in the surfaces. The chemical analysis in the scanning electron microscope is performed by measuring the energy and intensity distribution of the X-ray signal generated by a focussed electron beam on a particular area of the analysed specimen. Figure 4.21 shows the spectrum of elements present in the surface of unworn high carbon chrome steel ball or roller (SAE 52100). Also, Figure 4.22 shows the spectrum of elements present in the surface of unworn martensitic stainless steel balls (AISI 420). Looking carefully at the two figures, one can notice clearly the existence of α-Fe and Cr as indicated by the X-ray diffraction examination described earlier. Also, there are higher percentages of Cr and Mn in unworn stainless steel (AISI 420) compared with those observed in unworn (SAE 52100) steel which resulted from the difference of Cr content. This confirms the chemical composition of the two materials given in detail in Section 2.4. The structure of both materials also was examined by the SEM after the unworn surface from each of them had been etched as shown in Figures 4.23 and 4.24.

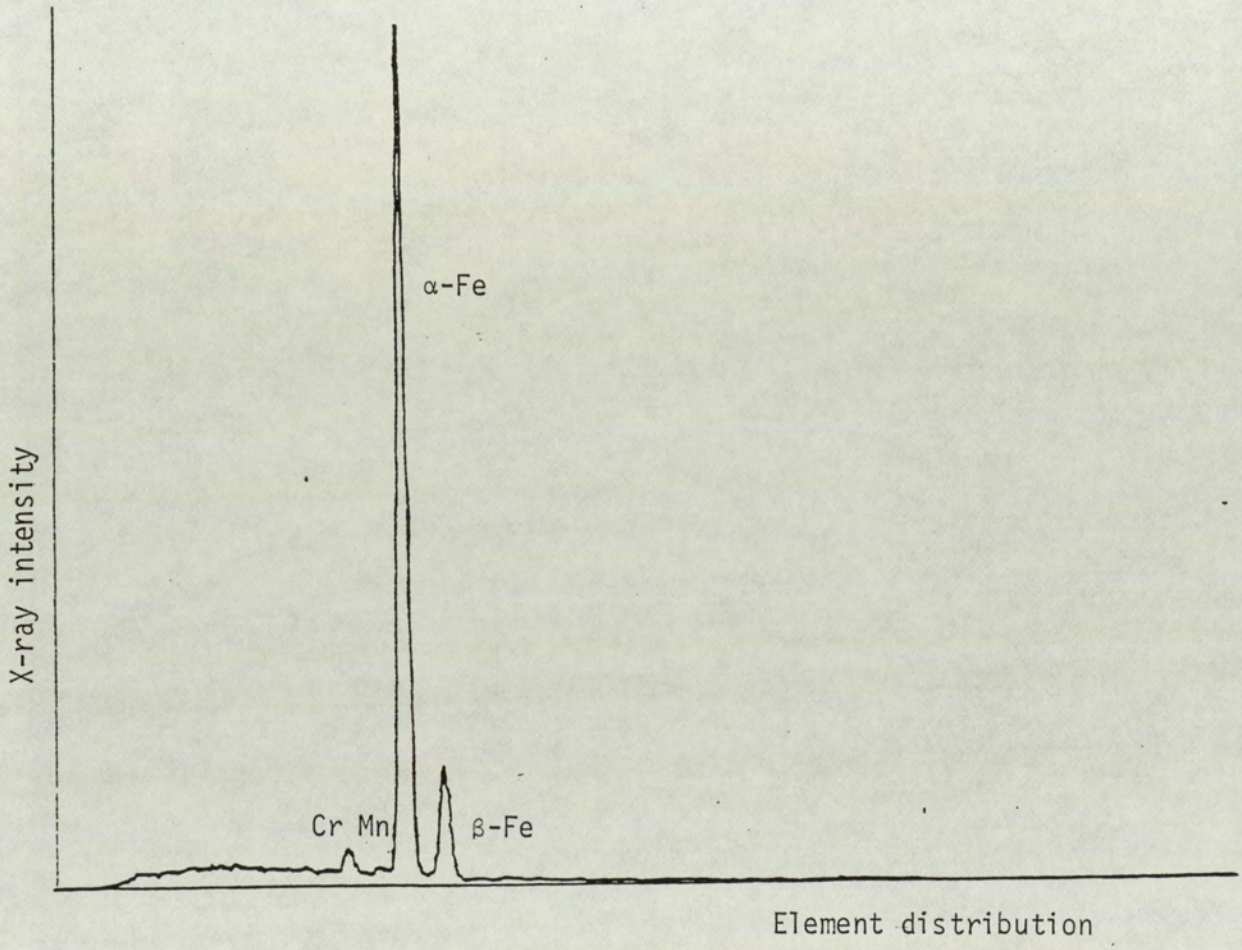

Figure 4.21 X-ray chart of unworn SAE 52100 steel surface.

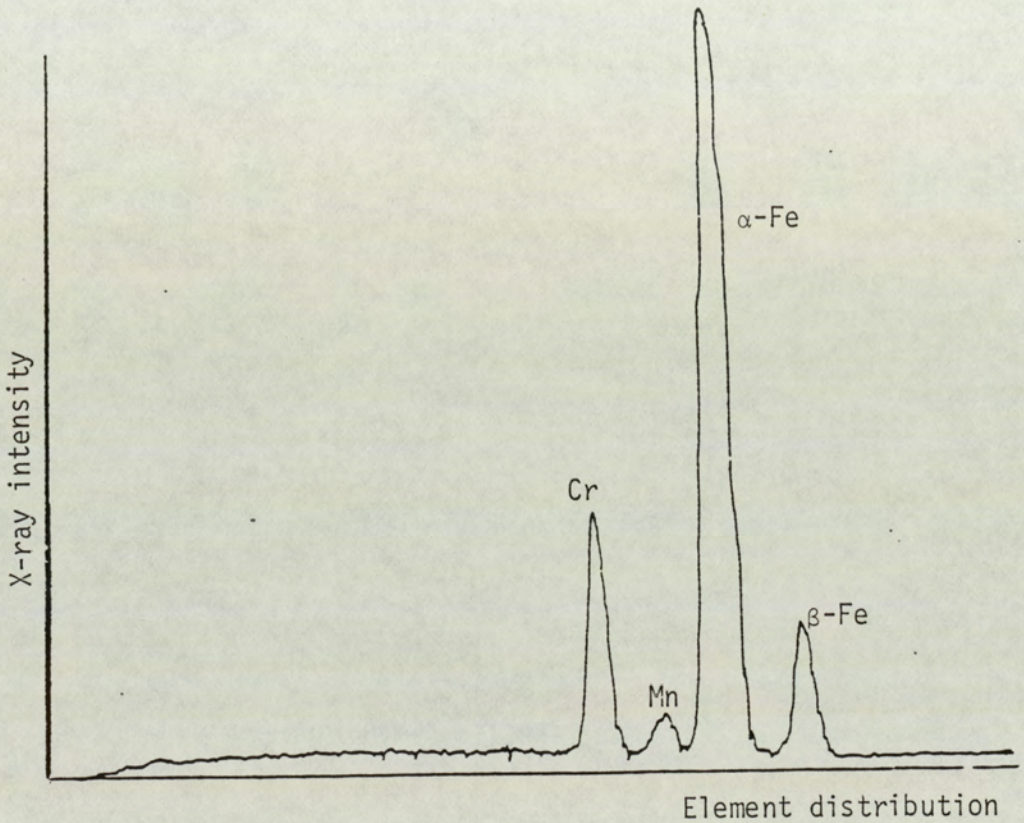

Figure 4.22 X-ray chart of unworn AISI 420 stainless steel surface.

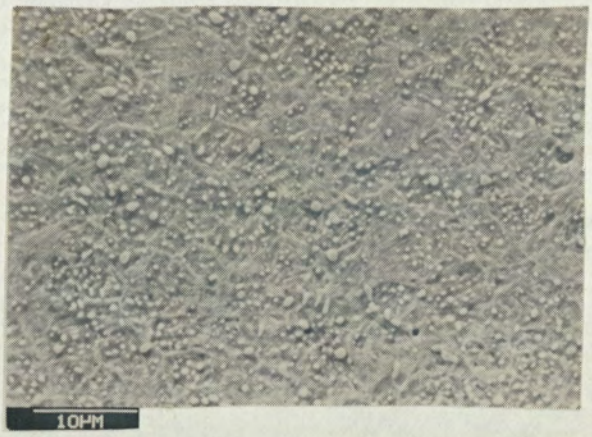

Figure 4.23 SEM micrograph of unworn (SAE 52100) steel, etched with 2% of Nital reagent.

Figure 4.24 SEM micrograph of unworn (AISI 420) stainless steel, etched with Vilalla's reagent.

4.3:4 Scanning electron microscopy of surfaces worn with no additive

The use of the SEM was based, specifically, on investigating the effects of the additives and the material used on the wear scar topography, the distribution of the elements in the scar, and the structure of the worn balls or rollers in both AW and EP regions.

When no additive was used the topography of the wear scar had a rough surface and no film on it. The roughness of the scar surface was observed to increase with increasing applied load regardless of the combination of materials (see Figure 4.25).

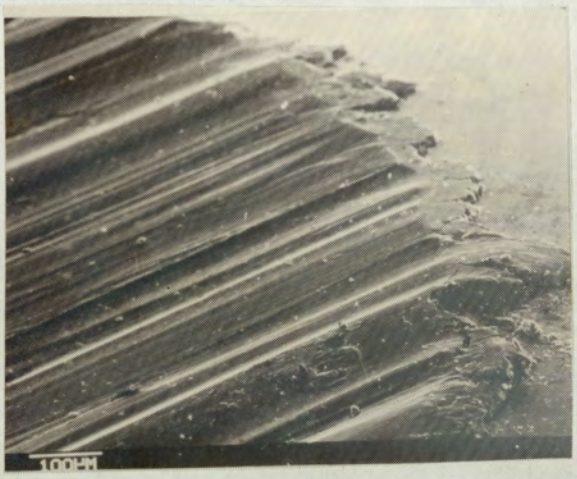

Figure 4.25 SEM micrograph of wear scar formed on (SAE 52100) steel roller by the rotating (AISI 420) stainless steel with R32 under 400 N.

4.3:5 Scanning electron microscopy of worn surfaces in the presence of sulphur additive

The effects of using sulphur additive were observed to be a coating of the wear with a visible surface film and the scar roughness was much less than that seen with R32, as shown in Figure 4.26. Also there was an increase in the amount of sulphur in the scar surface (see Figure 4.27). But the roughness of the scar was increased as a result of the extreme pressure condition. This is shown in Figure 4.28. Looking at Figure 4.29 one can see that there are considerable amounts of sulphur and chromium in the scar surface. While the appearance of chromium to this extent could be related to the use of martensitic stainless steel as stationary balls.

Figure 4.26 Scanning electron microscopy of wear scar formed on a stationary high carbon chrome steel roller (SAE 52100), with R32 + S0.25% by martensitic stainless steel rotating ball under 500 N.

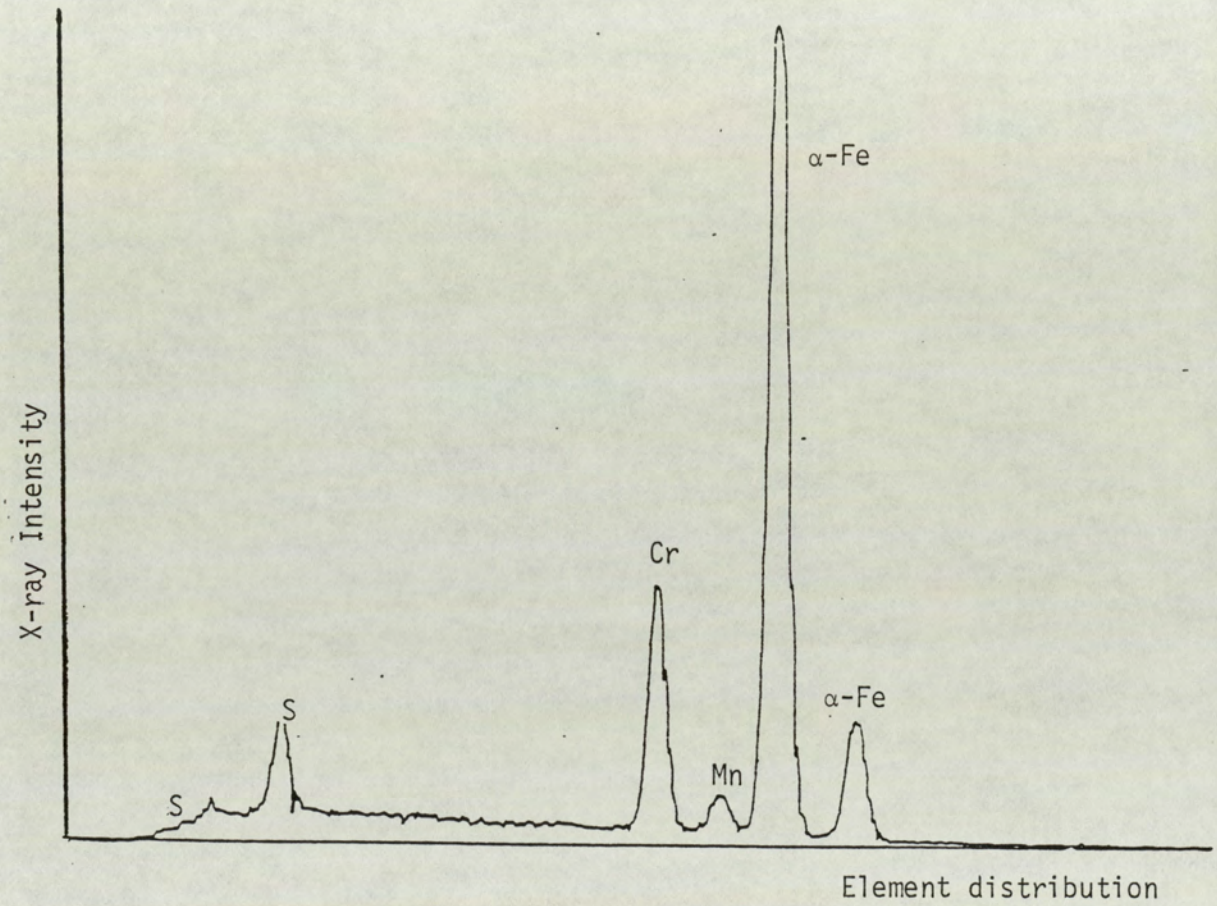

Figure 4.27 X-ray chart of SAE 52100 steel surface worn by AISI 420 stainless steel.
Lubricant: R32 + S 0.25%.
Load: 500 N.

Cr

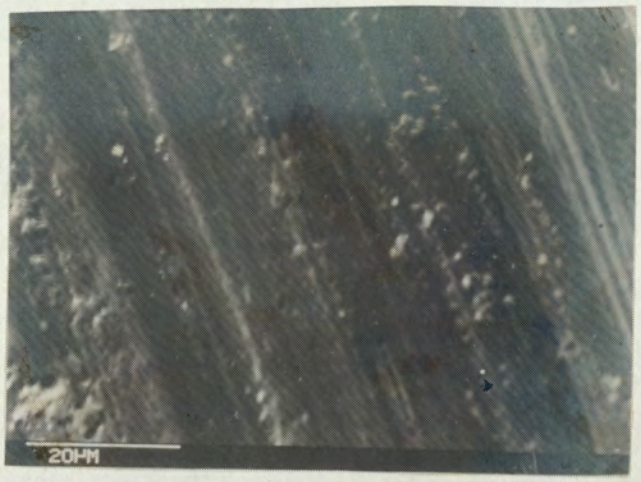

Figure 4.28 Scanning electron microscopy of wear scar formed on a stationary high carbon chrome steel roller (SAE 52100) by martensitic stainless steel (AISI 420).
Lubricant: R32 + S0.25%
Load: 16000 N

S

Fe

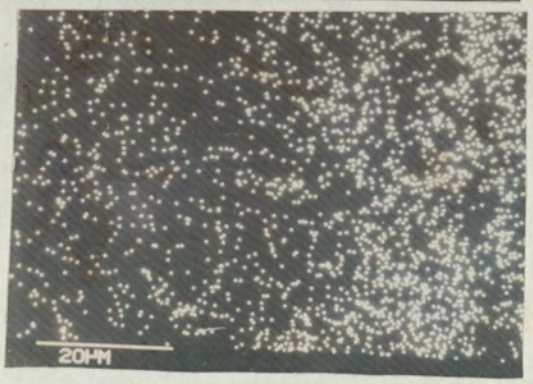

Mn

Figure 4.29 X-ray image showing the elemental distribution of Cr, S and Fe.
Lubricant: R32 + S0.25%
Load: 1600 N
AISI 420 stainless steel ball run on three 52100 steel balls.

When (SAE 52100) steel was involved as stationary balls with sulphur additive, there was no significant microstructural change either in the subsurface or in the bulk, under AW conditions, as shown in Figure 4.30, but the microstructural change was observed under the EP conditions, as shown in Figure 4.30.

Using (AISI 420) stainless steel as rotating and stationary balls, one can see that there is a more noticeable microstructural change in the bulk of the stationary ball than in the subsurface of that ball, under both AW and EP conditions, as shown in Figure 4.31.

The microstructural change was clearer in the subsurface of (AISI 420) stainless steel worn by (SAE 52100) steel under EP conditions, where the grain boundaries disappeared under a load of 4000 N.
No such change was observed under the AW conditions.

It is interesting to note that clear microstructural changes took place in the wear scars of such surfaces as (AISI 420) stainless steel worn by (SAE 52100) steel under EP conditions, as shown in Figure 4.32. In the above-mentioned Figure the microstructure of the subsurface along the wear scar had no noticeable grains as can be observed in the bulk.

4.3:6 Scanning electron microscopy of surfaces worn with Dibenzyl Disulphide (DBDS) additive

Use of DBDS additive had a slightly different effects on the topography and the microstructure of the materials used. The scar topography was smoother and brighter than that obtained with sulphur additive, as seen in Figure 4.33. The analyses of X-ray images taken of Cr, S, Fe and Mn

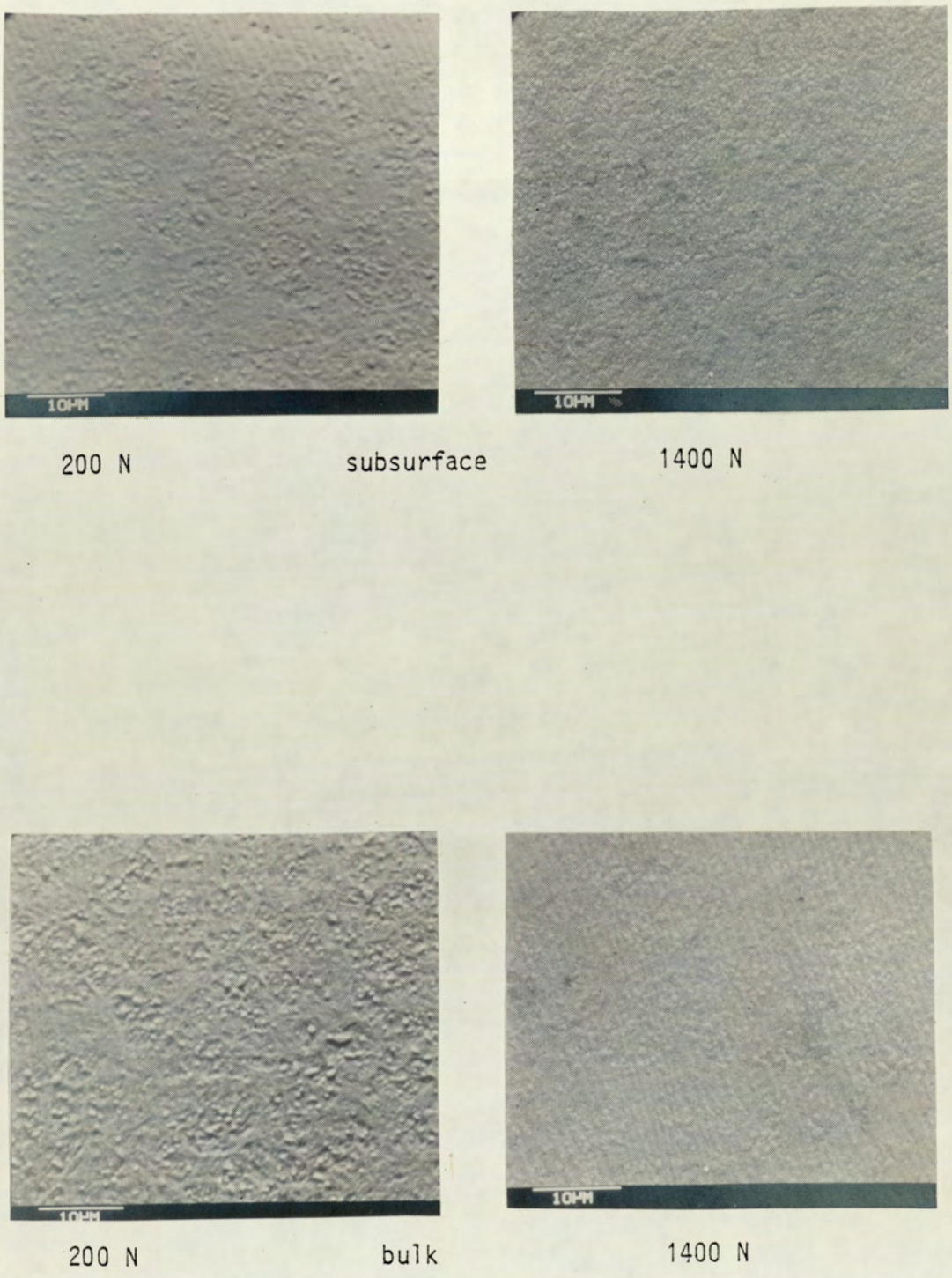

Figure 4.30 SEM micrograph shows the microstructural change in the subsurface and in the bulk of (SAE 52100) steel worn by (AISI 420) stainless steel under AW and EP with sulphur additive.

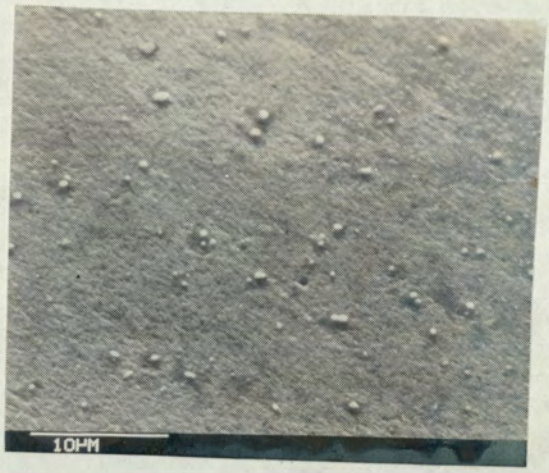

200 N subsurface 1400 N

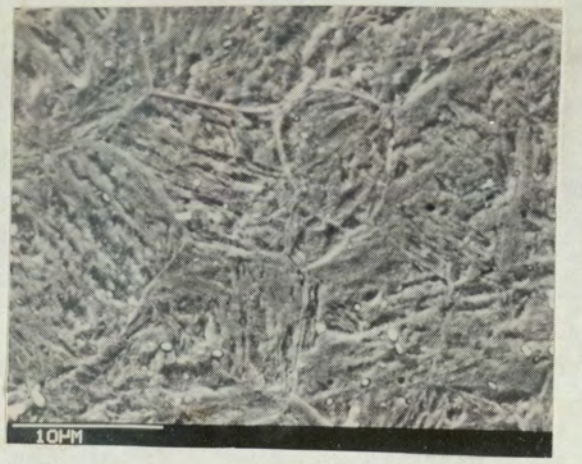

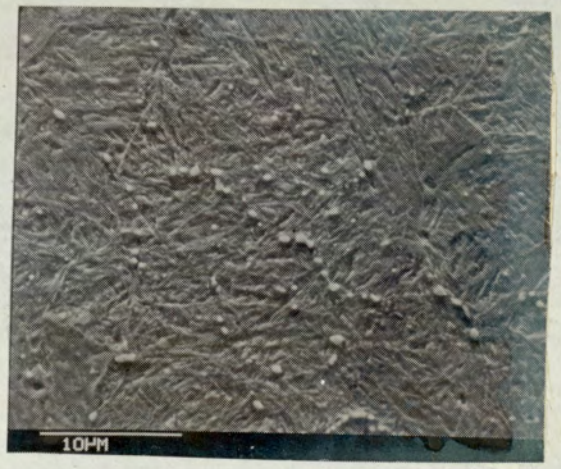

200 N bulk 1400 N

Figure 4.31 SEM micrograph shows the microstructural change in the subsurface and in the bulk of (AISI 420) stainless steel worn by similar stainless steel under AW and EP conditions with sulphur additive.

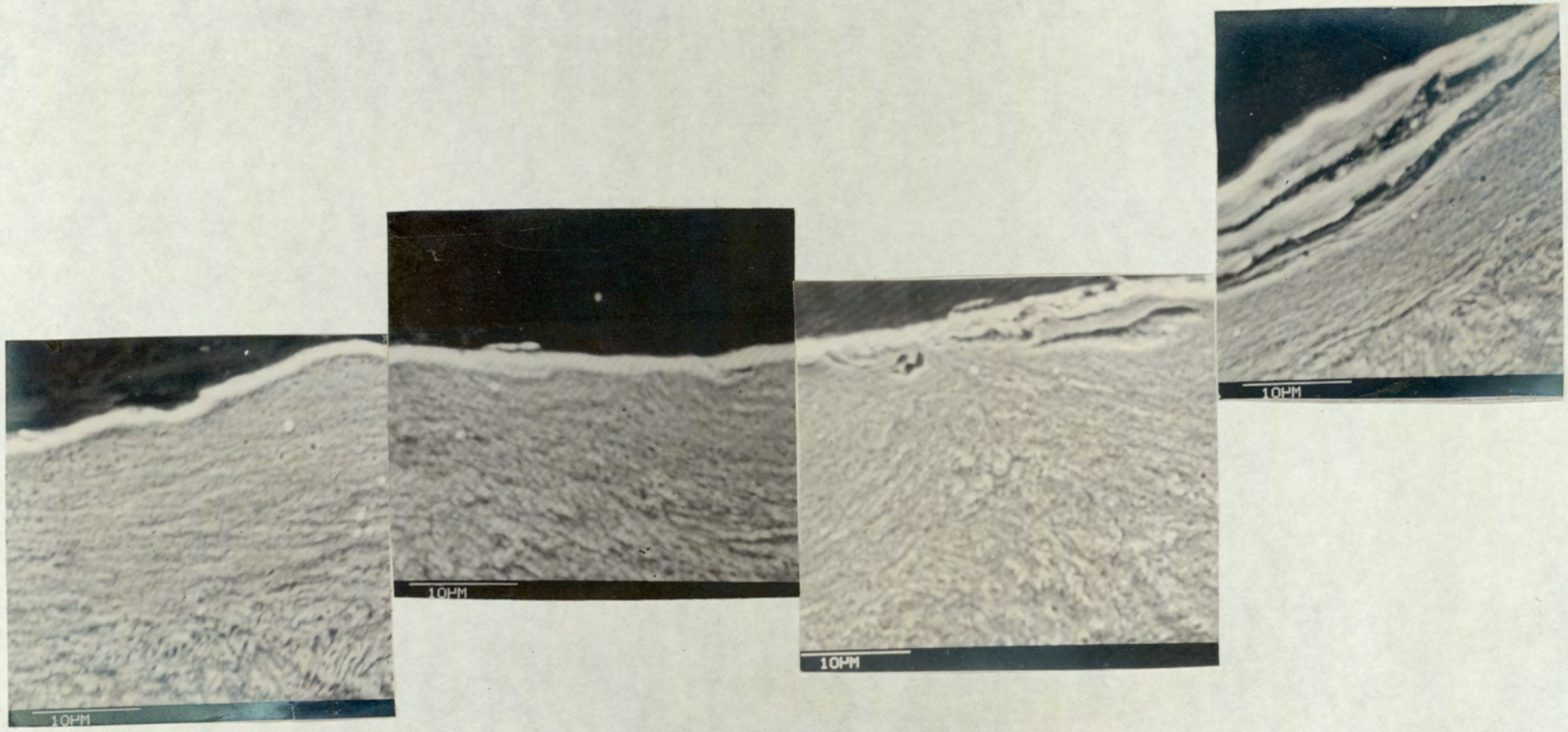

Figure 4.32 SEM micrograph showing the microstructure of the subsurface of wear scar produced on (AISI 420) stainless steel ball by (SAE 52100) steel with sulphur additive under load of 1400 N.

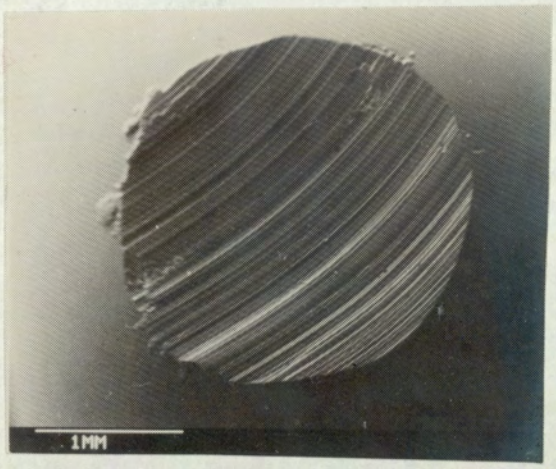

Load of 1400 N

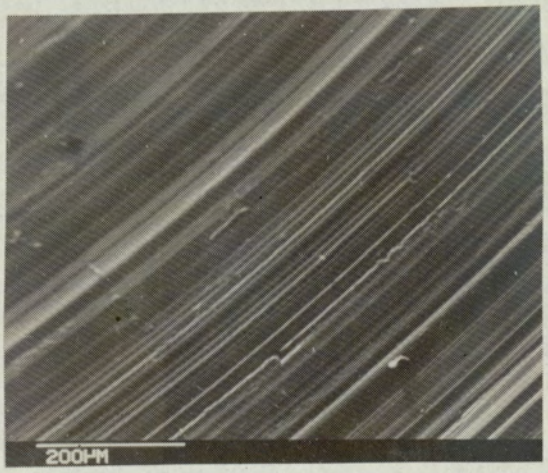

Load of 1400 N

Figure 4.33 SEM micrograph showing the topography of wear scar produced on (SAE 52100) by (AISI 420) stainless steel with DBDS additive.

distributions in the wear scars show (in Figure 4.34) that the concentration of each of the above-mentioned elements was much more than that seen in the wear scars produced with sulphur additive under AW conditions.

When (SAE 52100) steel was run on (AISI 420) stainless steel, microstructural changes were observed in the subsurface. This was clearly demonstrated in Figure 4.35 which shows a wide strip with no grain boundaries where plastic deformation has occurred. in the susbsurface (20 μ). This is in contrast to that seen in the bulk under the same EP conditions. However, when (AISI 420) was involved in the wear tests, as rotating and stationary balls, the microstructures indicated that there was some growth of chromium carbides and the appearance of irregularity in the microstructure under EP conditions, as shown in Figure 4.36.

On the other hand the microstructure of the wear scar produced under the AW conditions showed the same irregularity, but with less chromium carbides. This is shown in Figure 4.37, where the black particles are the Cr carbides.

No signfiicant microstructural changes can be seen in the subsurfaces of the wear scars and in the bulk of specimens selected from the stationary steel balls worn by (AISI 420) stainless steel. There is no noticeable difference seen between the grain boundaries under the EP conditions and those found under the AW conditions, as shown in Figure 4.38.

Running high carbon chrome steel on similar steel balls caused no significant changes in the microstructure of the wear scar subsurfaces or in the bulk. However, when (AISI 420) stainless steel was used for the stations balls the appearance of the grain boundaries was different in the bulk to those in the subsurface of the wear scar, as shown in Figure 4.39.

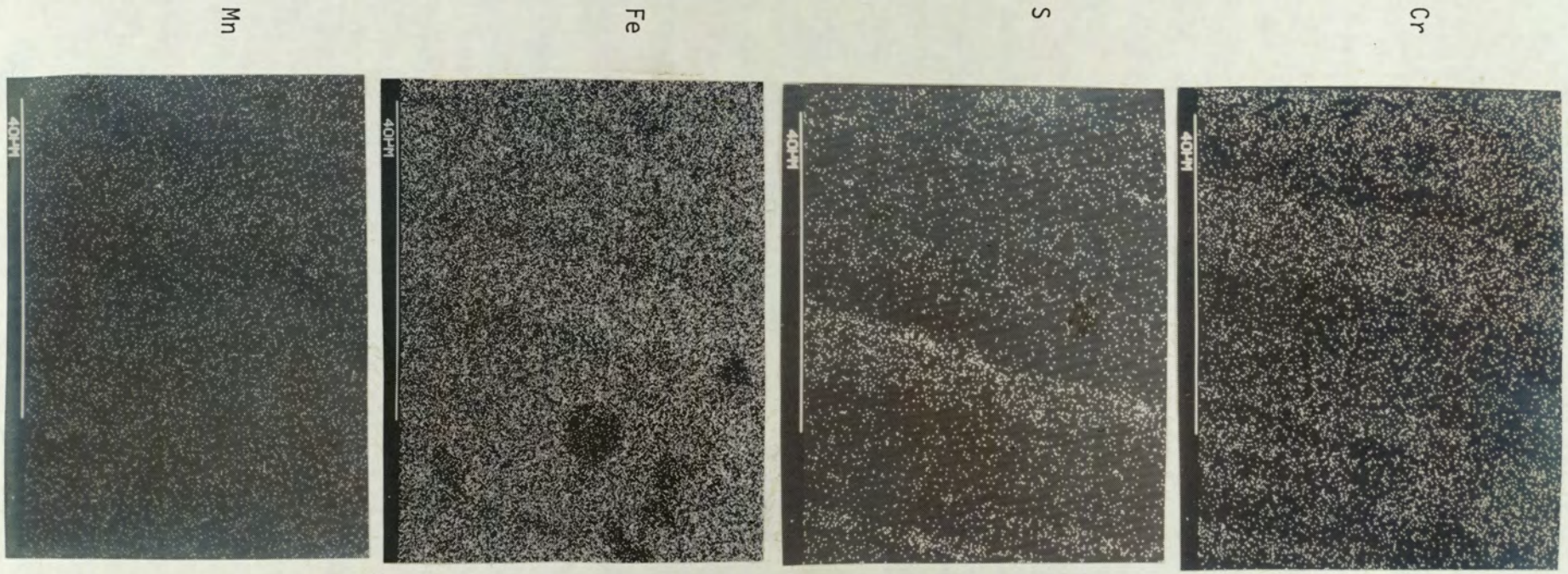

Figure 4.34 X-ray image of elements distributed in the wear scar formed on (SAE 52100) steel worn by (AISI 420) stainless steel. Lubricant: R32 + DBDS. Load: 1400 N.

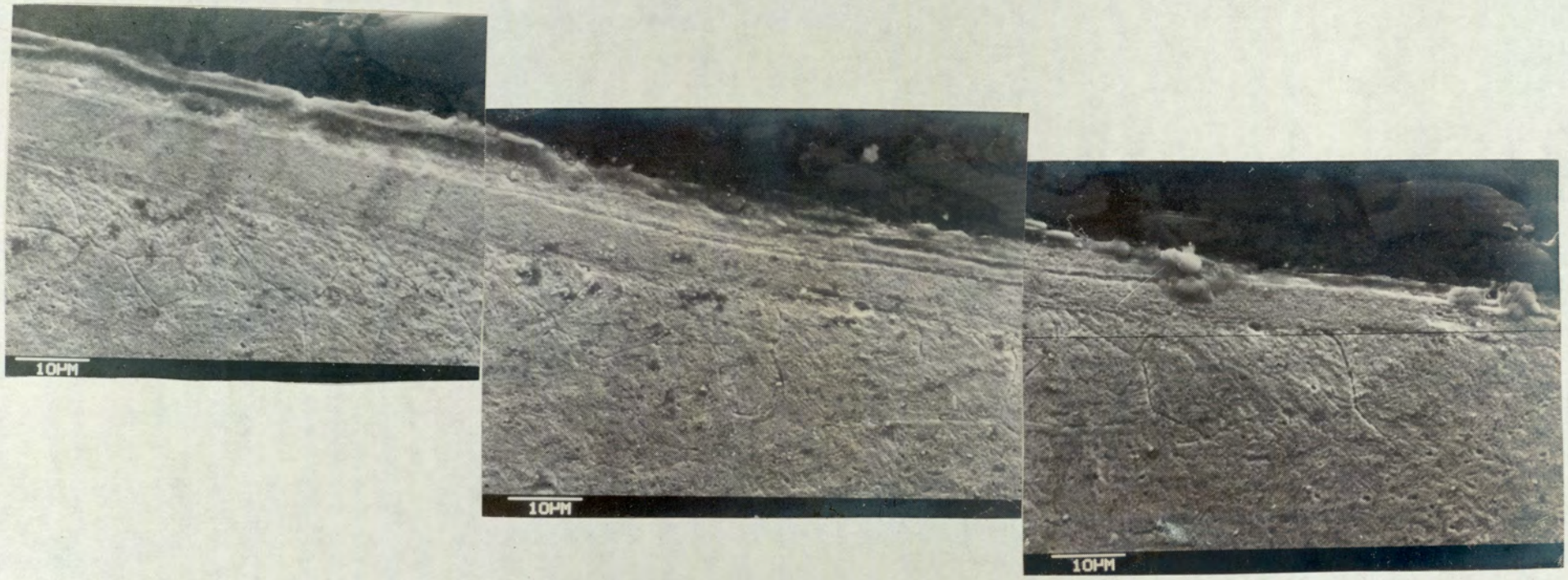

Figure 4.35 SEM micrographs showing the microstructure of the subsurface of the wear scar produced on AISI 420 stainless steel worn by SAE 52100 steel.

Lubricant: R32 + 0.886% DPDS. Load: 1400 N.

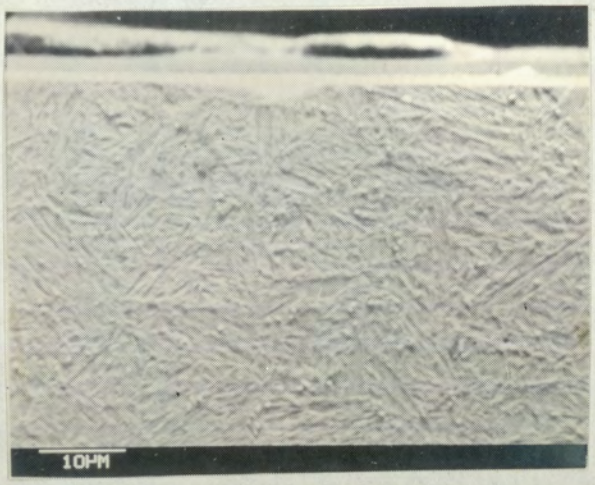

subsurface

bulk

Figure 4.36 SEM micrographs show the microstructure of AISI 420 stainless steel worn by similar stainless steel.
Lubricant: R32 + 1.00% DBDS.
Load: 1400 N.

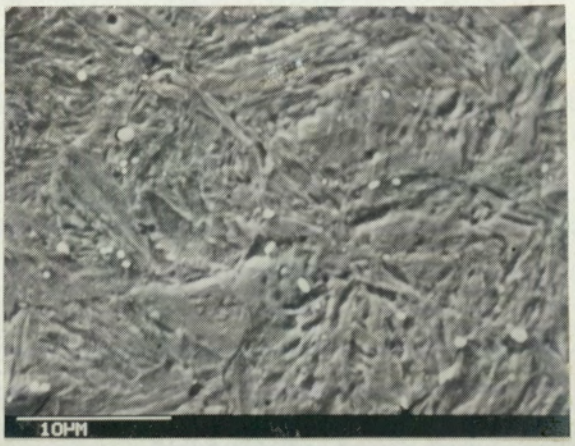

subsurface

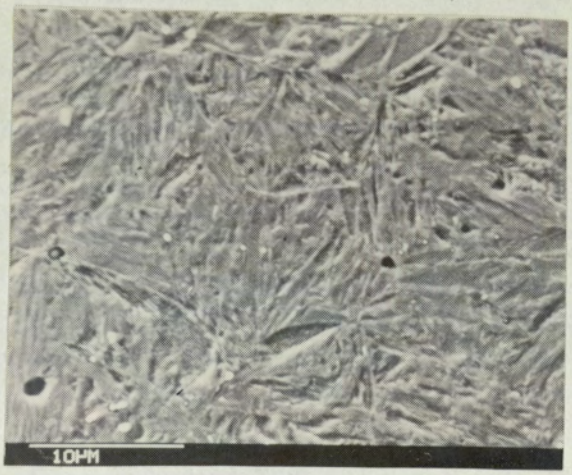

bulk

Figure 4.37 SEM micrographs show the microstructure of AISI 420 stainless steel worn by similar stainless steel.
Lubricant: R32 + 1.00% DBDS.
Load: 200 N.

Antiwear region at 200 N

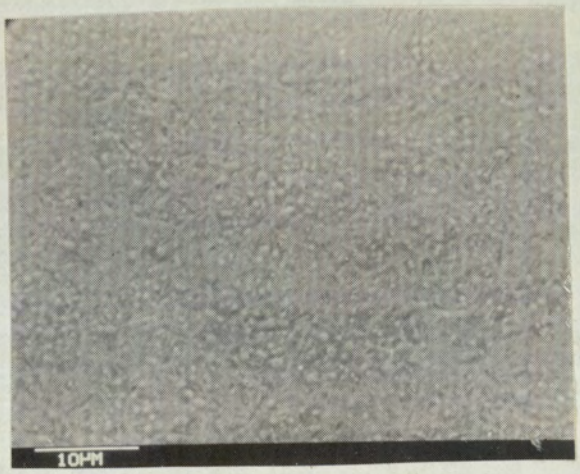

Extreme pressure region at 1400 N

Figure 4.38 SEM micrographs show the microstructure of AISI 420 stainless steel worn by SAE 52100 steel with R32 containing 1.00% DBDS.

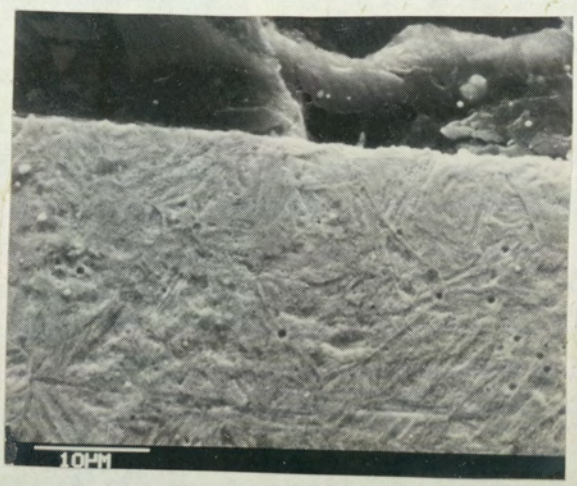

subsurface at load 200 N

Bulk at load 200 N

Figure 4.39 SEM micrographs showing the microstructural change in the subsurface and in the bulk of the worn (AISI 420) stainless steel with DBDS additive.

4.3:7 Scanning electron microscopy of worn surfaces in the presence of Diphenzyl Disulphide (DPDS) additive

When the DPDS additive was used in all cases of rotation, mentioned in Section 3.1, the surface topographies of the wear scars were obviously rough and accompanied by deep grooves (Figure 4.24) compared with those that had been seen with S and DBDS additives. This was probably because the surface films formed on the wear scar were thin, as a result of the general severe wear behaviour which could be seen with the DPDS additive. Differences were also observed in the elemental distributions present at the surface of the wear scar, where chromium and sulphur concentrations were much less than those observed with S and DBDS additives (see Figure 4.41).

Both (SAE 52100) steel and (AISI 420) stainless steel have shown more microstructural changes in the subsurfaces of the wear scar than in the bulk. One would expect any structural change to occur close to the wearing surface (see Figures 4.42 and 4.43).

4.3:8 Preliminary discussion on the SEM analysis

The XEM and X-ray energy spectrum revealed the expected presence of the elements Fe, Cr and Mn in the unworn (SAE 52100) steel and (AISI 420) stainless steel. This confirms the chemical compositions of the two above mentioned materials (see article 2.4).

Only Fe, Cr and Mn were found in the wear scar formed with R32.

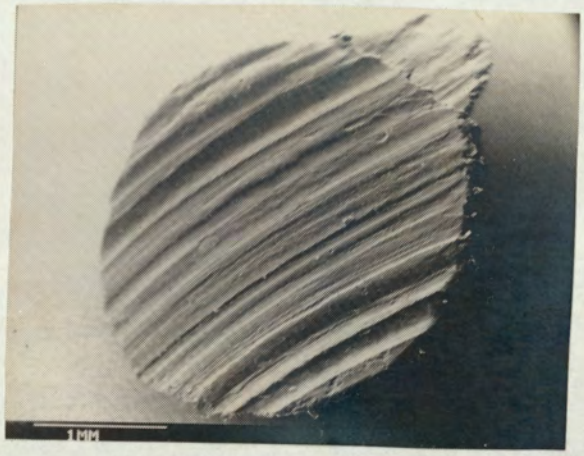

Figure 4.40 SEM micrograph showing the topography of wear scar formed under rotating a martensitic stainless steel ball on three stationary high carbon chrome steel rollers of applied load of 400 N.

Cr

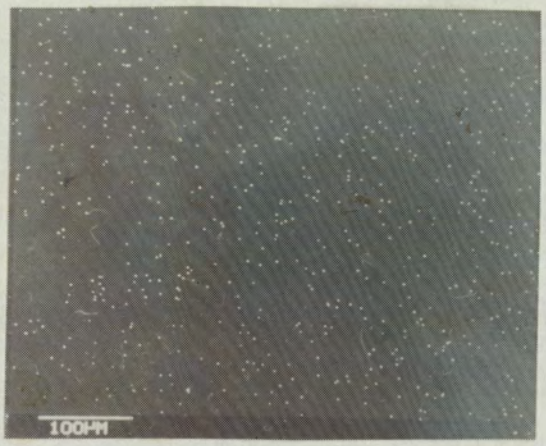

S

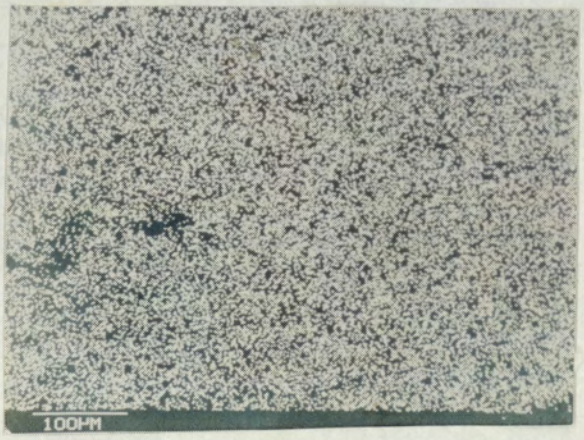

Fe

Figure 4.41 X-ray image of the elmental distribution in wear scar surface formed in the stationary high carbon steel rollers by martensitic stainless steel AISI 420 load of 1000 N. Lubricant: R32 + 0.886% DPDS.

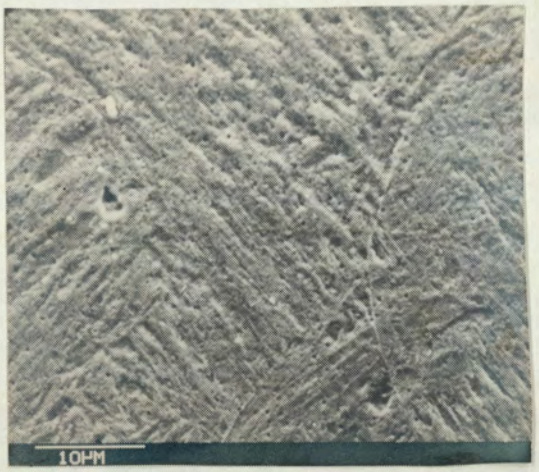

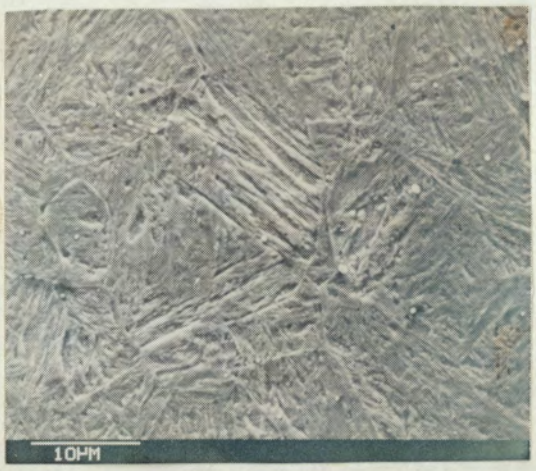

200 N (subsurface)

200 N (bulk)

Figure 4.42 SEM micrographs showing the microstructural changes in the subsurface and in the bulk of (AISI 420) with DPDS.

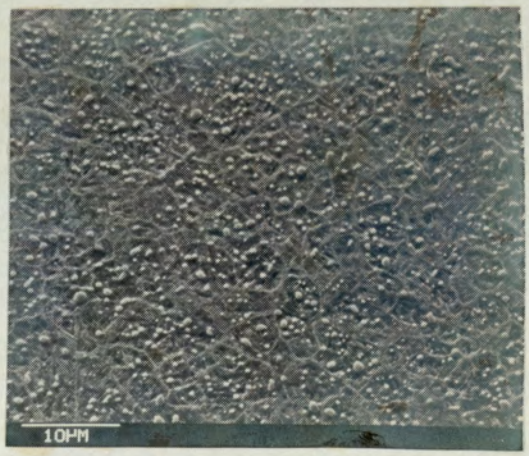

Subsurface

Bulk

1400 N

Figure 4.43 SEM micrographs showing the microstructural changes in the subsurface and in the bulk of (SAE 52100) steel worn by (AISI 420) stainless steel DPDS additive.

The existence of sulphur was noticeable in all wear scars produced in wear tests carried out with sulphur and disulphide additives. The visibility of finely scored wear scars and the shine of the surface films were due to the presence of sulphur.

The SEM micrographs of the wear scars indicated that the DBDS and sulphur provide similar smooth topographies, while DPDS topography was characterized by roughness. This may be the result of the surface films of DPDS additive being especially thin giving poor protection.

Dealing with the effects of the use of various combinations of materials, it has been seen that the microstructure does change within the processes of wear. The change in the wear scar subsurface under EP conditions was more obvious than in the antiwear region , (see Figure 4.30). But the change in the microstructure in the bulk of the selected specimen was much less than in the subsurface. Also, the bulk of the specimen subjected to the EP conditions suffered from microstructural changes more than that in the bulk of the specimen under the AW conditions (see Figure 4.31).

In Figure 4.32 there is a clear change in the microstructure of the specimen under EP conditions, which can be seen by the disappearance of the grain boundaries and the existence of a clear strip along the subsurface of the wear scar. This was due to the plastic deformation which caused a breaking off the grain boundaries in the subsurface. This plastic deformation resulted from an internal stress caused by the increasing applied load. The constituents of this strip were mainly Fe and Cr.

The use of the additives had a strong effect on the wear conditions. DBDS additive provides good protection to the sliding materials compared with dPDS additive. Therefore, DPDS additive failed to maintain sufficient protection or to diminish the wear.

The microstructural changes in the four combinations of materials were expected. It was found that if the sliding pairs were similar, the microstructure would suffer less changes than with dissimilar ones, particularly in the EP region.

It is quite interesting to note that the X-ray images of the surface film coating the wear scar of the selected specimens (produced with S, DBDS and DPDS addtiives) exhibit considerable amounts of Fe, Cr and S.

CHAPTER 5

DISCUSSION

5.1 Introduction

The purpose of this investigation was to demonstrate the very different wear behaviour obtained with similar and dissimilar sliding metallic materials under antiwear and extreme pressure conditions, and in particular to note the role of chromium in the wear behaviour of steels.

5.2 The Wear Behaviour of SAE 52100 and AISI 420 Steels

The high carbon chrome steel used for the basic work was SAE 52100 steel. This is very little different from the normal ball-bearing steel used in the U.K. (namely EN31 steel) and used previously on similar work in this laboratory (Coy and Quinn[28,32]).

Coy and Quinn[28] found that the initial seizure loads using similar stationary and rotating EN31 balls using R32, DBDS and DPDS were 45, 45 and 55 N respectively. This investigation indicates, however, that initial and final seizure almost coincide and that the final seizure loads were the same in all combinations. When R32 is present there is little if any boundary action. Hence protection in the AW region is due to mixed elastohydrodynamic lubrication. When the degree of metallic contact increases to a certain level, seizure occurs.

R32 itself is unable to interact with the metal surface, and in order for it to function as a boundary lubricant capable of bringing about such an interaction, additives must be added. The general performance of S, DBDS and DPDS additives show a noticeable initial seizure in all

combinations and that the wear behaviour takes the following pattern:

	Rotating Balls	Stationary Balls
Worst	S/S	S/S
	S/S	52100
Best	52100	S/S
	52100	52100

The additives DBDS and DPDS have good antiwear regions using similar rotating and stationary SAE 52100 steel balls where the initial seizure load was 600 and 700 N respectively. The initial seizure load was much lower if AISI 420 stainless steel balls were involved and the antiwear regions were suppressed to 100 N or less. The suppression of antiwear activity is clearly connected with the presence of a high concentration of Cr in the rotating and stationary balls (see Table 3.1).

Referring to the EP action, one can see from Table 3.1 that sulphur has the best EP action when compared to the DBDS additive, especially when SAE 52100 steel used as both rotating and stationary balls, where the EP region extended to 4000 N $(\frac{52100}{52100})$, 2000 N $(\frac{52100}{\text{AISI 420}})$, 1800 $(\frac{\text{AISI 420}}{\text{AISI 420}})$ and 2400 N $(\frac{\text{AISI 420}}{52100})$ in the four combinations of materials. While the EP action of DBDS was less than that of sulphur additive, where the EP region extended to 2600 N, 2000 N, 1800 N and 2000 N respectively. DPDS action was generally less than both the above mentioned additives, which reduced the EP region to 1600 N, 1400 N, 1600 N and 1400 N respectively.

The use of the four-ball machine in wear tests carried out with these combinations of materials has shown that the wear scar diameters depend on (i) the lubricant used in the wear test, (ii) the type of material,

(iii) the load-carrying capacity of the additives. The wear scar diameters become large when the AISI 420 stainless steel is used for the stationary balls. This shows that the presence of chromium does have a considerable effect in this variation of the wear scar diameters. This may relate to the actual role of chromium, which can cause a considerable increase in hardness with some loss in the ductility. Higgins[1] pointed out that the increase in hardness is due to the fact that chromium is regarded as a carbide stabiliser, and can form the hard carbides such as Cr_7C_3.

The wear tests carried out with S, DBDS and DPDS in the four-ball machine showed that wear behaviour of the four combinations of materials was much better than those carried out with no additive. This illustrates the advantages of using additives in AW and EP conditions which have widely been studied by many tribologists, such as Allum and Forbes[27,39], Coy and Quinn[28,32], Davey and Edwards[17]. Figure 3.6 shows that the wear scar diameters produced with sulphur were the smallest amongst those obtained by all additives used in this investigation. The sulphur additive does not show good AW action and this is regarded as one of the main disadvantages. This is due to the fact that sulphur is a corrosive material if blended with higher than 2% concentration.

5.3 Mechanism of the Disulphides Action in AW and EP Conditions

Here we are concerned with the overall mechanism of protection afforded by S, DBDS and DPDS in the AW and EP conditions. It is generally understood that intermittent penetration of the oil film by the surface asperities occurs during elastohydrodynamic lubrication. As the load is increased

metallic contact will increase until finally when the temperature of the contact reaches a certain value, the bulk of the oil film collapses producing a large increase in both temperature and wear. In the AW region the additive adsorbed into the surface will resist the penetration and reduce metallic contact. In this AW region it is suggested that the sulphur is initially adsorbed onto the metal surface after the cleavage[30] of the sulphur-sulphur bond occurs followed by the formation of an iron mercaptide layer. In the chemical reaction of disulphides the sulphur-sulphur bond is known to be the weakest part of the molecule. Allum and Forbes[41] expected that the order of increasing case of scission is

benzyle < phenyl

Diphenyle disulphide would be expected to have the weakest sulphur-sulphur bond. As loads approaching EP conditions are reached, much higher temperatures are found in the contact zone, and cleavage of the carbon-sulphur bond to form an inorganic sulphur-containing-layer occurs. Allum and Forbes[40] found that the EP activity of di-n-alkyl disulphides increased as the chain length decreased. Therefore the EP activity of sulphur additives is dependent on the ease of cleavage of the carbon-sulphur bond in the molecule so that an inorganic iron-sulphur layer is formed. Allum and Forbes[30] had found that the following order of increasing EP activity of these disulphides are as follows:

diphenyl < di-n-butyl < di-sec-butyl < di-tert-butyl < dibenzyl, diallyl

The results obtained in this work are in agreement with Allum and Forbes[30] regarding the performance of DBDS and DPDS in EP conditions. Table 3.1 shows that in all combinations of materials the final seizure

load of DBDS were higher than those obtained with DPDS. But in the AW conditions the DPDS activity was equal or larger than the DBDS activity which also agrees with the work of Allum and Forbes[30,40], and Forbes[13] and is supported by Coy and Quinn[28,32]. The wear tests carried out with the disulphides show that the order of EP activity of these disulphides is

diphenyle < dibenzyl

This work has shown that there is no advantage in the use of DPDS. Therefore, it is more useful to choose Zinc Dialkyle dithiophsophate (ZDP) as used by Barton[41], Coy and Quinn[28] since ZDP has good AW regions, than choosing DPDS.

5.4 Discussion on the Surface Analysis

The electron probe microanalyses, glancing angle X-ray diffraction and scanning electron microscopy techniques have been used to examine the surface films produced in AW and EP wear tests.

The electron probe analysis has mainly been used to find out the relative concentrations of Cr, Fe and S in the surface film in relation to increasing applied loads. These analyses may not give accurate representation of surface concentration due to the fact that the sampling depth of 1-1.5μ of the electron beam penetration produces a large contribution from sub-surface layers. The EPMA was used to measure the concentration of Cr, Fe and S experimentally, and the oxygen, carbon were calculated by difference. In fact carbon can be measured experimentally by the EPMA and oxygen can be measured by using Auger Electron Spectroscopy (A.E.S.) but the efforts were

denoted to Cr, Fe and S, because A.E.S. was not available in the University. Sulphur is present in the wear scar and its content in the surface film generally decreases in the AW region, reaching the minimum amount at the I.S. load, and then starts to increase with increasing applied load, as seen in Figure (5.1).

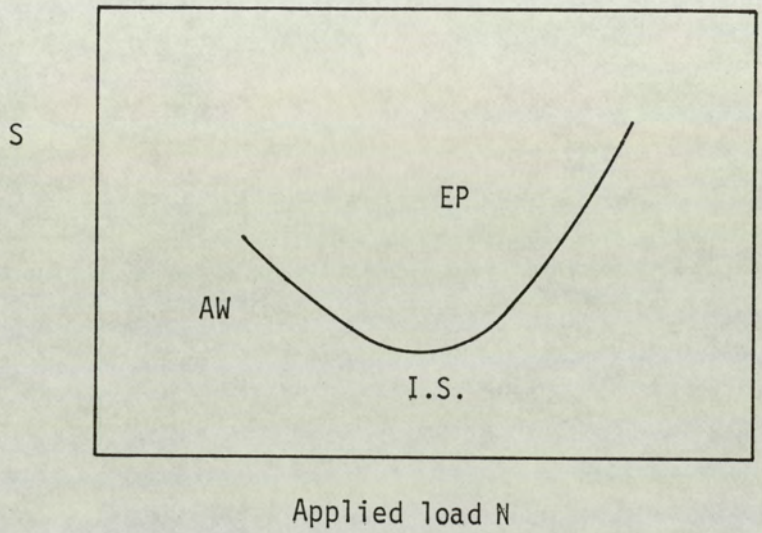

Figure 5.1 Variation of amount of sulphur with applied load N.

In the AW region, sulphur decreases due to increasing desorption and removal of the sulphur containing molecules with increase in energy dissipation at the surface. After I.S. the molecules break up to release free sulphur which then interacts with the surface, resuling in increasing sulphur concentration and the formation of iron sulphide.

The decrease of sulphur in Figure 4.12 may be related to the failure of cleavage of the sulphur-sulphur bonds of the DPDS.

The EPMA show that the preferential formation of FeS and iron oxides results in an apparent decrease in Cr.

Also, the analysis shows that the relationship between FeS, Cr and O/C are all interdependent. When initial seizure occurs large quantities of FeS are formed at the surface together with iron oxides, which leads to the above mentioned apparent decrease in Cr and O/C since results are normalized to 100%.

Allum and Forbes[30] found that the oxygen content of the wear scar decreases with increasing sulphur content, which is not in agreement with the results obtained in this investigation.

The X-ray analysis shows that iron oxides were more detectable than chromium oxides. Iron carbides and chromium carbides were detectable in the X-ray analysis and their presence in the EP region was more noticeable than in the AW region. In the X-rays photograph the iron oxide lines were always more intense than those of Cr oxides. Cr_7C_3 was detectable by the X-ray analysis (see Tables 4.2-4.4). But, Cr_7C_3 was not seen when the combination was totally of SAE 52100 steel. This was due to the low percentage of chromium in this type of steel compared to the AISI 420 stainless steel where Cr_7C_3 is much more noticeable. Debris analysis should have been done in order to identify the presence of iron and chromium oxides.

SEM was used rather than the optical microscope because of its depth of field. The most interesting features found by the SEM are the changes in microstructure (shown in Figures 4.32 and 4.35) in the subsurface. These changes were produced due to the plastic deformation and were more noticeable in the subsurface and particularly in the EP regions.

CHAPTER 6

CONCLUSIONS AND FUTURE WORK

6.1 Conclusions

This investigation has shown that the chemical composition of the material used should be taken into account. The general pattern for wear is that in order of improvement for all additives.

	Rotating Balls	Stationary Balls
Worst	S/S	S/S
	S/S	52100
Best	52100	S/S
	52100	52100

The mean behaviour of SAE 52100 (of similar sliding pairs) was much better than that of similar sliding pairs of AISI 420. This was due to the higher percentage of chromium (12-14%) in AISI 420. Such a percentage does have a deleterious effect on the wear behaviour. It has been seen throughout this investigation that the AW and EP actions were suppressed due to this percentage of Cr. Also, it was found that the wear scar formed under the rotating AISI 420 stainless steel balls are much larger than those formed with SAE 52100 steel.

The sulphur additive had very good EP activity compared to DBDS and DPDS, but DBDS and DPDS show good AW activity.

The AW activity of the disulphides takes the following order:

benzyle < phenyle.

But, in the EP activity of the disulphides, the following order was obtained:

diphenyle < dibenzyle.

The analysis of the worn surfaces obtained by EPMA, X-ray diffraction and SEM techniques showed that there is a clear presence to iron and chromium in the surface films. Sulphur was decreased to its minimum at the initial seizure loads. After the initial seizure load sulphur content increases with increasing applied load. Chromium generally decreased with increasing applied load, while oxygen/carbon concentrations increased with the applied loads.

The SEM analysis has shown that the sliding pairs do suffer a change of subsurface microstructure due to plastic deformation caused by the applied load, and this change decreases towards the material bulk.

6.2 Future Work

This investigation has shown that there are several areas of research which can be conducted. These areas are as follows:

1). Studying the tribological behaviour of different types of stainless steels (Ferritic and Austenitic) using similar sliding pairs and dissimilar ones.

2). Comparing several combinations of different types of stainless steels and high carbon chrome steels.

3). The work can be extended to investigate widely the role of chromium and molybdenum in the above mentioned stainless steels.

4). It would be interesting to study the micro-structure of the wear scar subsurface using various techniques of analysis, among them SEM, EPMA, X-ray diffraction, photo-Electron Spectroscopy and Optical Electron Microscopy combined with sectioning and microhardness testing.

5). It would be useful to try other additives, such as organo chlorine and phosphorous additives in any future work, in addition to other disulphide additives.

6). The mechanism of the formation of the surface film produced in the four-ball machine wear tests needs to be investigated in line with the role of Fe, Cr in the above mentioned stainless steels.

REFERENCES

(1) Engineering Metallurgy, Applied Physics Metallurgy, R.A. Higgins p. 225.

(2) Oxidational and Tribological Studies of Austenitic Stainless Steel Under CO_2-Based Environments. L.R. Wallace, Ph.D. 1980.

(3) Archard, J.S. and Hirst, W., "The Wear of Metals Under Lubricated Conditions", Proc. Roy. Soc. (London), Series A, 1956, Vol. 236, pp. 397-410.

(4) Quinn, T.F. (1978). Proc. Int. Conf. on Fundamentals of Tribology, MIT Press, Cambridge, Massachussetts (1980). "The classifications, laws, mechanisms and theories of wear", pp. 477-492.

(5) Burwell, J.F., Strange, C.D., (1952), Proc. Roy. Soc., 212, "Metallic wear".

(6) Waterhouse, R.B., Int. Conf. of Wear Mater., St. Louis, No. Apr. 25-28/971, ASME, NY. 1977, p.55-59. "Role of adhesion and delamination in the fretting wear of metallic materials".

(7) Holliday, J.S. and Hirst, W., Proc. Roy. Soc. A., Vol. 236, pp. 411-425, "The fretting corrosion of mild steel".

(8) Dowson, D., "Transition of boundary lubrication from elasto-hydrodynamic lubrication", Boundary lubrication. An appraisal of world literature. Ed. Ling, F.F., Klaus, E.E. and Fein, R.S., A.S.M.E., (1969), pp. 229-240.

(9) Rowe, G.W., "Boundary lubrication", The principle of lubrication, A. Cameron, Loneman Green & Co., Ltd., (1966), Chap. 20.

(10) Bieber, H.E., Klauz, and Tewksbury, E.J., "A study of tricresyl phosphate as an additive for boundary lubrication", Transactions 11, 155-161 (1968),

(11) Bowden, F.P. and Ridler, E.W., "Physical properties of surfaces, III - The surface temperature of sliding metals, The temperature of lubricated surfaces", Proc. Roy. Soc. A., 1936 (154), pp. 640-656.

(12) Borsoff, V.N., Wagner, C.D., "Studies of formation and behaviour of an extreme pressure film", Vol. 13, Part 2 (1957), pp. 91-99.

(13) Forbes, E.S., "Antiwear and extreme pressure additives for lubricants", Tribology (1970), pp. 145-152.

(14) Davey, W., "The extreme pressure lubricating properties of some sulphides and disulphides in mineral oil as assessed by the four-ball machine", Wear, 1, pp. 291-304, (1957/58).

(15) Prutton, C.F. and Turbuli, D. and Dlough, G., "Mechanism of action of organic chlorine and sulphur compounds in extreme pressure lubrication", J. Inst. Pet., 32 (1946), p.90.

(16) Hamilton, L.A. and Woods, W.W., Ind. and Eng. Chem., 42, (1950), pp. 513-519, "Reaction of iron with organic sulphur compounds".

(17) Davey, W. and Edwards, E.D., "The extreme pressure lubricating properties of some sulphides and disulphides, in mineral oil, as assessed by the four-ball machine", Wear, Vol. 1, (1957), pp. 291-304.

(18) Godfrey, D., "Chemical changes in steel surfaces during extreme pressure lubrication", Trans. ASLE, Vol. 5, (1962), pp. 57-66.

(19) Greenhill, E.B., "The lubrication of metals by compounds containing sulphur", J. Inst., Pet. Vol. 34, (1948), p.659.

(20) Sakuria, T., Ikeda, S. and Okabe, H., "The mechism of the reaction of sulphur compounds with steel surfaces during boundary lubrication using S^{35} as a tracer", Trans. ASLE, Vol. 5, (1962), pp. 67-74.

(21) Sakurai, T., and Sato, K., "Study of corrossinity and correlation between chemical reactivity and load-carrying capacity of oils containing extreme pressure agents",AASLE, Transactions, 9, pp. 77-87 (1966).

(22) Loeser, E.H., Twiss, S.B. and Teague, D.M., "Cam and Tappet test for lubricants, I - Anti-scuff evaluation". Lubrication Engineering, Vol. 13, no. 4, April 1957, pp. 1961-6.

(23) Loeser, E.H., Twiss, S.B., and Teague, D.M., "Cam and Tappet test for lubricants, II", Wear evaluation, (1957), Vol. 13, pp. 269-274.

(24) Loeser, E.H., Wiquert and Twiss, S.B., "Cam and Tappet lubrication, III - Radiative study of phosphorous in the EP film", (1958), Vol. 1, No. 2, pp. 329-335.

(25) Loeser, E.H., Wiquert and Twiss, S.B., "Cam and Tappet lubrication, IV - Radiation study of sulphur in the EP film". (1959), Vol. 2, pp. 199-207.

(26) Bewnett, P.A., "A surface effect associated with the use of oils containing zinc Dialkyle Dithophosphate", ASLE Trans. 2, pp. 78-90, (1959).

(27) Allum, K.G. and Forbes, E.S., "The load-carrying properties of metal Dialkyle Dithrophosphates: The effect of chemical structures, (1968), Vol. 183, Part 3, p. 7.

(28) Coy, R.C., and Quinn, T.F.J., "The use of physical methods of analysis to identify surface layers formed by organosulphur compounds in wear tests", ASLE Transactions, Vol. 18, 3, pp. 163-174.

(29) Godfrey, D., "The lubrication mechanism of tricresyl phosphate on steel", ASLE, Transactions, 8, pp. 1-11 (1965).

(30) Allume, K.G. and Forbes, E.S., "The load-carrying mechanism of organic sulphur compounds - application of electron probe microanalysis", ASLE Transactions 11, pp. 162-175, (1968).

(31) Czidhos, H. and Kirnchke, K., "Investigations into film failure (transition point) of lubricated concentration contacts", Wear 22 (1972), pp. 321-336.

(32) Coy, R.C. and Quinn, T.F.J., "An application of electron probe microanalysis and X-ray diffraction to the study of surfaces worn under extreme pressure lubrication", Proc. Inst. Mech. Engrs., Lubrication Conference, September 1972.

(33) Brainard, William, A. and Buckly, Donald, H., "Adhesion and function of PTFE in contact with metals as studied by Auger spectroscopy, field iron and scanning electron microscopy".

(34) Isherwood, B.J. and Quinn, T.F.J., "The application of a glancing-angle X-ray diffraction film technique to the study of the low-temperature oxidation of iron-chromium alloys", Brit. J. Appl., Phys. (1967), Vol. 18.

(35) Boerlage, Engineering, 136, pp. 46-47 (1933). "Four-ball testing apparatus for extreme pressure lubricants".

(36) Timoshenko, S. and Gooder, J.N., "Theory of elasticity, McGraw-Hill Book Company, Inc., (1951), p. 372.

(37) "The mechanical and physical properties of the British Standard EN steels", J. Woolman and A.A. Noltram, Vol. 3, BIRA, Pergamon Press, (1969).

(38) Modern physical techniques in modern materials technology, Edited by T. Mulvey and R.K. Webster.

(39) Allum and Forbes, "The load-carrying properties of organic sulphur compound", J. Inst. Petrol, (1967), Vol. 53, pp. 173-185.

(40) Allum, K.G. and Forbes, E.S., "The load-carrying properties of organic sulphur compounds, Part II, The influence of chemical structure on the antiwear properties of organic Disulphides", J. Inst. Appl., 53, pp. 173-185, (1967).

(41) Barton, D.B., Klaus, E.E.,Tewksbury, E.J., Strange, J.R., "Preferential adsorption in the lubrication process of zinc Dialkyldithiophosphate". Vol. 16, 3, pp. 161-167.